

A THEORETICAL INVESTIGATION OF OPTICAL  
ABSORPTION INTENSITIES IN TRANSITION METAL COMPLEXES

BY

LOUIS NOODLEMAN

S.B., Massachusetts Institute of Technology

1971

S.M., Massachusetts Institute of Technology

1972

Submitted in partial fulfillment of the requirements  
for the degree of  
DOCTOR OF PHILOSOPHY  
at the  
Massachusetts Institute of Technology  
September, 1975

Signature of Author Signature redacted  
Department of Materials Science and  
Engineering, August 11, 1975  
Certified by Signature redacted  
Thesis Supervisor  
Accepted by Signature redacted  
Chairman, Departmental Committee on  
Graduate Students



Thesis  
Mat. Sci. + E  
1975  
Ph.D.



A THEORETICAL INVESTIGATION OF OPTICAL  
ABSORPTION INTENSITIES IN TRANSITION METAL COMPLEXES

BY

LOUIS NOODLEMAN

Submitted to the Department of Materials Science and Engineering on August 11, 1975 in partial fulfillment of the requirements for the degree of Doctor of Philosophy.

---

ABSTRACT

A density matrix formulation for optical absorption is developed within the framework of the  $X_\alpha$  scattered wave theory. In this approach, the transition state orbitals are used as an approximation to the natural orbitals of the system. It is shown that this concept enters in a natural way into the formalism. Through the use of commutation relations, we show that the three oscillator strength forms,  $f(x)$ ,  $f(\vec{V})$ , and  $f(\vec{V}\vec{V})$  are equivalent in the  $X_\alpha$  theory, in contrast to the Hartree-Fock method. In the present work, the  $f(\vec{V}\vec{V})$  form is used exclusively for computation since in the scattered wave method this form may be evaluated without integrating over the intersphere region. The method is first applied to intensities in the simple diatomic molecules  $H_2^+$ ,  $H_2$ , and  $CO^+$ , with results generally accurate to 5% (at the equilibrium nuclear separation) in  $H_2^+$ , and of order of magnitude accuracy for the weak transitions in  $CO^+$ . In  $H_2$ , the  ${}^1\Sigma_g^+ \rightarrow {}^1\Sigma_u$  transition is very accurately described, but the  ${}^1\Sigma_g^+ \rightarrow {}^1\Pi_u$  intensity is not satisfactory due to the diffuse character of the  ${}^1\Pi_u$  state. We then computed intensities in the transition metal complexes  $MnO_4^{-1}$ ,  $FeCl_4^{-1}$ ,  $CoCl_4^{-2}$ , and  $Cr(CO)_6$ . Relative intensities of the dipole allowed charge transfer transitions in  $FeCl_4^{-1}$  and  $CoCl_4^{-2}$  are reasonably accurate. The crystal field intensity in  $CoCl_4^{-2}$  is unsatisfactory due to the low excitation energy,  $\Delta E < 1\text{ eV}$ . Intensity considerations in  $Cr(CO)_6$  yield a new spectral assignment. In  $MnO_4^{-1}$ , the scale factor between the theoretical and the experimental intensities is 17, which is quite large. We postulate that this is due to an incorrect boundary condition for the cluster. The discrepancies in the absolute intensities between theory and experiment in transition metal complexes are discussed in terms of correlation effects, local field effects, and boundary conditions.

## ABSTRACT (continued)

Thesis Supervisor: Professor Keith H. Johnson

Title: Professor of Materials Science and  
Engineering

## TABLE OF CONTENTS

<u>Chapter Number</u>		<u>Page Number</u>
	ABSTRACT	2
	LIST OF FIGURES	7
	LIST OF TABLES	8
	ACKNOWLEDGEMENTS	10
I	Introduction	11
II	Experimental Background	23
III	Previous Theoretical Work on Optical Intensities	30
	A. Atoms	30
	B. Simple Molecules	35
	C. Transition Metal Complexes	42
IV	A Critical Discussion of Conventional Theoretical Approaches to Intensities	46
	A. Configuration Interaction Theory	46
	B. Hartree-Fock LCAO Theory	48
	C. The Effects of Molecular Vibrations on Spectra	52
	D. Boundary Conditions and Local Field Effects	62
V	The $X_{\alpha}$ Scattered Wave Method	70
	A. The $X_{\alpha}$ Theory	70
	B. The Transition State Concept	79

<u>Chapter Number</u>		<u>Page Number</u>
	C. The Scattered Wave Method	82
	D. The Use of Overlapping Atomic Spheres	87
VI.	The Development of a New Approach to Calculating Optical Intensities Based on the $X_{\alpha}$ Scattered Wave Method	95
	A. Application of Density Matrices to Optical Absorption	95
	B. Symmetry and Degeneracy	106
	C. Commutation Relations, Local Fields, and the $\vec{V}V$ Formalism	111
VII.	Applications of the $\vec{V}V$ Form of the Oscillator Strength in the $X_{\alpha}$ Scattered Wave Method	120
	A. Test Cases	120
	1. Hydrogen Molecular Ion	120
	2. Hydrogen Molecule	128
	3. Carbon Monoxide Positive Ion	135
	B. Transition Metal Complexes	139
	1. Permanganate	141
	2. Iron Tetrachloride	153
	3. Cobalt Tetrachloride	161
	4. Chromium Hexacarbonyl	165
VIII.	Conclusions	178
IX.	Suggestions for Further Work	182
X.	Appendix A- Listing and Description of the Computer Program	188
	Appendix B- Detailed Derivation of Matrix Element Formulae in the $\vec{V}V$ Formalism	236

<u>Chapter Number</u>		<u>Page Number</u>
	Appendix C- Relation of the Molar Extinction Coefficient $\epsilon_m$ and the Oscillator Strength $f$ to the Ab- sorption Coefficient $\eta$	243
	Appendix D- Photoemission using the $\bar{V}V$ Formalism	245
	References-	247
	Biographical Note-	253

## LIST OF FIGURES

<u>Figure Number</u>		<u>Page Number</u>
1	$\text{MnO}_4^{-1}$ Energy Levels	152
2	$\text{FeCl}_4^{-1}$ Energy Levels	160
3	$\text{Cr}(\text{CO})_6$ Energy Levels	173
4	Vibrational Overlap in Vibronic Transitions	174

## LIST OF TABLES

<u>Table Number</u>		<u>Page Number</u>
1	Oscillator Strengths in Several Light Ions	33
2	Oscillator Strengths in Alkali Atoms	34
3	Hartree-Fock Electronic Oscillator Strengths for Some 13 Electron Systems	40
4	$H_2^+$ Optical Properties - Oscillator Strengths	124
5	$H_2^+$ Energy Eigenvalues	126
6	$H_2^+$ Optical Properties - Comparison of Oscillator Strengths by Scattered Wave Method with Gaussian Results	127
7	$H_2$ Optical Properties	132
8	$CO^+$ Oscillator Strengths	138
9	$MnO_4^{-1}$ Energy Levels by the $X_\alpha$ Scattered Wave Method with Non-Overlapping Spheres	148
10	$MnO_4^{-1}$ Optical Properties	149
11	Comparison of $X_\alpha$ Theory $f(\vec{V})$ Intensities with the $f$ values of Mortola and Coworkers for $MnO_4^{-1}$	150
12	Amplitude for $1t_1 \rightarrow 2e$ (col. 1 $\rightarrow$ col. 2) in $MnO_4^{-1}$	151
13	Energy Levels in $FeCl_4^{-1}$	156
14	$FeCl_4^{-1}$ Optical Properties	157
15	Optical Properties of $FeCl_4^{-1}$ from the Work of Averill and Ellis	159

<u>Table Number</u>		<u>Page Number</u>
16	$\text{CoCl}_4^{-2}$ Optical Properties	164
17	$\text{Cr}(\text{CO})_6$ Energy Levels	170
18	$\text{Cr}(\text{CO})_6$ Optical Properties	172
19	Symmetry Information for $T_d$ Group	176



### Acknowledgments

This work would have been an almost impossible undertaking without a great deal of help from many people. The author is particularly indebted to Professor Keith Johnson for his guidance and encouragement. The author is also grateful to Chiang Yang, Carl Russo, Nick DeCristoforo and Professor Roy Kaplow for many stimulating discussions.

Discussions with the thesis review committee, consisting of Professors Rose and Gatos, and Dr. Messmer of the General Electric Company, were very useful, especially in appreciating the broader implications of this work. An additional note of thanks is due Dr. Messmer for his contributions to the work on oscillator strengths, done in collaboration with Dr. D. Salahub.

The author thanks Dagmar Hon for typing the rough draft, and Stephanie Lowe, Maureen Forte and Pat McSweeney for their work on the final draft. This work was financed through a National Science Foundation Grant administered through the M.I.T. Department of Materials Science and Engineering, and in part by the Shell Foundation, and the General Electric Research Foundation.

My parents' encouragement is deeply appreciated. Finally, I want to thank Miss Carol Giorgetti, whose warmth, support, and love have brought me through many troubled times.

## CHAPTER I

## INTRODUCTION

In the history of modern physics, the complexities of optical spectra in atoms and molecules have played a major role. The appearance of discrete spectral lines in atoms contradicted classical radiation theory and led to the development of quantum mechanics.<sup>1</sup> The first major success of the theory was then in understanding atomic multiplet structure.<sup>2</sup> The fields of atomic and molecular spectroscopy have expanded enormously since this time, but many problems still persist. In particular, the calculation from first principles of excitation energies in molecules is still a difficult task. Even more difficult is the accurate determination of theoretical absorption intensities.<sup>3</sup>

On the other hand, reliable calculations of spectral intensities in molecules would be very valuable. Such calculations would establish spectral assignments which were uncertain due to overlapping bands, or due to errors in calculated excitation energies. These spectral assignments, in turn, can yield valuable information about the bonding

and reactivity of different states (ground and excited) of the molecule.<sup>4</sup>

We are also interested in such issues as the comparative intensities of dipole allowed and vibrationally induced (vibronic) transitions, and the effects of the molecular environment on spectral intensities. In addition, since experimental measurements of absolute intensities are often difficult, further theoretical progress may stimulate new experimental efforts in this area.<sup>3</sup>

To solve these problems, a new theoretical framework for determining optical absorption intensities in molecules was developed based on the  $X_\alpha$  scattered wave method.<sup>5,6</sup> This new approach was applied to a series of systems from simple diatomic molecules like  $H_2^+$  and  $H_2$  to transition metal complexes, with emphasis on the latter. We will calculate the intensities of electric dipole allowed transitions in these molecules. We will also discuss transitions which become dipole allowed via molecular vibrations.<sup>7</sup> We will not treat higher order multipole transitions and spin forbidden transitions which generally have much lower intensities.<sup>4</sup>

A theory of spectra based on a molecular orbital approach has a wide range of applicability.<sup>8,9</sup> Localized states in solids (for example, impurity states and exciton states in semiconductors) or localized states at surfaces (in the neighborhood of a chemisorptive bond) may be represented in a molecular orbital framework through the use of a small

cluster of atoms. Many important systems of this type contain transition metal atoms coordinated at least in part by non-metallic ligands. In addition, the active centers of many biological macromolecules (hemoglobin, myoglobin, and cytochromes) also contain transition metal atoms coordinated by non-metallic ligands. For example, the biological molecules just mentioned all contain a heme complex in which an iron atom is coordinated by a planar array of four nitrogen atoms, with a fifth ligand which attaches the heme complex to a protein polypeptide chain below this plane, via an amino acid. In the case of hemoglobin, any one of a number of ligands ( $O_2$ , CO, NO, and so on) may be attached to the complex. Many of the systems cited above have interesting optical properties. For example, metallic impurities such as Cu, Ag, Au, and Mu may be introduced substitutionally into a host lattice of ZnS and CdS to produce specific luminescence bands (Cu impurities in ZnS produce green and blue emission bands, for instance). In myoglobin, CO chemisorbed on the heme complex may be photo-desorbed with ultraviolet light.<sup>10</sup> An analysis of spectral assignments and intensities in such systems would be valuable, and will be the subject of future work. For the present, we note that these systems are closely related to the transition metal complexes we will study.

One further topic for future work should be mentioned -- photoemission. Once a reasonable model for the final (continuum) states is obtained, the methods developed here

are applicable to determining photo-emission intensities in molecules and clusters. The author's preliminary attempts to evaluate photo-emission intensities in  $\text{CH}_4$  are described in Appendix D. Suggestions for future approaches in this area are presented in Chapter 9.

The organization of the work is as follows. A summary of the previous experimental and theoretical work on optical intensities is given in Chapters II and III. In Chapter IV, we discuss the conventional theoretical methods for treating intensities, and the problems these methods encounter especially in complex systems. In Chapter V, the  $X_\alpha$  scattered wave theory of electronic structure is presented. This theory was developed by Slater and Johnson as an alternative to the conventional configuration interaction (CI) and Hartree-Fock LCAO (linear combination of atomic orbitals) theories for electronic structure.<sup>3,5,6,11</sup> We present our new approach for calculating intensities in Chapter VI, and we apply this method to simple molecules and to transition metal complexes in Chapter VII. Chapters VIII, IX, and X contain our conclusions, suggestions for future work, and appendices respectively.

We can gain perspective on the comparative accuracies of the various theories of electronic structure by considering the problem of evaluating excitation energies in molecules. The results will be suggestive of the value of the different theories for determining optical intensities.

The conventional Hartree-Fock theory uses a single

determinantal wave function to find the many electron eigenstates and energies of a system.<sup>3</sup> The spin orbitals of a single determinant are varied to obtain the minimum total energy for a particular state. Therefore, as applied rigorously, separate variational calculations are required for initial and final state wave functions  $\psi_m$  and  $\psi_n$ . Yet even in rigorous form the Hartree-Fock theory predicts total energies in molecules to about 2ev. accuracy, which is often insufficient for problems of chemical interest. In complex molecules, such as those containing transition metal atoms, various approximations are required, and excited states are evaluated using the inaccurate virtual orbital theory.<sup>11</sup> A further analysis of Hartree-Fock theory and the approximations made to implement it is given in Chapter IV.

The method of configuration interaction (CI) utilizes a linear combination of determinants to describe the many electron wave functions and energies of the initial and final states.<sup>3</sup> This more accurate method yields excitation energies accurate to within less than 1ev. in simple molecules like CN, but the method is intractable in complex systems (see Chapter IV).

More recently, the  $X_\alpha$  scattered wave method has been developed to calculate electronic properties in both simple and complex molecules.<sup>5,6</sup> The  $X_\alpha$  method is based on a statistical expression for the total energy of a system. As a consequence, it is not necessary to assume a particular

form for the many electron wave functions in the theory. In addition, a local exchange term is used in the expression for the molecular total energy, unlike the more complex non-local exchange of Hartree-Fock theory. The  $X_\alpha$  theory yields accurate excitation energies (to less than 1 eV.) and accurate molecular potential energy curves in most cases.<sup>8</sup>

In view of these successes, the  $X_\alpha$  theory provides a good basis for a theory of optical intensities. A comparative study of intensities over the range of systems we have chosen should reveal which errors are intrinsic to the approximation methods used, and which arise only in the more complex systems.

Progress in evaluating intensities in transition metal complexes is particularly desirable.<sup>4,12</sup> The current theoretical situation in this area is very unsatisfactory. Of the various approximate Hartree-Fock calculations on transition metal complexes, only the intensity results of Van der Avoird and Ros on  $\text{CuCl}_4^{2-}$  are in relative agreement with the experimental values (that is, the theoretical and experimental intensities are related by a single proportionality constant).<sup>13,14</sup> Since this calculation does not predict excitation energies accurately, its validity for evaluating intensities is doubtful. In no case do the experimental and theoretical intensities agree in absolute value. For many cases, theoretical intensities in relative agreement with experiment would be sufficient to clarify spectral assignments,

and to determine the various types of optical absorption occurring in a system.

We now consider briefly the theory of optical intensities. Absorption intensities in molecules are generally given in terms of the absorption oscillator strength  $f$  which is defined as<sup>15</sup>

$$1.1) \quad f = \frac{2m\Delta E}{3\hbar^2 d_m} \sum_{i,k} |\langle \psi_{m_k} | \sum_{j=1}^N \vec{x}_j | \psi_{n_i} \rangle|^2 = \frac{2m\Delta E}{3\hbar^2 d_m} \cdot S$$

In this equation,  $d_m$  is the initial state degeneracy,  $\psi_{m_k}$  and  $\psi_{n_i}$  the initial and final state many particle wave functions,  $\Delta E$  is the excitation energy for the transition, and the sum over  $i, k$  goes over all degenerate partners of the initial and final states. The matrix element is expressed in Dirac notation, with the integration being over the nuclear as well as the electronic coordinates. The vector  $\vec{x}_j$  is the position vector of electron  $j$ .  $N$  is the total number of electrons in the system.  $f$  is a measure of the amount of energy absorbed per unit energy input to the molecule.  $S$  is called the absolute line strength. It is a more symmetrical quantity than  $f$ , and is easily related to the spontaneous emission probability from the upper state  $\psi_n$  to the lower state  $\psi_m$ , to the corresponding radiative lifetime of the excited state, as well as to the stimulated emission oscillator strength. These relations were formulated by Einstein.<sup>16,17</sup> Since all these quantities are interrelated, the measurement of any one of them is sufficient to obtain the absorption oscillator strength.



Although  $f$  is generally defined in terms of a matrix element of the position operator  $\vec{x}$ , equivalent definitions for exact wave functions may be formulated in terms of the momentum operator  $-i\hbar\vec{\nabla}$ , or the gradient of the one electron potential  $-\vec{\nabla}V$ .<sup>3</sup> In the scattered wave method,  $f(\vec{\nabla}V)$  assumes a particularly simple structure, and we have therefore used this form exclusively for our calculations. The  $f(\vec{\nabla}V)$  form, however, is generally thought to be unreliable for use with approximate wave functions.<sup>18</sup> An additional purpose of the present study is then to evaluate the accuracy of  $f(\vec{\nabla}V)$  compared with the other forms of  $f$ .

The many particle wave functions  $\psi_m$  and  $\psi_n$  include a factor dependent on the respective vibrational sublevels  $v'$  and  $v''$ . In the Born Oppenheimer approximation<sup>19</sup>

$$1.2) \psi_m = \psi_m^{el}(1, 2, \dots, N, R_1 \dots R_M) \psi_{v'}(\vec{R}_1 \dots \vec{R}_M)$$

$\psi_m$  is factored into an electronic part which depends parametrically on the nuclear positions  $R_1 \dots R_M$ , and into a second part which is simply the vibrational wave function for sublevel  $v'$ . The electronic coordinates  $1, 2, \dots, N$  include the spin coordinates, and the previous integration therefore includes sums over spin coordinates.<sup>5</sup> In principle, then, it is necessary to know both the vibrational and electronic wave functions to evaluate the oscillator strength  $f_{v', v''}$  between specific vibrational sublevels. As we shall see in Chapter IV, an approximate value for  $f$  summed over  $v''$  sublevels and averaged over  $v'$  sublevels may be found by evaluating  $\psi_m$  and  $\psi_n$  at

the equilibrium nuclear positions, and integrating only over electronic coordinates in equation 1.1. Only the electronic parts of the wave functions are used in this case. The result is a measure of the total area under an absorption curve (for absorption versus frequency) for a single electronic transition.<sup>7,15</sup> The  $f_{v',v''}$  appears as the vibrational superstructure of the peak.<sup>20</sup> In the present work, we will concentrate on obtaining the total  $f$  values for electronic transitions. For some molecules, we will evaluate  $f$  at different internuclear distances, but not at a sufficient number of points to directly evaluate  $f_{v',v''}$ . This would be an especially difficult task in polyatomic molecules, since the number of data points required goes up as the power of the number of normal mode coordinates. In diatomic molecules, the vibrational wave functions may be evaluated using the experimental Rydberg-Klein-Rees potential curves.<sup>3</sup> In polyatomic molecules, one similarly attempts to match force constants to the observed vibrational frequencies, and then compute the vibrational wave functions. This is again more difficult than in the diatomic case.<sup>21</sup>

In diatomic molecules, it is often the practice to obtain the "experimental"  $f$  value at equilibrium nuclear separation  $R_e$  from a set of measured radiative lifetimes between vibrational sublevels  $t_{v',v''}$ . (An example of this is found in the Popkie and Henneker "experimental"  $f$  values for some simple diatomics discussed in Chapter 2.)<sup>22</sup> The present discussion of diatomics forms a basis for the more

general discussion of vibrational effects on spectra developed in Chapter IV. Let the internuclear distance for the diatomic be  $R$ . Then<sup>22</sup>

$$1.3) f(R_e) = \frac{2m\Delta E}{3\hbar^2} \frac{S(R_e)}{d_m}$$

$$1.4) S(R) = \sum_{i,k} |\langle \psi_{m_k}^{el} (1\dots N, R) | \sum_{j=1}^N \vec{x}_j | \psi_{n_i}^{el} (1\dots N, R) \rangle|^2 \\ = \sum_{i,k} |\vec{M}_{ik}(R)|^2$$

$$1.5) f_{v',v''} = \frac{2m}{3\hbar^2} \frac{\Delta E}{d_m} \sum_{i,k} |\langle \psi_{v'}(R) | \vec{M}_{ik}(R) | \psi_{v''}(R) \rangle|^2$$

The integration in equation 1.4 is only over electronic coordinates; in equation 1.5, only the internuclear distance  $R$  is integrated over.  $M(R)$  is the transition moment. Equations 1.3 and 1.4 are definitions. Equation 1.5 then follows from equation 1.1.  $f_{v',v''}$  is directly related to the measured lifetime between vibrational sublevels  $t_{v',v''}$ . To invert the data and obtain  $f(R_e)$ , the functional form for  $M(R)$  must be found. It is perfectly general to expand  $M(R)$  as a Taylor series<sup>7,22</sup>

$$1.6) M(R) = \sum_i M_i R^i$$

One must then assume a specific polynomial form for  $M(R)$  (for example, a quadratic form) to determine  $f(R_e)$ . Accurate vibrational wave functions for the states are also required.

From a theoretical point of view, the evaluation of the electronic oscillator strength at fixed nuclear position

$f(R)$  in the case of a diatomic molecule requires a knowledge only of the electronic parts  $\psi_m$  and  $\psi_n$  of the total wave

function. The conventional theories of electronic structure outlined at the beginning of the chapter are used to obtain approximate forms for the electronic wave functions. However, a theory of optical properties using many electron wave functions is inappropriate for the  $X_\alpha$  scattered wave theory.<sup>5</sup> A new density matrix approach to optical absorption was therefore developed by the author which is better adapted to the concepts of the  $X_\alpha$  scattered wave theory (Chapter VI).

A final problem of interest is the dependence of optical absorption in molecules on the surrounding environment. The environment effects optical absorption in two ways.<sup>7,20,23</sup> 1) Specific molecular interactions alter the states (both ground and excited) of the absorbing molecule. A detailed knowledge of the boundary conditions appropriate to a given environment is therefore necessary to determine the molecular eigenstates and the associated oscillator strengths. 2) The electromagnetic wave incident on a material is modified by the medium surrounding an absorbing molecule (local field effects). This implies that equation 1.1 for the absorption intensity is not correct.

These effects are most significant in solution spectra, where the absorbing molecule is embedded in a fairly dense medium.<sup>7,23</sup> In the case of ions in solution (or ionic crystals), the additional problem of how the oppositely charged ions interact, and how these ions interact with the electromagnetic field is introduced. In vapor spectra, where the density of the medium is low, these problems are not

important. We will discuss boundary conditions and local field effects in detail in Chapter IV, though many problems remain unsolved.

In conclusion, the difficulties in obtaining reliable absorption oscillator strengths are formidable. In view of its previous success, the  $X_\alpha$  scattered wave theory is a good prospect for further advances on this problem.

## CHAPTER II

## EXPERIMENTAL BACKGROUND

First we consider experimental intensities for atoms. For light atoms and ions, oscillator strengths may be obtained by the accurate beam foil method developed by Bashkin and co-workers.<sup>24</sup> In this method, ions are sent through a thin foil of carbon. In the process, the ions may be excited, ionized further, or neutralized. A measurement of the resulting radiative lifetime  $\tau$  of the excited state then yields an oscillator strength generally accurate to 3-11%, better than any other method used.<sup>25</sup> A number of authors have applied this technique to the ions  $C^+$ ,  $N^+$ ,  $F^+$ , and  $Ne^+$  (see Table 1).<sup>26-29</sup> There is good agreement among the various experimental results.

Experimental  $f$  values have also been obtained by several workers for  $s \rightarrow p$  transitions in the alkali atoms Li, Na, and K.<sup>30</sup> For lithium, Anderson and co-workers have used the beam foil technique.<sup>31</sup> Link has used an accurate fluorescence method to obtain the Li  $2s \rightarrow 2p$ , Na  $3s \rightarrow 3p$ , and K  $4s \rightarrow 4p$  oscillator strengths.<sup>32</sup> Other less reliable methods have also been used

to obtain  $f$  values in these atoms. Ellis and Goscinski have summarized the different experimental intensities for alkali atoms, including the estimated uncertainties in the experimental values (see Table 2).<sup>30</sup> Some of the uncertainties are quite large (for example, Na  $4s \rightarrow 4p$  and K  $5s \rightarrow 5p$ ).

We now consider experimental intensities in some simple molecules. The intensities for the two lowest bands in  $H_2$  are not available from experiment, since the lowest lying Lyman band ( $X^1\Sigma_g \rightarrow B^1\Sigma_u$ ) overlaps the higher Werner band ( $X^1\Sigma_g \rightarrow C^1\Pi_u$ ).<sup>33</sup> The experimental  $f$  value for the sum of the two bands is roughly 0.65 as determined by Mulliken and Rieke from dispersion measurements for hydrogen gas.<sup>7,34</sup> This is only a rough estimate of the true  $f$  value.

Extensive measurements have been made of radiative lifetimes in the 13 electron systems  $C_2^-$ ,  $N_2^+$ , CN, and  $CO^+$ .<sup>35</sup> "Experimental" oscillator strengths are obtained by an analysis of the radiative lifetimes between vibrational sublevels  $t_{v',v''}$ . Popkie and Henneker's "experimental"  $f$  values (at the ground state equilibrium nuclear separation  $R_e$ ) are given in Table 3.<sup>22</sup> As discussed in Chapter I, the  $t_{v',v''}$  data may be inverted to obtain  $f$  (experiment) only if a specific functional form for the transition moment  $M(R)$  is assumed. There are, in addition, substantial problems in measuring the radiative lifetimes in these systems.<sup>35</sup> Since the lifetimes are in the 10 microsecond region, there is sufficient time for de-excitation by collisions with other molecules. For

example,  $N_2^+$  may de-excite when colliding with neutral  $N_2$ , either by a change of the vibrational state of  $N_2^+$  or by electron transfer. As a result, measured lifetimes often differ by a factor of two or more.<sup>35,36</sup> The experimental inaccuracies are indicated by the two different  $f$  values for  $N_2^+$  in Table 3.<sup>22</sup>

Johnson, Capelle, and Broida have measured the radiative lifetimes  $t_{ov}$  of AlO by fluorescence with a pulsed tunable dye laser.<sup>37</sup> An  $f_{oo}$  value of 0.021 was obtained, which will be compared with the theoretical value in Chapter 3. These workers have found that the radiative lifetimes of AlO using this method are independent of the vapor pressure of the gases (including the AlO vapor pressure) in the observation chamber. This indicates that collisional quenching (the collisional de-excitation of a molecule, such as in the  $N_2^+$  case) is negligible. Since this is the source of much of the error in measuring radiative lifetimes, we may conclude that the AlO lifetimes are reasonably accurate.

In contrast to many of the previous examples, oscillator strengths in transition metal complexes are generally measured directly via the absorption intensities rather than by means of radiative lifetimes. There are still problems in measuring absolute spectral intensities, and, in addition, these intensities are often dependent on the surrounding medium. We will, therefore, find it necessary to specify the medium in discussing optical intensities in these systems.



$\text{MnO}_4^{-1}$  is a tetrahedrally coordinated molecule which may appear either as a component of an ionic crystal or as an anion in solution.<sup>9</sup> The molecule has a characteristic purple color which is associated with an absorption band of oscillator strength  $f=0.03$  occurring in the green part of the spectrum  $\Delta E=2.3$  ev.<sup>9,11</sup> Permanganate also has a weak Van Vleck type paramagnetism indicating a closed shell electronic structure for the ground state. Crystalline  $\text{KMnO}_4$  has an orthorhombic structure, with each unit cell consisting of four  $\text{K}^+$  and four  $\text{MnO}_4^{-1}$  ions.<sup>38</sup> X-ray diffraction measurements on this structure have established that the manganese-oxygen distance is between  $1.54\text{\AA}$  and  $1.63\text{\AA}$ .<sup>39,40</sup> For most of our calculations (Chapter VII), the intermediate value found by Mooney of  $1.59\text{\AA}$  will be used.<sup>38</sup>

Holt and Ballhausen have measured the optical absorption of a dilute solid solution of  $\text{KMnO}_4$  in  $\text{KClO}_4$ .<sup>41</sup> They found three bands at 2.3, 4.0, and 5.5 ev., and a weaker shoulder at 3.5 ev. However, they did not report absolute band intensities, so we have used the earlier experimental intensities of Tetlow (1938-1939) on the same solid solution in Table 10.<sup>42</sup> The bands at 3.5 ev. and 4.0 ev. are unresolved in Tetlow's measurements, so the intensities have been assigned in the proportions found from the Holt and Ballhausen spectrum. The resulting spectral intensities are necessarily approximate. Den Boef and co-workers (1958) have measured the intensity of the 2.3 ev. band for  $\text{KMnO}_4$  in aqueous solution, and have found substantial

agreement with Tetlow's value.<sup>43</sup> This would indicate, on a preliminary basis, that permanganate absorption is not strongly dependent on the surrounding environment. However, this proposition should be checked by measuring absorption spectra in various crystalline environments and solutions. This is particularly important since both the den Boef and Tetlow measurements are quite old. In the isoelectronic chromate ion  $\text{CrO}_4^{-2}$ , the oscillator strength for the lowest energy dipole allowed transition is  $f=0.08$  compared with  $f=0.03$  for the same transition in  $\text{MnO}_4^{-1}$ .<sup>44</sup> This suggests that the  $\text{MnO}_4^{-1}$  intensities are very sensitive to the precise form of the wave functions. This will be an important point in our later discussion of the  $\text{MnO}_4^{-1}$  spectrum.

$\text{FeCl}_4^{-1}$  is a tetrahedrally coordinated complex with high net spin ( $S=\frac{+5}{2}$ ).<sup>4</sup> The Fe-Cl bond length is  $2.196\text{\AA}$ .<sup>45</sup> Bird and Day have measured the absorption spectrum of this system, and found four peaks of moderate intensity ( $f=0.07-0.28$ , see Table 14).<sup>4</sup> For these experiments, samples of  $\text{FeCl}_4^{-1}$  anions were prepared as tetramethylammonium  $\text{N}(\text{CH}_3)_4^+$  and tetraethylammonium  $\text{N}(\text{C}_2\text{H}_5)_4^+$  salts which were then dissolved in ethanol. Spectra were measured at  $77^\circ\text{K}$ . At this temperature, a rigid glass was obtained containing a dilute solution of  $\text{FeCl}_4^{-1}$  anions. An excess of chlorine ions is required to suppress the reaction of the  $\text{FeCl}_4^{-1}$  with the solvent (solvolysis). The glass often cracks, which introduces errors into the spectrum. In addition, the effects of the medium on the

spectral intensities in this rather complex system remain unresolved.

The electronic structure of  $\text{CoCl}_4^{-2}$  is similar to the  $\text{FeCl}_4^{-1}$  structure, except for the addition of 2 electrons to d orbitals which are unoccupied in  $\text{FeCl}_4^{-1}$ .<sup>4</sup> The chlorine tetrahedron in the  $\text{CoCl}_4^{-2}$  complex is known to be distorted.<sup>46</sup> The experimental Co-Cl bond distance is 2.28Å.<sup>47</sup> The net spin in this system is  $S = \frac{+3}{2}$ .<sup>4</sup> Three spectral peaks have been found at low energy  $\Delta E = 0.4, 0.7,$  and  $1.8 \text{ ev.}$  due to d→d crystal field transitions.<sup>48-50</sup> The peak intensities for the last two are extremely small  $f = 7.2 \times 10^{-4}$  and  $5.1 \times 10^{-3}$  (see Table 16).<sup>48,49</sup> The peak intensity at  $\Delta E = 0.4 \text{ ev.}$  has not been measured, but is thought to be small and dependent on the amount of tetragonal distortion of the  $\text{CoCl}_4^{-2}$  complex.<sup>50</sup> The spectral measurements discussed above are due to Cotton and co-workers, Ferguson, and Quinn and Smith. Day and Jorgensen have found a transition of moderate intensity at higher energy,  $f = 0.065$  at  $\Delta E = 5.3 \text{ ev.}$ <sup>47</sup> Most of these workers made measurements on tetra-alkylammonium salts either in pure crystalline form or in ethanol solution. In these cases, the  $\text{CoCl}_4^{-2}$  environment is similar to the  $\text{FeCl}_4^{-1}$  environment in the experiments of Bird and Day. The experimental errors encountered in  $\text{CoCl}_4^{-2}$  are therefore similar to those found in  $\text{FeCl}_4^{-1}$ .

Beach and Gray have measured the spectral intensities of the octahedral complex  $\text{Cr}(\text{CO})_6$  in both vapor form and in

solution (see Table 18).<sup>51</sup> The Cr-C and C-O internuclear distances are  $1.92\text{\AA}$  and  $1.13\text{\AA}$  respectively.<sup>52</sup> There are five major spectral peaks at 3.91, 4.44, 4.83, 5.48, and 6.31 eV., with a smaller intensity peak at 3.69 eV.<sup>51</sup> Transitions at 3.59 and 3.91 eV. cause the photo-dissociation of neutral CO from  $\text{Cr}(\text{CO})_6$ .<sup>52</sup> Where comparisons are available, solution spectra of  $\text{Cr}(\text{CO})_6$  in EPA (a mixture of ethanol, isopentane, and ethyl ether) yield intensities which are lower than the vapor spectra values by 40-50% (with both sets of measurements being made at  $300^\circ\text{K}$ ). This is a clear case where the molecular environment strongly affects spectral intensities.

## CHAPTER III

## PREVIOUS THEORETICAL WORK ON OPTICAL INTENSITIES

## ATOMS

In Table 1, we give the comparative results of Hartree-Fock theory, Sinanoglu's many electron theory (a type of CI theory), and experiment for the oscillator strengths of the ions  $C^+$ ,  $N^+$ ,  $F^+$ , and  $Ne^+$ .<sup>25-29</sup> While there is good agreement between many electron theory and experiment, about a 10% discrepancy, the Hartree-Fock results are too high by a factor of 2-3. This shows that the Hartree-Fock theory does not give accurate absolute intensities even in simple systems.

Ellis and Goscinski have reported oscillator strengths for Li, Na, and K by the  $X_\alpha$  method.<sup>30</sup> These have been compared with a summary of experimental  $f$  values and with the Hartree-Fock values. The  $X_\alpha$  calculated intensities are in good absolute agreement with experiment, the average error being 5.12% (with the Latter correction potential), versus 14.7% for the Hartree-Fock method. The transition state was used to find the  $X_\alpha$  orbitals for the calculation, and the oscillator strength was evaluated using the length form.

(See Chapters 5 and 6 for a thorough discussion of these concepts.) The  $X_\alpha$  oscillator strengths are presented in Table 2.

The oscillator strengths labeled  $f(X_\alpha)$  in Table 2 are calculated using the standard  $X_\alpha$  orbitals. The orbitals  $f(X_\alpha, \text{Latter})$ , however, were computed using the Latter correction for the potential, which is defined as follows.<sup>30</sup> At small and intermediate distances the standard  $X_\alpha$  potential is used. At large distances  $r \geq r_0$ ,  $V(r) = \frac{-2(Z-N+1)}{r}$ , where  $Z$  is the nuclear charge, and  $N$  the number of electrons in the atom. When an electron is far away from the nucleus, its potential is assumed to be purely electrostatic as given in the formula above. The distance  $r_0$  is fixed by requiring the continuity of  $V(r)$ . It is known that many important consequences of the  $X_\alpha$  theory no longer hold when the Latter correction potential is used.<sup>53</sup> In particular, the virial theorem which is satisfied both in the  $X_\alpha$  theory and in an exact theoretical framework, fails upon application of the Latter correction potential. For these reasons, we will use the standard  $X_\alpha$  theory without the Latter correction in our own calculations. From Table 2, the accuracy of the two theoretical approaches is comparable, except that  $f(X_\alpha)$  seems to display a larger error for very small intensities  $f < 0.01$ . The evaluation of  $X_\alpha$  oscillator strengths for atoms is elementary when compared with the general formulation for determining intensities in polyatomic molecules which is

developed in Chapter VI.

It would also be valuable to widen the range of atomic systems for which  $X_\alpha$  oscillator strengths are available. Alkali atoms, having only a single electron outside a closed shell, are very simple systems from a quantum theoretical point of view. (This is evident if one compares the accuracy of the Hartree-Fock intensities for the alkali atoms with the accuracy of the Hartree-Fock values for the ions  $C^+$ ,  $N^+$ ,  $F^+$ , and  $Ne^+$ . By this criterion, the light ions are more complicated in structure than the alkali atoms.) There are, therefore, far more critical tests of the  $X_\alpha$  intensities for atoms than those which have been considered so far.

Table 1  
Oscillator Strengths in Several Light Ions<sup>a</sup>

	Transitions	f (Hartree-Fock)	f(MET)	f(experiment)
CII	$2p^2 \ ^2P \rightarrow 2p^2 \ ^2D$	0.263	0.125	0.114
NII	$2p^2 \ ^3P \rightarrow 2p^3 \ ^3D$	0.236	0.100	0.101, 0.109
NII	$2p^2 \ ^3P \rightarrow 2p^3 \ ^3P$	0.170	0.137	0.131
FII	$2p^4 \ ^3P \rightarrow 2p^5 \ ^3P$	0.322	0.140	
NeII	$2p^5 \ ^2P \rightarrow 2p^6 \ ^2S$	0.176	0.073	0.035, 0.055

(MET is Sinanoglu's many electron theory.)

<sup>a</sup> Reference 25.



Table 2  
Oscillator Strengths in Alkali Atoms<sup>a</sup>

Transition	$f(x_\alpha)$	$f(x_\alpha, \text{Latter})$	Experimental $f$
Li 2s→2p	0.7529	0.7629	0.75 ± 0.01
2s→3p	0.00125	0.00479	0.0055 ± 0.0002
3s→2p	0.2612	0.3269	0.345 ± 0.035
3s→3p	1.1019	1.1615	1.23 ± 0.12
Na 3s→3p	0.9305	0.9783	0.975 ± 0.04
3s→4p	0.01731	0.01319	0.0140 ± 0.002
4s→3p	0.4647	0.5089	0.489 ± 0.12
4s→4p	1.4004	1.4344	1.35 ± 0.34
K 4s→4p	1.0298	1.0542	0.99 ± 0.04
4s→5p	0.01618	0.0100	0.0089 ± 0.0001
5s→4p	0.5044	0.5492	0.55 ± 0.14
5s→5p	1.4742	1.5093	1.5 ± 0.75

( $f(x_\alpha)$  is the oscillator strength using the standard  $x_\alpha$  approximation.  $f(x_\alpha, \text{Latter})$  uses the  $x_\alpha$  approximation at small and intermediate distances, and the Latter correction at large distances.  $V(r) = \frac{-2(Z-N+1)}{r}$   $r \geq r_0$ , with  $Z$  the nuclear charge, and  $N$  the number of electrons.)

<sup>a</sup> Reference 30.

## SIMPLE MOLECULES

The simplest molecule is  $H_2^+$ , which has only one electron. Bates and co-workers have calculated the exact electronic wave functions of the  $1\sigma_g$ ,  $1\sigma_u$ , and  $1\Pi_u$  states in this system as a function of internuclear distance  $R$ , as well as the resultant  $f$  values.<sup>54,55</sup> Lamb, Young, and La Paglia have compared these  $f$  values with approximate linear combination of atomic orbitals (LCAO) and Gaussian lobe basis calculations.<sup>56</sup> The basis set of six Gaussians at each nucleus and one at the molecular midpoint allow for an accurate description of both excitation energies (with an error of less than 0.27eV.) and oscillator strengths. The simple LCAO results are distinctly inferior. In Table 6, the  $f$  values for the Gaussian basis are listed for three different forms  $f(\vec{x})$ ,  $f(\vec{V})$ , and  $f(\vec{x}, \vec{V})$  (the dipole length, momentum, and mixed forms of the oscillator strength -- the last being the geometrical mean of the first two forms). The exact  $f$  values of Bates and co-workers are also given in Table 6. Since there are no electron-electron interactions in  $H_2^+$ , this example allows one to evaluate the accuracy with which a known Schrodinger equation is solved by a given method. For the Gaussian basis method, the discrepancies between the different oscillator strength forms result from the truncation of the basis set (see Chapter IV). These discrepancies are significant for  $R \geq 3.0$  bohr radii. Similar truncation problems are encountered

in the  $X_\alpha$  scattered wave intensities (see Chapter 7, Section A). Although the Gaussian basis method yields a generally good description of intensities in  $H_2^+$ , it is still an LCAO method. Such methods have serious deficiencies in complicated systems.

The  $H_2$  molecule is a more complex system than  $H_2^+$ , since there is a single electron-electron interaction in this molecule. The appropriate configurations for the  $X^1\Sigma_g$  ground state, and the  $B^1\Sigma_u$  and  $C^1\Pi_u$  excited states are  $(1\sigma_g)^2$ ,  $(1\sigma_g 1\sigma_u)$ , and  $(1\sigma_g 1\Pi_u)$ .<sup>33</sup> Kolos and Wolniewicz have done very accurate CI calculations for these three states as well as the  $^3\Sigma_u(1\sigma_g \uparrow 1\sigma_u \uparrow)$  state, and  $f$  values for the bands were obtained.<sup>57</sup> Previously, Ehrenson and Phillipson used a simple CI wave function for the ground state and a self-consistent wave function for the  $1\sigma_g 1\sigma_u$  configuration to calculate the  $(1\sigma_g)^2 \rightarrow (1\sigma_g 1\sigma_u)$  oscillator strength.<sup>33</sup> The oscillator strength values from these calculations may be found in Table 7. The Kolos-Wolniewicz approach of calculating wave functions as explicit functions of the electron-electron distance has not been applied to systems with more than two electrons. Nonetheless, their calculations on  $H_2$  are among the most accurate to have been done on atomic and molecular systems.<sup>3</sup> The total theoretical  $f$  value for the two bands  $1_{\Sigma_g} \rightarrow 1_{\Sigma_u}$  and  $1_{\Sigma_g} \rightarrow 1_{\Pi_u}$  is 0.656, in good agreement with the less accurate experimental value  $f=0.65$ .

Popkie and Henneker have made an extensive study of diatomic molecules with 13 electrons ( $C_2^-$ ,  $N_2^+$ , CN, and  $CO^-$ ).<sup>22</sup> Optical intensities were obtained from the Hartree-Fock wave functions of Cade and co-workers.<sup>58</sup> These wave functions were obtained by separate determinantal calculations for the ground and excited states with an extensive basis set (rigorous Hartree-Fock method). The resulting Hartree-Fock oscillator strengths of Table 3 are about 3-5 times the experimental values. However, we have found that the formula in Popkie and Henneker's paper for  $f(\text{Hartree-Fock})$  is too large by a factor of 2 for  ${}^2\Pi \rightarrow {}^2\Sigma^+$  type transitions. (We discuss a general method for calculating the necessary degeneracy factor in Chapter VI.) Utilizing this correction, the Hartree-Fock  $f$  values are 1.5-5 times the experimental values. The largest discrepancy is in the  $B^2\Sigma_u^+ \rightarrow X^2\Sigma_g^+$  transition in  $N_2^+$  with  $f(\text{Hartree-Fock})=0.193$ ,  $f(\text{experiment})=0.038$ . The theoretical oscillator strengths of Table 3 were evaluated using the mixed form  $f(\vec{X}, \vec{V})$  which yields better results than  $f(\vec{X})$  or  $f(\vec{V})$  for these systems within the Hartree-Fock method; yet significant discrepancies exist between theory and experiment. In the current state of the problem, it is not clear whether the theoretical or the experimental  $f$  values have the larger error.

Very recently, M $\ddot{e}$ ssmer and Salahub have calculated the intensities of the  $1\Pi \rightarrow 5\sigma$  ( $X^2\Sigma^+ \rightarrow A^2\Pi$ ) and  $5\sigma \rightarrow 2\Pi$  ( $X^2\Sigma^+ \rightarrow 2\Pi_r$ ) transitions in  $CO^+$  using the  $X_\alpha$  method with overlapping

spheres (see especially Chapter V ).<sup>59</sup> The dipole length form of  $f$  was used in the calculation. The atomic wave functions were matched to approximate single center forms (Hankel functions) in the interatomic region. The integrations were then done explicitly over all regions of space to obtain the matrix elements (see Chapter VI C). These oscillator strengths  $f(\vec{x})$  are given in Table 8. (We should emphasize that in all atomic and molecular cases we report absorption oscillator strengths independent of whether measurements were made of emission processes or of absorption.) For the  $1\Pi \rightarrow 5\sigma$  transition, the  $X_\alpha$  theory  $f(\vec{x})$  value of 0.0088 may be compared with the Hartree-Fock  $f$  value of 0.0177 (uncorrected) and 0.0089 (corrected) as well as with the experimental  $f$  value 0.0056.<sup>22,59</sup> The  $X_\alpha$  scattered wave theory  $f$  value is very close to the rigorous Hartree-Fock result (corrected), the latter being evaluated with the mixed form of  $f$ . These theoretical results are in very good agreement with the experimental  $f$  value, especially in view of the uncertainty in the experimental value. For the  $5\sigma \rightarrow 2\Pi$  transition, the respective intensities are  $f(\text{Hartree-Fock})=0.105$  (uncorrected), 0.053 (corrected), and  $X_\alpha$  theory  $f(x)=0.048$ . Experimental intensities are not available for this transition. Messmer and Salahub found that the oscillator strength was very sensitive to the type of matching functions used, and that Hankel functions are superior to Bessel functions in the calculations.<sup>59</sup> The  $f(\vec{x})$  form in the  $X_\alpha$  theory has not as yet been applied to

more complex systems, so its overall value is still to be determined. These preliminary results are very encouraging. Later, we will compare these  $f$  values with the author's  $f(\vec{V})$  values on  $\text{CO}^+$  (Chapter VII A).

Michels has done a limited CI calculation for the  $B^2\Sigma^+ \rightarrow X^2\Sigma^+$  transition in  $\text{AlO}$ .<sup>60</sup> Using accurate vibrational wave functions, he has found an  $f_{00}$  value of 0.012. Johnson, Capelle, and Broida obtained an experimental  $f_{00}$  value of 0.021, or about 2 times the theoretical value.<sup>37</sup> Several CI calculations of intensities have been made on diatomic and triatomic molecules. Comparison with experimental intensities, where these are available, generally yields values of comparable accuracy to the  $\text{AlO}$  results.<sup>61,62</sup>

We may conclude that for diatomic molecules of moderate complexity, the accuracies of limited CI theory, the rigorous Hartree-Fock method, and the  $X_\alpha$  scattered wave method seem comparable. For very simple molecules like  $\text{H}_2$ , an extensive CI calculation is the best method, but this type of calculation is not easily generalizable to more complex systems. Further theoretical and experimental work is again necessary to clarify the situation.

Table 3

Hartree-Fock Electronic Oscillator Strengths for  
Some 13 Electron Systems.

Theoretical and experimental values given at ground state  
equilibrium separation  $R_e$ .<sup>a</sup>

Transition	$f^{\text{HF}}$	f(experiment)
$(A^2\Pi_u \rightarrow X^2\Sigma_g^+)$		
$C_2^-$	0.0166	
$N_2^+$	0.252	0.0029, 0.0064
$(B^2\Sigma_u \rightarrow X^2\Sigma_g^+)$		
$C_2^-$	0.224	
$N_2^+$	0.193	0.038
$(A^2\Pi_i \rightarrow X^2\Sigma^+)$		
CN	0.0168	0.0058
$CO^+$	0.0177	0.0056

<sup>a</sup> Reference 22.

Table 3  
(continued)

Configurations for these systems:<sup>b</sup>

$X^2\Sigma_g^+$	$1\sigma_g^2$	$1\sigma_u^2$	$2\sigma_g^2$	$2\sigma_u^2$	$3\sigma_g$
$A^2\Pi_u$	$1\sigma_g^2$	$1\sigma_u^2$	$2\sigma_g^2$	$2\sigma_u^2$	$3\sigma_g^2$
$B^2\Sigma_u^+$	$1\sigma_g^2$	$1\sigma_u^2$	$2\sigma_g^2$	$2\sigma_u$	$3\sigma_g^2$
$X^2\Sigma^+$	$1\sigma^2$	$2\sigma^2$	$3\sigma^2$	$4\sigma^2$	$5\sigma$
$A^2\Pi_i$	$1\sigma^2$	$2\sigma^2$	$3\sigma^2$	$4\sigma^2$	$5\sigma^2$

<sup>b</sup> Reference 3.



## TRANSITION METAL COMPLEXES

Permanganate has been studied theoretically by many workers, but the spectrum in this system (apart from the  $X_{\alpha}$  scattered wave results) is still not understood. Different spectral assignments have been made by Wolfsberg and Helmholz, Ballhausen and Liehr, Viste and Gray, and Mortola and co-workers.<sup>63-66</sup> All of these calculations were of the semi-empirical Hartree-Fock LCAO type. Fenske and Sweeney have computed  $f$  values based on the calculations of Ballhausen and Liehr (1958) and Wolfsberg and Helmholz (1952).<sup>12</sup> The results are highly unsatisfactory. For example, for the  $1t_1 \rightarrow 2e$  (oxygen  $2p \rightarrow$  manganese  $3d$ ) transition, the Ballhausen and Liehr intensity is 34 times the experimental value. The Ballhausen and Liehr calculation also indicates that the first band is more intense than the second and third bands combined, while the reverse is true. The Wolfsberg and Helmholz spectral assignment has the  $7t_2$  (manganese  $3d$ ) level as the lowest unoccupied state, lying below the  $2e$ . This contradicts both the prediction of crystal field theory for tetrahedral complexes, and the results of electron spin resonance measurements on  $\text{MnO}_4^{-2}$ .<sup>67,68</sup> The latter establish that the extra electron is in the  $2e$  level.

Recently, Mortola and co-workers (1973) have completed a self-consistent approximate Hartree-Fock calculation using a Gaussian basis set for  $\text{MnO}_4^{-1}$ .<sup>66</sup> A comparison of their

theoretical intensities with experiment is given in Table 11. The Gaussian wave functions do not yield correct relative intensities for the various bands. In particular, the  $1t_{1} \rightarrow 7t_{2}$  transition has a smaller intensity than either the  $1t_{1} \rightarrow 2e$  or the  $6t_{2} \rightarrow 2e$  in contradiction to the experimental band intensities. The commonly used dipole length oscillator strengths are much larger than the experimental  $f$  values, and the three different oscillator strength forms differ substantially. The disagreement of the different oscillator strength forms is a consequence of the non-local nature of the Hartree-Fock exchange potential (we will discuss this problem in Chapter VI), as well as of the limited basis set used in the calculations (this was discussed earlier in regard to the  $H_2^+$  intensities). The Mortola spectral assignments were obtained by using the formula

$$\Delta E_{ij} = \frac{\langle u_i | \nabla_x | u_j \rangle}{\langle u_i | x | u_j \rangle}$$

to find the excitation energy for the corresponding transition (excitation energies by virtual orbital theory are in error by 2.0-4.5ev., and are therefore unreliable). Such a procedure is not justified with a non-local exchange potential (see Chapter VI C).

In conclusion, the previous intensity calculations for  $MnO_4^{-1}$  have not clarified the spectral assignments, and these intensities bear no relation to the experimental spectral intensities.

Ellis and Averill have calculated excitation energies and intensities for  $\text{FeCl}_4^{-1}$  using the spin restricted  $X_\alpha$  method and the dipole length form of the oscillator strength.<sup>69</sup> As shown in Table 14, both the calculated intensities and the calculated excitation energies are in poor agreement with experiment. Their methods may be criticized on several grounds. 1) Their oscillator strength formula is wrong, and should be multiplied by the orbital degeneracy of the initial (lower) level  $q_{10}$ . This is why their intensities are too small as shown by the corrected values. 2) The spin restricted formalism is unreliable for  $\text{FeCl}_4^{-1}$ . The excitation energies have large errors, and the orbitals are highly spin dependent. Spin unrestricted calculations are required for high spin complexes like  $\text{FeCl}_4^{-1}$ . 3) An incorrect ground state configuration was used in the calculation. 4) Ground state orbitals and one electron energies rather than transition state orbitals and energies were used in the calculation. 5) The muffin tin approximation for the potential was used rather than the overlapping sphere approach. These issues will be discussed in Chapters V and VI. In view of these assumptions, the resulting inaccurate intensities and excitation energies should be expected. These errors are not intrinsic to  $X_\alpha$  scattered wave calculations on  $\text{FeCl}_4^{-1}$  (see Chapter VII).

Jaeger and Englman have calculated  $d \rightarrow d$  intensities in tetrahedral complexes using a crystal field model and including the temperature dependence of the intensity.<sup>70</sup>

$\text{CoCl}_4^{-2}$  was among the complexes considered. However, these authors conclude that the crystal field model is unreliable for determining intensities in these systems.

There have been no previous intensity calculations on the complex  $\text{Cr}(\text{CO})_6$ . Beach and Gray have made a semi-empirical LCAO calculation on  $\text{Cr}(\text{CO})_6$  using the assumption that the lowest energy band is due to the  $t_{2g} \rightarrow e_g$  (Cr 3d  $\rightarrow$  Cr 3d) transition.<sup>51</sup> We will analyze this assumption, and present our intensity calculations for this complex in Chapter VII.

Overall, little work has been done in evaluating spectral intensities in transition metal complexes. With the exception of the  $\text{CuCl}_4^{-2}$  calculation discussed in Chapter I, no useful information on electronic structure can be deduced from the previous oscillator strength values. As can be seen from the  $\text{FeCl}_4^{-1}$  results, a clear understanding of the  $X_\alpha$  method concepts is required to properly treat the problem with the  $X_\alpha$  approach. Because of the approximations required to implement the Hartree-Fock method on transition metal complexes, future progress on intensities with this method should be difficult (Chapter IV).

## CHAPTER IV

A CRITICAL DISCUSSION OF CONVENTIONAL THEORETICAL APPROACHES  
TO INTENSITIES

## CONFIGURATION INTERACTION THEORY

The configuration interaction theory is an approximate method for finding the many electron wave functions  $\psi^{el}$  of a system.

The many electron wave function of a molecule is a solution of the Schrodinger equation<sup>19</sup>

$$4.1) H(\vec{x}_1 \dots \vec{x}_N, \vec{R}_1 \dots \vec{R}_M) \psi(1, 2, \dots, N, \vec{R}_1 \dots \vec{R}_M) = E(\vec{R}_1 \dots \vec{R}_M) \cdot \psi(1, 2, \dots, N, \vec{R}_1, \dots, \vec{R}_M)$$

with  $H(\vec{x}_1 \dots \vec{x}_N, \vec{R}_1 \dots \vec{R}_M)$  the full many electron Hamiltonian at fixed nuclear position. (We suppress the superscript indicating an electronic wave function). As a consequence of equation 4.1 the total energy  $\langle \psi | H | \psi \rangle$  (integration only over electronic coordinates) is a minimum when the true many electron wave function is used in the expression. This is true for both ground and excited states. Given a complete, orthonormal set of spin orbitals  $w_1, w_2, \dots, w_\infty$ , a linear combination of determinants with coefficients  $c_i, \sum_i c_i D_i$  may

be formed to represent the wave function  $\psi$ .<sup>3</sup> One may vary the  $c_i$  to obtain the minimum total energy, and in the limit of an infinite number of terms, the true wave function results. In practice, expansions are limited to a few hundred configurations; each configuration is a linear combination of determinants satisfying the symmetry requirements of the many electron wave functions. In the most general form of the CI method, both the orthonormal basis set and the coefficients of the determinants are varied to obtain an approximate total energy and wave function. Various techniques, such as Sinanoglu's many electron theory, allow one to classify which configurations will be most important in the expansion, and thus to limit the number of configurations which must be considered.<sup>25</sup> CI methods are quite powerful for obtaining accurate wave functions, but the range of systems that can be treated is very limited. CI calculations are computationally prohibitive on molecules much larger than  $O_2$  and  $AlO$ .<sup>3,60</sup>

## HARTREE-FOCK LCAO THEORY

The Hartree-Fock theory is based on approximating the  $N$  electron wave function of an atomic or molecular system by a single determinant<sup>71</sup>

$$4.2) \quad \psi(1,2,\dots,N) = (N!)^{-\frac{1}{2}} A w_1(1) w_2(2) \dots w_N(N)$$

with  $A$  the antisymmetrizing operator. The one electron spin orbitals  $w_i$  are chosen to be orthonormal, and are factorizable as a space part times a spin part

$$4.3) \quad w_i(1) = \phi_i(\vec{x}_1) X_i(\sigma_1)$$

with  $X_i(\sigma_1) = \uparrow$  or  $\downarrow$  spinor function and  $\sigma_1$  the two valued spin variable  $\sigma_1 = +1, -1$ . By minimizing the expectation value of the total energy  $\langle \psi | H | \psi \rangle$  (in Dirac notation) with respect to a variation of the  $\phi_i$ , an optimum set of spin orbitals is obtained. The resultant spin orbitals  $w_i$  satisfy the Hartree-Fock equations

$$4.4) \quad H_{\text{eff}}(1)w_i(1) = \varepsilon_i w_i(1)$$

$$H_{\text{eff}} = -\nabla_1^2 - \sum_g \frac{2Zg}{|\vec{x}_1 - \vec{R}_g|} + \int d\nu_2 \sum_{\text{occupied } k} w_k^*(2) \frac{2(1-P_{12})}{|\vec{x}_1 - \vec{x}_2|} w_k(2)$$

in Rydberg units. The integration is over both space and spin coordinates. (In these units, energies are in Rydbergs, distances in bohr radii, and  $\frac{\hbar^2}{2m} = 1$ ). The index  $g$  denotes the various nuclei of the system. The operator  $P_{12}$  permutes the coordinates of electrons 1 and 2.

In the LCAO (linear combination of atomic orbitals) approach to solving molecular problems, the orbitals  $\phi_i$  are

approximated by a linear combination of orthonormal basis functions<sup>72</sup>

$$4.5) \quad \phi_i(\vec{x}) = \sum_{j=1}^M C_{ji} a_j(\vec{x}) \quad \begin{array}{l} i=1,2,\dots,N \\ j=1,2,\dots,M \text{ (M=size of the basis set)} \end{array}$$

Here the  $a_j(\vec{x})$  constitute a fixed atomic orbital basis set.

This leads to a set of self-consistent equations for the  $C_{ji}$  which must be solved iteratively. These are matrix equations of the general form<sup>11</sup>

$$4.6) \quad \sum_{j=1}^M (F_{rj} - \epsilon_i S_{rj}) C_{ji} = 0 \quad r=1,\dots,M$$

Non-trivial solutions for the  $C_{ji}$  exist when  $|F - \epsilon_i S| = 0$ . The solutions of this equation are a set of  $\epsilon_i$  from which the  $C_{ji}$  are then obtained. There are two difficulties: one is that the matrix elements  $F_{rj}$  depend on the charge distribution and consequently on the  $C_{ji}$ . This is what necessitates an iterative solution. The more serious difficulty is that the  $F_{rj}$  contain three and four center Coulomb and exchange integrals when a multi-center atomic basis set (with atomic orbitals centered on each nuclear site) is used. The most general of these is the four-center integral<sup>73</sup>

$$4.7) \quad \langle AB|CD \rangle = \int a_1^*(\vec{x}_{A1}) a_2(\vec{x}_{B1}) \frac{1}{|\vec{x}_1 - \vec{x}_2|} a_3^*(\vec{x}_{C2}) a_4(\vec{x}_{D2}) dv_1 dv_2$$

In this equation  $\vec{x}_{A1}$  is the vector distance of electron 1 from the origin at nucleus A. The orbitals  $a_1, a_2, a_3, a_4$  are atomic orbitals centered at sites A, B, C, and D.

Although various analytic basis sets have been used for the  $a_j(\vec{x})$ , the most reliable has proved to be the exponential



Slater basis

$$4.8) \quad a_{n\ell m} = N_{n\ell m} r^{n-1} e^{-\xi r} Y_{\ell m}(\theta, \phi)$$

with  $N$  the normalization constant,  $Y_{\ell m}(\theta, \phi)$  a real spherical harmonic, and  $r$  the radial distance from a given atomic center. Calculations of this type are very complex and require large amounts of computer time. Optimal minimal Slater basis calculations using a few functions at each center have been performed on  $H_2O$ ,  $CH_4$ ,  $PH_4$  and other systems of similar complexity.<sup>73</sup> Calculations on larger systems become feasible only if the multi-center integrals are approximated semi-empirically as in the extended Huckel method, or as in the CNDO (complete neglect of differential overlap) method.<sup>11</sup> Another approach is to abandon the multicenter basis set, and instead use a single center basis as in Ellis's calculations on  $KNiF_3$ .<sup>73</sup>

The source of much of the difficulty is the non-local exchange term in the effective Hamiltonian

$$4.9) \quad \int d\mathbf{v}_2 \sum_k^{occ.} w_k^*(2) \frac{-2P_{12}}{|\mathbf{x}_1 - \mathbf{x}_2|} w_k(2)$$

As we shall see later, when this term is replaced by a local exchange term, an approximate numerical solution of Schrodinger's equation becomes feasible. The use of analytic basis sets in solving the Hartree-Fock equations further compounds the problem, since such basis sets are characterized by slow convergence and complicated mathematical properties. This problem is especially serious in complicated systems

such as transition metal complexes.<sup>74</sup> A further consequence lies in the treatment of excited states. When unoccupied (virtual) orbitals are calculated via the Hartree-Fock equations, the exchange term displays unphysical features. Specifically, the excited state electron moves in the field of all  $N$  electrons, and thus behaves as if it were an additional test charge added to the  $N$ -electron system. The resulting virtual orbitals are not good excited state orbitals, and the excitation energies of the system are far too high.<sup>11</sup> Since dipole matrix elements  $\langle \phi_i | \vec{x} | \phi_j \rangle$  of the orbitals must be evaluated to obtain absorption intensities, these will not be reliable either. The alternative of solving a separate determinantal problem for each excited state configuration -- the rigorous Hartree-Fock method -- is intractable in complex systems because of the computer time required.

We will also show in Chapter VI C that the different forms of the oscillator strength are theoretically equivalent only for the case of local potentials. As previously described, this condition is not met by the Hartree-Fock method.

In this section, we have seen that a method using a local exchange term, if this term is well founded in terms of basic theory, offers several advantages over Hartree-Fock theory.

THE EFFECTS OF MOLECULAR VIBRATIONS ON SPECTRA

We present in this section a discussion of molecular vibrations based on a paper by Mulliken and Rieke.<sup>7</sup> The derivations in this section are more general than theirs in that we allow the equilibrium nuclear positions for the excited states of a system to be different from those of the ground state. It was well known at the time of the Mulliken and Rieke paper that the same theorems hold in this case as hold in the case of no change in the nuclear configuration. From the standard theory of molecular vibrations, we derive one new result, that the mean excitation energy for a vibronic transition lies below the value determined by the Franck-Condon principle (the vertical excitation energy).

In the Introduction, we discussed the distinction between the oscillator strength as a function of internuclear separation  $f(R)$ , and the oscillator strength between specific vibrational sublevels  $f_{v',v''}$  for a diatomic molecule. To find the total absorption from a specific vibrational sublevel of the ground state, we must take  $\sum_{v''} f_{v',v''}$ .<sup>7</sup> Similarly, for a thermal ensemble of initial vibrational sublevels  $v'$ , we find (average  $v'$ )  $\sum_{v''} f_{v',v''}$ . This is the quantity which we are attempting to evaluate and compare with experiment. In general, the electronic oscillator strength is a function of the normal mode displacements  $q_m$ ,  $f(q_1, \dots, q_m, \dots)$ , as is

the electron transition moment we have previously defined  $M(q_1, \dots, q_m, \dots)$ . The appropriate generalization of the formula for  $f_{v', v''}$  is then<sup>7,22</sup>

$$4.10) \quad f_{v', v''} = \frac{2m}{3\hbar^2 d_i} \Delta E_{v', v''} \sum_{k, l} |\langle \psi_{v', i}(q_1 \dots q_m \dots) | \vec{M}_k(q_1 \dots q_m \dots) | \psi_{v'', j}(q_1 \dots q_m \dots) \rangle|^2$$

Here  $\psi_{v', i}$  and  $\psi_{v'', j}$  are the total vibrational wave functions for the initial and final electronic states  $i$  and  $j$ , with sublevels  $v'$  and  $v''$ , and  $\Delta E_{v', v''}$  is the corresponding excitation energy. The sum over  $k, l$  is over all degenerate initial and final state partners, as before.

In the harmonic approximation, the total initial state vibrational wave function is given by

$$\psi_{v', i} = \phi_1^i(n_1) \phi_2^i(n_2) \phi_3^i(n_3) \dots, \text{ with the final state given by } \psi_{v'', j} = \phi_1^j(\bar{n}_1) \phi_2^j(\bar{n}_2) \phi_3^j(\bar{n}_3) \dots \quad .7,75 \quad \text{Here } n_1, n_2, \dots$$

are the excitation numbers of the normal modes  $1, 2, \dots$  for the initial state, and  $\bar{n}_1, \bar{n}_2, \bar{n}_3 \dots$  have the same meaning for the final state. The functions  $\phi_r^i(n_r)$  are harmonic oscillator wave functions for the  $n_r$  excitation of normal mode  $r$ . Because the potential energy curves are different for the electronic states  $i$  and  $j$ , the harmonic oscillator wave functions are also different, as are the normal mode displacements,  $q_r$  for state  $i$ ,  $\bar{q}_r$  for state  $j$ . (Since the normal mode displacements are measured with respect to the equilibrium nuclear configuration,  $\bar{q}_r = q_r + \xi_r$ . Here  $\xi_r$  is the change in normal mode coordinate  $q_r$  which results

from the change in the equilibrium nuclear configuration of states  $i$  and  $j$ ).

From the preceding considerations, the evaluation of  $f_{v',v''}$  should prove difficult. However, the approximate evaluation of (average  $v'$ )  $\sum_{v''} f_{v',v''}$  is quite feasible. We first expand the transition moment  $M(q_1, \dots, q_m, \dots)$  as a Taylor series in the normal mode displacements about the equilibrium point  $q_m = 0$  (for all  $m$ )<sup>7</sup>

$$4.11) \quad M = M_0 + \sum_n M_1^n q_n + \sum_{m,n} M_2^{mn} q_m q_n + \dots$$

The coefficients  $M_1^n$ ,  $M_2^{mn}$  may be found by evaluating  $M_1^n = \left. \frac{\partial M}{\partial q_n} \right|_0$  and we can proceed similarly for the higher order terms.  $M_0$  is just the transition moment at equilibrium for the ground state nuclear configuration,  $M_0 = M(R_{1e}, \dots, R_{ke})$ . If  $M_0 \neq 0$ , as is the case for a dipole allowed transition,  $M_0$  constitutes a first approximation to  $M$ . This approximation is reasonable if  $M$  is a slowly varying function near equilibrium, and if the initial vibrational states for the transition are of low order, especially  $v' = 0$  ( $n_r = 0$  for all modes). In practice, this condition often holds at room temperature and below as we shall see later.<sup>7</sup> An indication of the reliability of this approximation is given by the temperature dependence of the measured absorption for an allowed transition. The quantity (average  $v'$ )  $\sum_{v''} f_{v',v''}$  is temperature independent if  $M = M_0$ , but is temperature dependent when higher order terms are included.

We consider the quantity  $\sum_{v''} f_{v'v''}$  with  $M = M_0$ . We then obtain

$$4.12) \quad \sum_{v''} f_{v'v''} = \frac{2m}{3\hbar^2} \Delta E \sum_{k,l} |\vec{M}_{0,k\ell}|^2 \sum_{v''} |\langle \psi_{v'i}(q_1 \dots q_m \dots) | \psi_{v''j}(q_1 \dots q_m \dots) \rangle|^2$$

$\Delta E$  is an average excitation energy, which will be defined more precisely later. Since  $\psi_{v''j}(q_1 \dots q_m \dots)$  constitute a complete set of states over the space of the normal mode displacements  $q_r$ , we find

$$4.13) \quad \sum_{v''} f_{v'v''} = \frac{2m}{3\hbar^2} \Delta E \sum_{k,l} |\vec{M}_{0,k\ell}|^2$$

The sum over  $v''$  reduces to  $\langle \psi_{v'i}(q_1 \dots q_m \dots) | \psi_{v'i}(q_1 \dots q_m \dots) \rangle = 1$ .

As a further consequence, since equation 4.13 holds for any state  $v'$ , it is also true for a thermal ensemble of such states

4.14) (average  $v'$ )

$$\sum_{v''} f_{v'v''} = \frac{2m}{3\hbar^2} \Delta E \sum_{k,l} |\vec{M}_{0,k\ell}|^2 \cong f(R_{1e}, R_{2e}, \dots, R_{ke})$$

The measured absorption  $f$  value is, therefore, approximately the oscillator strength at equilibrium,  $f(R_{1e}, R_{2e}, \dots, R_{ke})$ .

This is the mathematical statement of the Franck-Condon principle. The physical idea is that the electronic transition takes place very quickly with respect to the nuclear motions. The transitions occur primarily from the  $v' = 0$  sublevel (a symmetric state with maximum amplitude at equilibrium) to  $v''$  sublevels which have a large amplitude near  $R_{1e}, R_{2e}, \dots, R_{ke}$ . Classically, the nuclear positions do not change during the

excitation, and the important  $v''$  sublevels have a turning point near this nuclear configuration. The excitation energy  $\Delta E$  is given by the total energy difference at equilibrium, representing a weighted average of vibrational sublevel excitation energies

$$4.15) \quad \Delta E = \sum_{v''} \Delta E_{v',v''} |\langle \psi_{v',i}(q_1 \dots q_m \dots) | \psi_{v'',j}(q_1 \dots q_m \dots) \rangle|^2 \\ \cong \Delta E(R_{1e}, R_{2e}, \dots, R_{ke})$$

(By defining  $\Delta E$  as a weighted average of  $\Delta E_{v',v''}$  we may justify the factorization of  $\Delta E$  out of the sum over  $v''$  in equation 4.12. To see this, simply substitute the weighted average over  $\Delta E_{v',v''}$  into equation 4.12, which then becomes an identity). The statement  $\Delta E \cong \Delta E(R_{1e}, R_{2e}, \dots, R_{ke})$  is not precisely true. However, it is a consequence of the behavior of typical excited state potential energy curves when  $v' = 0$ .<sup>20</sup> (See Figure 4). Transitions of the type just described are called vertical transitions since  $\Delta E(R_{1e}, R_{2e}, \dots, R_{ke})$  is a vertical energy difference between the potential energy surfaces in configuration space. We should note that alternative definitions of  $\Delta E$  are possible; for example,  $\Delta E$  could be defined as the value of  $\Delta E_{v',v''}$  for which  $f_{v',v''}$  is a maximum. This definition would still satisfy  $\Delta E \cong \Delta E(R_{1e}, R_{2e}, \dots, R_{ke})$ , and would differ from the previous definition by only about 0.1 ev. We may, therefore, use the alternative definitions interchangeably.

Now we consider a dipole forbidden transition,  $M_0 = 0$ .<sup>7</sup>

A concrete example would be a  $g \rightarrow g$  type transition (even parity  $\rightarrow$  even parity) in a molecule with an inversion center. The most important example in the present work is the  $2t_{2g} \rightarrow 9a_{1g}$  excitation in  $\text{Cr}(\text{CO})_6$ . The transition will remain forbidden,  $M = 0$ , unless the inversion center of the molecule is destroyed. This can be done only by an odd normal mode displacement. The resulting transition is called a vibronic transition. The Taylor expansion to second order is then

$M = \sum_{r=\text{odd}} M_1^r q_r$ . We are interested in

$$4.16) \quad \sum_{v''} f_{v',v''} = \frac{2m\Delta E}{3\hbar^2 d_i} \sum_{k,\ell,v''} |\langle \psi_{v',i}(q_1 \dots q_m \dots) | \sum_{r=\text{odd}} \vec{M}_{1,k\ell}^r q_r | \psi_{v'',j}(q_1 \dots q_m \dots) \rangle|^2$$

$$= \frac{2m\Delta E}{3\hbar^2 d_i} \sum_{k,\ell} \sum_{r=\text{odd}} |\vec{M}_{1,k\ell}^r|^2 \sum_{v''} |\langle \psi_{v',i}(q_1 \dots q_m) | q_r | \psi_{v'',j}(q_1 \dots q_m) \rangle|^2$$

The last expression in this equation is not obvious, but follows from using the completeness of the  $\psi_{v'',j}$  wave functions, and the fact that  $\psi_{v',i}$  has definite parity with respect to each normal mode  $q_m$ . Now consider a particular odd normal mode coordinate  $q_1$ . To find the intensity via  $q_1$ , we first evaluate

$$4.17) \quad \int \psi_{v',i} q_1 \psi_{v'',j} dq_1 \dots dq_p = \int \phi_1^i(n_1) q_1 \phi_1^j(\bar{n}_1) dq_1$$

$$\int \phi_2^i(n_2) \phi_3^i(n_3) \dots \phi_p^i(n_p) \phi_2^j(\bar{n}_2) \phi_3^j(\bar{n}_3) \dots \phi_p^j(\bar{n}_p) dq_2 \dots dq_p$$

with a total of  $p$  normal modes in the molecule. One then must take the sum after squaring over final states  $v''$ , of the expression in equation 4.17 and substitute into equation 4.16.



To simplify, let  $\bar{\psi}_{v'i} = \phi_2^i(n_2)\phi_3^i(n_3)\dots\phi_p^i(n_p)$  and  $\bar{\psi}_{v''j} = \phi_2^j(\bar{n}_2)\phi_3^j(\bar{n}_3)\dots\phi_p^j(\bar{n}_p)$ , resulting in

$$4.18) \quad \sum_{v''} \left[ \int \phi_1^i(n_1) q_1 \phi_1^j(\bar{n}_1) dq_1 \int \bar{\psi}_{v'i} \bar{\psi}_{v''j} dq_2 \dots dq_p \right]^2 \\ = \frac{\hbar}{2m_1\omega_1} (2n_1+1)$$

The derivation of 4.18 is fairly simple. Each  $v''$  is a set of labels  $\{\bar{n}_1, \bar{n}_2, \dots, \bar{n}_p\}$ . From the properties of harmonic oscillator wave functions<sup>75</sup>

$$4.19) \quad \phi_1^i(n_1) q_1 = \left( \frac{\hbar}{2m_1\omega_1} \right)^{1/2} \left( \sqrt{n_1} \phi_1^i(n_1-1) + \sqrt{n_1+1} \phi_1^i(n_1+1) \right)$$

$\omega_1$  is the harmonic oscillator frequency for the normal mode  $q_1$ , with  $m_1$  the corresponding reduced mass of the nuclei.

We sum first over  $\{\bar{n}_2 \dots \bar{n}_p\}$  and then over  $\bar{n}_1$  using the completeness of  $\bar{\psi}_{v''j}$  and  $\phi_1^j(\bar{n}_1)$  to obtain equation 4.18. The matrix elements for the other odd modes are found in the same manner yielding

$$4.20) \quad \sum_{v''} f_{v'v''} = \frac{m_e \Delta E}{3\hbar d_i} \sum_{k,\ell} \sum_{r=\text{odd}} \frac{(2n_r+1) \left| \vec{M}_{1,k\ell} \right|^2}{m_r \omega_r}$$

The electron mass is denoted by  $m_e$ , to distinguish it from the reduced nuclear mass  $m_r$ . This is the total vibronic intensity from an initial vibrational state  $v'$ , with normal mode quantum number  $n_r$ . It would also be the first order correction to the Franck-Condon result, equation 4.14.

To obtain the thermal average of this equation, we recall that the average excitation of a normal mode is given by

$$n_r = \frac{1}{e^{\hbar\omega_r/kT} - 1}, \text{ which is the Bose factor.}^{75}$$

Since  $2\langle n_r \rangle + 1 = \frac{2}{e^{\hbar\omega_r/KT} - 1} + 1 = \coth\left(\frac{\hbar\omega_r}{2KT}\right)$ , we find

$$4.21) \quad (\text{average } v') \\ \sum_{v''} f_{v',v''} = \frac{m_e \Delta E}{3\hbar d_i} \sum_{k,\ell} \sum_{r=\text{odd}} \frac{\coth\left(\frac{\hbar\omega_r}{2KT}\right) |\vec{M}_{1,k\ell}^r|^2}{m_r \omega_r}$$

Qualitatively, the temperature dependence of  $f$  goes as  $\coth\left(\frac{\hbar\omega_r}{2KT}\right)$  for a typical mode, which is a slowly increasing function of temperature for  $\hbar\omega_r > KT$ .<sup>70</sup> The same condition implies that the system is mostly in the ground vibrational state  $v' = 0$ .

We now show that the average excitation energy for a vibronic transition lies below the value determined by applying the Franck-Condon principle. Although this idea is a direct consequence of the theory of vibronic excitations as presented by Mulliken and Rieke, we have not found any discussion of this issue in the literature.<sup>7</sup>

In our derivation for vibronic transitions, we have again replaced the true vibrational excitation energies  $\Delta E_{v',v''}$  by an average  $\Delta E$ . By analogy with our previous definition,  $\Delta E$  has a different structure for vibronic transitions

$$4.22) \quad \Delta E_{\text{vibronic}} = C \sum_{v''} \left[ \Delta E_{v',v''} \sum_{k,\ell,r=\text{odd}} \frac{|\langle \psi_{v',i}(q_1 \dots q_m \dots) | \psi_{v'',j}(q_1 \dots q_m \dots) \rangle|^2}{|\vec{M}_{1,k\ell}^r|^2} \right]$$

with  $C$  a normalization constant. Before,  $\Delta E_{v',v''}$  was weighted simply by the square of the overlap of the initial and final vibrational wave functions,  $|\langle \psi_{v',i}(q_1 \dots q_m \dots) | \psi_{v'',j}(q_1 \dots q_m \dots) \rangle|^2$ .

In the present case, if  $v' = 0$ ,

$$\psi_{v', i, q_r} = C' \phi_1^i(0) \phi_2^i(0) \dots \phi_r^i(1) \dots \phi_p^i(0), \text{ with } C' \text{ a constant.}$$

Therefore,  $\Delta E_{\text{vibronic}}$  is determined by  $v''$  states having a large overlap with the first order harmonic oscillator function  $\phi_r^i(1)$ , which has odd parity, as well as with the zeroth order oscillators for the other modes. The primary overlap will then come from lower  $v''$  sublevels than was the case for an allowed transition. (See Figure 4). The net result is a shift of the spectrum to lower excitation energies,  $\Delta E_{\text{vibronic}} < \Delta E(R_{1e}, R_{2e}, \dots, R_{ke})$ . The value of the shift depends on which mode  $q_r$  makes the primary contribution to the vibronic intensity. These are simply the respective terms for the various modes in equation 4.21. For such a mode, the energy shift is approximately equal to the vibrational energy separation between oscillators  $\hbar\omega_r$  (typically about 0.1 - 0.3 eV). In addition, we notice that the calculation of vibronic intensities via equation 4.21 is quite feasible by our methods, though none have been attempted in the present work.

We should also comment on the validity of the approximations made in this section. We have used the harmonic oscillator wave functions for the initial and final vibrational states. This approximation is physically reasonable for the initial electronic state  $i$ , but is not reasonable for the electronic state  $j$  which may undergo molecular dissociation or have other anharmonic properties. However, the proofs

in this section rely only on the completeness of the  $\psi_{v''j}$  functions, on a harmonic oscillator type behavior near the classical excited state turning points, and on an absence of coupling between normal modes. Any physically reasonable vibrational wave function should obey the first two conditions. In particular, anharmonic effects at large distances from equilibrium should not affect our results. The assumption of no coupling between the normal modes is, however, unsatisfactory for many molecules. We should therefore consider the results of this section as characteristic of a reasonable physical model for molecular vibrations. The behavior of real physical systems may be more complex than we have portrayed here.

Summarizing, for a dipole allowed transition, the measured absorption intensity is given by (average  $v'$ )

$$\sum_{v''} f_{v'v''} = f(R_{1e}, R_{2e}, \dots, R_{ke})$$

at an average excitation energy  $\Delta E = \Delta E(R_{1e}, R_{2e}, \dots, R_{ke})$ . For a dipole forbidden transition, vibronic coupling causes absorption (at lower intensity) which is a slowly increasing function of temperature. The average excitation energy shifts to lower energies,  $\Delta E < \Delta E(R_{1e}, R_{2e}, \dots, R_{ke})$  by about 0.1 - 0.3 eV.

## BOUNDARY CONDITIONS AND LOCAL FIELD EFFECTS

We are concerned here with the effects on the absorbing molecule of the surrounding medium. Much of the original work in this area was done by Chako, with later contributions by Onsager, Person, and others.<sup>76-79</sup> As we indicated earlier, the issue is not important in the case of vapor spectra where the diffuseness of the medium (other absorbing molecules) renders the various molecules independent with respect to absorption (except for molecular collisions).<sup>7</sup> The issue arises in the case of absorbing molecules dissolved in a medium of a different type, or of absorption by a homogeneous material (for example, in a crystal such as  $\text{SiO}_2$ ). The later instance forms an important limiting case and shows the value of including boundary conditions as well as local field effects in our considerations.

We begin by considering a dilute solution of absorbing molecules of type A in a medium B, which is transparent at the absorption frequencies of A. Each molecule A lies in an assumed spherical cavity in medium B. Let an applied electric field  $\vec{E}_0$  cause a uniform polarization of B with polarization vector  $\vec{P}$ . (Since the molecule A is treated as an object which responds as a whole to the effective field  $E'$ , the field  $E'$  may not include a direct contribution from the polarization of A). The effective field at A is that of a spherical cavity cut in a uniform polarized

medium.<sup>80</sup> The field in the cavity is the macroscopic field  $E_0$  minus the field due to the polarization of the dielectric which we have removed. The electric field inside a uniformly polarized sphere is constant and is given by  $\vec{E}_s = \frac{-4\pi}{3} \vec{P}$ .

Then, the field in the cavity is

$$4.23) \quad E' = E_0 - E_s = E_0 + \frac{4\pi}{3} P = \left(1 + \frac{4\pi}{3} \chi_e\right) E_0$$

with  $\chi_e = \frac{P}{E_0}$  the dielectric susceptibility. However, we also know that the electric displacement vector  $\vec{D}$  is given by

$$4.24) \quad \vec{D} = \epsilon \vec{E}_0 = \vec{E}_0 + 4\pi \vec{P} = (1 + 4\pi \chi_e) \vec{P}$$

with  $\epsilon$  the dielectric constant. Then we find

$$4.25) \quad \chi_e = \frac{\epsilon - 1}{4\pi}$$

$$\vec{E}' = \left(1 + \frac{4\pi}{3} \left(\frac{\epsilon - 1}{4\pi}\right)\right) \vec{E}_0 = \left(\frac{2 + \epsilon}{3}\right) \vec{E}_0$$

Since the medium is transparent,  $\epsilon = n_0^2$  with  $n_0$  the index of refraction in B, and

$$4.26) \quad E' = \left(\frac{n_0^2 + 2}{3}\right) E_0$$

The absorption coefficient is given by<sup>80,81</sup>

$$4.27) \quad \eta = \frac{\frac{1}{2} \text{Re}(\vec{J} \cdot \vec{E}'^*)}{\frac{c}{8\pi} \text{Re}(\vec{E}_0 \times \vec{B}_0^*)}$$

The effective field  $E'$  induces a current  $J = \sigma E'$ . The rate of energy flow, however, is determined by the macroscopic field amplitude  $E_0$  (since this is the true average field over the material). From Maxwell's equations, the magnetic field amplitude is given by  $\vec{B}_0 = N_0 \vec{e}_3 \times \vec{E}_0$ , with  $N_0 = n_0 + iK_0$  the complex index of refraction for the entire material,  $K_0$  the extinction

coefficient, and  $\vec{e}_3$  the unit vector in the direction of wave propagation. We then find

$$4.28) \quad \frac{c}{8\pi} |\operatorname{Re}(\vec{E}_0 \times \vec{B}_0^*)| = \frac{cn_0}{8\pi} |\vec{E}_0|^2 = \frac{3cn_0}{8\pi} |E_{0x}|^2$$

The absorption coefficient is

$$4.29) \quad \eta = \frac{4\pi}{3c} \frac{(n_0^2+2)^2}{9n_0} \frac{\operatorname{Re}\left(\sum_{j=1}^3 \sigma_{jj}\right) |E_{0x}|^2}{|E_{0x}|^2} = \frac{4\pi}{3c} \frac{n_0^2+2}{9n_0} \operatorname{Re}\left(\sum_{j=1}^3 \sigma_{jj}\right)$$

(The electric field amplitude  $E_{0x}(\ell)$  is a function of penetration  $\ell$  into the material, but this does not affect  $\eta$ .

$$E_x(\ell, t) = E_{0x}(\ell) \bar{e}^{-i\omega t}, \text{ where } E_{0x}(\ell) = \bar{E}_{0x} e^{i\left(\frac{n_0\omega}{c} \ell - \omega t\right)} e^{-\frac{\omega K_0 \ell}{c}}$$

and  $\bar{E}_{0x}$  is a constant vector).  $\eta$  and similarly  $f$  differ from the previous result by the factor  $\frac{(n_0^2+2)^2}{9n_0}$ , which is greater than 1 for  $n_0 > 1$ .<sup>76</sup> Since the value of  $f$  for a vapor of A molecules has no local field effects<sup>7</sup>

$$4.30) \quad \frac{f_{\text{solution}}}{f_{\text{vapor}}} = \frac{1}{\gamma} = \frac{(n_0^2+2)^2}{9n_0}$$

The previous value of  $f$  should be multiplied by  $\frac{1}{\gamma}$  when compared with the integrated molar extinction coefficient for a

solution. The field  $E'$  of equation 4.26 is known as the cavity field, and the correction factor  $\frac{(n_0^2+2)^2}{9n_0}$  is

called the Lorentz-Lorenz factor. (The Lorentz-Lorenz equation for the index of refraction of the medium B, in the absence of A, may be derived with the same assumptions we

have used.<sup>80</sup>  $P = \bar{N} \alpha_B E'$ , with  $\bar{N}$  the molecular density of B,

and  $\alpha_B$  the molecular polarizability of B.  $E' = E_0 + \frac{4\pi}{3} P$ .  $\frac{P}{E'} =$

$$\frac{P}{E_0 + 4\pi P} = \frac{\chi_e}{1 + 4\pi\chi_e} = \bar{N}\alpha_B. \quad \text{Therefore,}$$

$$\frac{3}{4\pi} \frac{\epsilon - 1}{\epsilon + 2} = \frac{3}{4\pi} \frac{n_0^2 - 1}{n_0^2 + 2} = \bar{N}\alpha_B.$$

The last equation, when expressed in terms of  $n_0$ , is the Lorentz-Lorenz formula. We may also say  $\frac{n_0^2 - 1}{n_0^2 + 2} \cdot \frac{1}{\bar{N}} = A_m =$  constant.  $A_m$  is the molar refractivity which should be constant for a given substance in both the vapor and liquid states. The relation  $A_m = \text{constant}$  has been confirmed for several substances, and provides some verification of the cavity field concept. However, the Lorentz-Lorenz factor is not a generally valid result for the correction factor  $\frac{1}{\gamma}$  (7,23.)

In the preceding derivation, we have assumed that the electromagnetic properties of the absorbing molecule, in particular its internal index of refraction  $n_A$  (the index of refraction in molecule A), does not modify the polarization of the induced dipoles in medium B. If such an interaction is allowed, the result is the Onsager equation <sup>77,78</sup>

$$4.31) E' = \left( \frac{n_A^2 + 2}{\frac{n_A}{n_0}^2 + 2} \right) E_0$$

Here  $E'$  consists of the cavity field of equation 4.26, plus a reaction field from the effect of A on the polarization of B. We then find

$$4.32) \frac{f_{\text{solution}}}{f_{\text{vapor}}} = \frac{1}{\gamma} = \frac{1}{n_0} \left[ \frac{n_A^2 + 2}{\left(\frac{n_A}{n_0}\right)^2 + 2} \right]^2$$



This formula, however, is open to serious objections.  $n_A$  may be a rapidly varying function near an absorption peak, and one does not know how  $n_A$  should then be evaluated.

The derivation of the Lorentz-Lorenz equation we have presented, and Onsager's derivation of equation 4.31, depend solely on electrostatic concepts. However, it is well known that a radiation field differs fundamentally from an electrostatic field. The Onsager and Lorentz-Lorenz results cannot, therefore, be accepted without proof via radiation theory. The proof of the Lorentz-Lorenz equation for  $E'$  may be found in Born's Optics, but no such proof has been given of the Onsager equation.<sup>81</sup>

The theoretical drawbacks of the Lorentz-Lorenz and Onsager results might be more acceptable if the predicted  $\frac{f_{\text{solution}}}{f_{\text{vapor}}}$  agreed with experiment, but here again the theories encounter difficulties. While Lorentz-Lorenz theory predicts a  $\frac{1}{\gamma}$  value of 1.30 for cyclopentadiene and cyclohexadiene in n-hexane, the measured values are 0.83 and 1.04.<sup>23</sup> This disagreement is typical for hydrocarbons. The Onsager theory also predicts too high a value for  $\frac{1}{\gamma}$  in these systems. In view of these results, we will let  $\frac{1}{\gamma} = 1$  in our calculations.

So far we have dealt only with the problem of evaluating the effective field  $E'$  at molecule A (local field effects). However, we should also consider the possible dependence of  $\frac{1}{\gamma}$  on specific molecular interactions (raising the issue of boundary conditions). (In this context,  $\frac{1}{\gamma}$  may be defined by

$f$  (in medium) =  $\frac{1}{\gamma}$   $f$  (isolated molecule). This definition is meaningful even when  $\frac{f_{\text{solution}}}{f_{\text{vapor}}}$  is not measurable, as is the case for many molecular anions). The molecular interactions to be considered are 1) electrostatic stabilization of ions in solutions or crystals, 2) permanent or fluctuating multiple fields and London dispersion forces, and 3) covalency between molecules.<sup>7</sup>

In the scattered wave method, electrostatic stabilization of an ion is achieved by surrounding the molecule with a neutralizing charged sphere of the opposite sign, generally at the outer sphere radius, simulating the external environment.<sup>9</sup> Neither the energy levels (aside from a constant shift) nor the wave functions are sensitive to the exact location of the charged sphere. (See Chapter 7.) Higher order multiple fields from other ions (in solution, the ions move and the fields fluctuate) will lower the degeneracies of the electronic wave functions, and cause additional splittings of the spectral peaks.<sup>46</sup>

In neutral molecules, solvent effects are governed by the polarity of the solute and solvent molecules.<sup>23</sup> An energy shift to lower wave numbers generally occurs for absorption bands of non-polar molecules in both polar and non-polar solvents. For polar molecules, the energy shift is to lower wave numbers if the dipole moment of the solute molecule increases on excitation, and generally to higher

wave numbers if the dipole moment decreases. These results follow simple energetic considerations of the relative stabilities of the ground and excited states for the absorbing molecule.

The preceding effects lead to energy shifts of about 0.0 - 0.2 ev., and would not be expected to cause significant changes in spectral peak intensities, at least for dipole allowed transitions.<sup>23</sup> Some dipole forbidden transitions may become weakly allowed via the electrostatic perturbations. However, covalent interactions between molecules can change intensities quite drastically.

Consider a system with strong covalent interactions between molecules. The electrons are no longer localized to individual molecules, but rather move throughout the system. The appropriate electromagnetic field is, therefore, not the cavity field  $E'$ , but instead the average field  $E_0$ .<sup>82</sup> The localized wave functions become more diffuse, and with strong interactions the discrete molecular energy levels are replaced by bands (if some localization remains, the bands are narrow). For a homogeneous material (for example,  $\text{SiO}_2$ ), we have

$$4.33) \quad \frac{1}{\gamma} = \frac{1}{n_0}$$

with  $n_0$  the index of refraction of the material. The absorption coefficient is

$$4.34) \quad \eta = \frac{4\pi}{cn_0} \frac{\operatorname{Re} \left( \sum_{j=1}^3 \sigma_{jj} \right)}{3}$$

$$\text{where } \frac{\operatorname{Re} \left( \sum_{j=1}^3 \sigma_{jj} \right)}{3} = \sigma_1 \text{ (average)}$$

To put this in a more familiar form,  $\epsilon_2 \omega = 2n_0 K_0 \omega = 4\pi \sigma_1$ , with the complex dielectric constant  $\epsilon$  defined as  $\epsilon = \epsilon_1 + i\epsilon_2$ .<sup>83</sup>

$$4.35) \quad \eta = \frac{4\pi \sigma_1}{n_0 c} = \frac{\epsilon_2 \omega}{n_0 c} = \frac{2K_0 \omega}{c}$$

This is the standard form for  $\eta$  in terms of the extinction coefficient  $K_0$  for a homogeneous material. As covalency increases,  $f$  is initially reduced due to the increasing diffuseness of the orbital wave functions, and due to the lower value of  $\frac{1}{\gamma}$  ( $\frac{1}{\gamma} < 1$ ). The limiting case where bands are formed should probably be solved separately.

We conclude that  $\frac{1}{\gamma}$  may be either greater than or less than 1 depending on the comparative importance of local field and covalency effects (the results we quoted for hydrocarbons are probably indicative of the compensating tendencies), but that a more comprehensive theory for intensity corrections is seriously needed.

## CHAPTER V

THE  $X_\alpha$  SCATTERED WAVE METHODTHE  $X_\alpha$  THEORY

The  $X_\alpha$  method arose from the attempt to find a local form for the exchange term which would be common to all the orbitals of an atom or molecule. In 1951, Slater suggested the use for an approximate exchange potential proportional to  $\rho^{1/3}$ , with  $\rho$  the local electronic charge density, to replace the Hartree-Fock exchange potential of equation 4.9.<sup>84</sup> Later, this work was put on a more rigorous basis by Hohenberg, Kohn, Sham, and Slater.<sup>5,85,86</sup> Our discussion of the  $X_\alpha$  theory will follow fairly closely the treatment of Slater.<sup>5</sup>

We begin by defining the charge densities of spin-up and spin-down electrons in a molecule by<sup>5</sup>

$$5.1) \quad \rho^\uparrow = \sum_{j^\uparrow} n_j u_j^* u_j, \rho^\downarrow = \sum_{j^\downarrow} n_j u_j^* u_j, \rho = \rho^\uparrow + \rho^\downarrow$$

where the  $n_j$  are the occupation numbers for the spin-up and spin-down orbitals  $u_j$ . In general, the spin-up orbitals are different from the spin-down orbitals. A charge density having the simple form of equation 5.1 corresponds to the more general diagonal first-order density matrix defined by

$$5.2) \quad \rho(\mathbf{x}, \mathbf{x}') = \sum_{j\uparrow} n_j u_j^*(\vec{x}') u_j(\vec{x}) + \sum_{j\downarrow} n_j u_j^*(\vec{x}') u_j(\vec{x})$$

Therefore,  $\rho(\mathbf{x}) = \rho(\mathbf{x}, \mathbf{x})$ . In general, the density matrix would also include terms of the form  $\gamma_{ij} u_i(\mathbf{x}) u_j^*(\mathbf{x}')$ .<sup>87</sup> As we will show in Chapter VI, a unitary transformation will reduce this expression to the form of equation 5.2. The resulting orbitals of the exact density matrix, when reduced to diagonal form, are called the natural orbitals, with occupation numbers  $n_i$ . The expression for the total energy of the molecule is then<sup>5,87</sup>

$$5.3) \quad E = \sum_i n_i \int u_i^*(1) f_1 u_i(1) dv_1 + \frac{1}{2} \int \rho(1) \rho(2) g_{12} dv_1 dv_2 + E_{xc}$$

Here,  $f_1$  is the one electron operator for electron 1,  $f_1 = -\nabla_1^2 + V_N$ , the sum of its kinetic energy and potential energy in the field of all the nuclei. The second term is the classical Coulomb interaction of a charge density with itself, with  $g_{12} = \frac{2}{|\vec{x}_1 - \vec{x}_2|}$  the Coulomb operator. The exchange-correlation term  $E_{xc}$  is a consequence of the antisymmetry of the many electron wave functions, and of the more general tendency of the electrons to stay away from one another (the electron motions are correlated). (Again, we are working in Rydberg units. Subsequently, all integrations are over space and spin coordinates). Although equation 5.3 is exact when the  $u_i$  are natural orbitals and the exact  $E_{xc}$  is used, it may also appear in approximate theories. For example, the Hartree-Fock total energy expression results when we substitute<sup>87</sup>

$$5.4) \quad E_{xc}(\text{Hartree-Fock}) = -\frac{1}{2} \sum_{i=1}^N \sum_{j=1}^N \int w_i^*(1) w_j^*(2) \frac{2}{|\vec{x}_1 - \vec{x}_2|} w_j(1) \\ \cdot w_i(2) dv_1 dv_2$$

( $w_i$  are the spin orbitals defined in the last chapter. The charge density in Hartree-Fock theory has the same form as equation 5.1.) What we are seeking is a simpler form of exchange to use in equation 5.3.

Hohenberg and Kohn have shown that for a many electron system in an external potential, (here the potential of the nuclei), the ground state total energy is a unique functional of the electron charge density  $\rho$  neglecting spin.<sup>85</sup> If we postulate that excited states obey the same condition, we find  $E_{xc} = E_{xc}(\rho \uparrow, \rho \downarrow)$  including the possible spin dependence. In order to understand the functional dependence of  $E_{xc}$ , we consider the electrostatic interaction energy of a system of  $N$  electrons. If the exact many electron wave function is  $\psi$ , the electrostatic interaction energy of the electrons is given by<sup>5</sup>

$$5.5) \quad \frac{1}{2} N(N-1) \int \psi^*(1, 2, \dots, N) g_{12} \psi(1, 2, \dots, N) dv_1 \dots dv_N$$

The integral represents the electrostatic interaction of the pair of electrons 1 and 2, there being  $\frac{1}{2}N(N-1)$  such pairwise interactions. In many electron language, the charge density  $\rho(1)$  and the joint probability density  $\rho_2(1, 2)$  (which represents the probability for finding an electron at 1, and another simultaneously at 2) are

$$5.6) \quad \rho(1) = N \int \psi^*(1, \dots, N) \psi(1, \dots, N) dv_2, \dots, dv_N$$

$$5.7) \quad \rho_2(1, 2) = N(N-1) \int \psi^*(1, 2, \dots, N) \psi(1, 2, \dots, N) dv_3, \dots, dv_N$$

Equation 5.5 is the same as the last two terms of equation 5.3. When the definition 5.7 is used, we find the electronic interaction energy

$$5.8) \quad \frac{1}{2} \int \rho_2(1, 2) g_{12} dv_1 dv_2 = \frac{1}{2} \int \rho(1) \rho(2) g_{12} dv_1 dv_2 + E_{xc}(\rho \uparrow, \rho \uparrow)$$

Solving for  $E_{xc}(\rho \uparrow, \rho \uparrow)$

$$\begin{aligned} 5.9) \quad E_{xc}(\rho \uparrow, \rho \uparrow) &= \frac{1}{2} \int (\rho_2(1, 2) - \rho(1)\rho(2)) g_{12} dv_1 dv_2 \\ &= \frac{1}{2} \int \rho(1) \left[ \left( \frac{\rho_2(1, 2)}{\rho(1)} - \rho(2) \right) g_{12} dv_2 \right] dv_1 \\ &= \frac{1}{2} \int \rho(1) W(1) dv_1 \end{aligned}$$

$W(1)$  (the expression in brackets) is the electrostatic potential of interaction of the charge density  $\rho(1)$  with the Fermi hole. The total charge associated with this potential is

$$\int \left( \frac{\rho_2(1, 2)}{\rho(1)} - \rho(2) \right) dv_2. \quad \text{From definitions 5.6 and 5.7}$$

$\int \rho_2(1, 2) dv_2 = (N-1)\rho(1)$ . The charge is then  $(N-1) - N = -1$  electron unit. The charge density  $\rho_h(2) = \frac{\rho_2(1, 2)}{\rho(1)} - \rho(2)$

is that of the Fermi hole density at position 2 acting on an electron at position 1. We can then evaluate the Fermi hole density at the electron position 1. (This means that

the Fermi hole and the electron must have the same spin coordinates  $\sigma_1$ , as well as the same position  $x_1$ ).  $\rho_h(1) =$

$$\frac{\rho_2(1, 1)}{\rho(1)} - \rho(1). \quad \text{Since } \rho_2(1, 1) = 0, \text{ as a consequence of the}$$

anti-symmetry of the wave function, we find  $\rho_h^\uparrow(x_1) = -\rho(x_1)$



for electrons spin-up. (The statement  $\rho_2(1,1) = 0$  means that there is 0 probability for 2 electrons to be simultaneously at the same location with the same spin).

Now, let us assume a uniform Fermi hole density of  $\rho_h^\uparrow(x_2) = -\rho(x_1)$  (this is the density at the center of the hole) throughout a sphere of radius  $R$ , and  $\rho_h(x_2) = 0$  outside  $R$ . Remembering that the total Fermi hole charge is -1 electron unit, we obtain

$$5.10) \quad -\frac{4}{3}\pi R^3 \rho^\uparrow(x_1) = -1, \quad R = \left(\frac{3}{4\pi\rho^\uparrow(x_1)}\right)^{1/3}$$

The electrostatic potential at the center of a uniformly charged sphere in Rydberg units is  $\frac{3}{R}$ . The potential at  $x_1$  is then

$$5.11) \quad -3 \left[\left(\frac{4\pi}{3}\right) \rho^\uparrow\right]^{1/3}$$

for spin-up electrons. A slightly more general potential is

$$5.12) \quad U_{x\alpha}^\uparrow(x_1) = -9\alpha \left[\left(\frac{3}{4\pi}\right) \rho^\uparrow\right]^{1/3}$$

Which is just proportional to expression 5.11. The exchange correlation energy is given by

$$5.13) \quad E_{xc} = \frac{1}{2} \int [\rho^\uparrow(x_1) U_{x\alpha}^\uparrow(x_1) + \rho^\downarrow(x_1) U_{x\alpha}^\downarrow(x_1)] dv_1$$

The  $X_\alpha$  total energy expression  $E_{x\alpha}$  results when  $E_{xc}$  is substituted into the total energy expression, with  $\rho$  defined by equation 5.1. The parameter  $\alpha$  is normally selected so that the  $X_\alpha$  total energy for an atom agrees with the corresponding Hartree-Fock total energy. The exchange-correlation energy of equation 5.13 is not exact, but it should be closely

related to the correct form.

To determine the orbitals  $u_i$ , we again require the total energy  $E_{x\alpha}$  to be stationary with respect to a variation of the spin orbitals for the eigenstates of the system.

$$5.14) \quad \delta E_{x\alpha} = 0, \int u_i^*(1) u_i(1) dv_1 = 1 \quad \text{or} \quad \int u_i^*(1) u_i(1) dv_1 = 0$$

where we include the constraint that all the orbitals be normalized. We fix the occupation numbers  $n_i$ , and apply the variational principle resulting in the one electron equations

$$5.15) \quad \left[ -\nabla_1^2 + V_c(1) + V_{x\alpha}^\uparrow(1) \right] u_i^\uparrow(1) = \epsilon_i^\uparrow u_i^\uparrow(1)$$

The first term is the kinetic energy,  $V_c(1)$  is the Coulomb potential acting on electron 1 as a result of both the nuclear and the total electronic charge density (including that of orbital  $u_i$ ), and  $V_{x\alpha}^\uparrow(1)$  is the one electron exchange correlation term with  $V_{x\alpha}^\uparrow(1) = \frac{2}{3} U_{x\alpha}^\uparrow(1)$ . Therefore,

$$5.16) \quad V_c(1) = V_N(1) + \int g_{12} \rho(2) dv_2, \quad V_{x\alpha}^\uparrow(1) = \frac{2}{3} U_{x\alpha}^\uparrow(1) \\ = -6\alpha \left[ \left( \frac{3}{4\pi} \right) \rho^\uparrow(1) \right]^{1/3}$$

The  $\epsilon_i$  are the Lagrange multipliers introduced into the constraint equations  $\int u_i(1) \delta u_i^*(1) dv_1 = 0$ . Further details are provided in Slater's Quantum Theory of Molecules and Solids, Vol. 4.<sup>74</sup> The solutions of equation 5.15 are an orthonormal set of spin orbitals  $u_i^\uparrow, u_i^\downarrow$  in a local potential which is common to all electrons of a given spin. The set of equations must be solved self-consistently since the Coulomb and exchange-correlation potentials involve the

orbitals  $u_i$ , and the  $u_i$  in turn are solutions for these potentials. The scattered wave method used to solve these equations is described in a later section.

The occupation numbers  $n_i$  in the  $X_\alpha$  theory are determined by requiring that they satisfy Fermi statistics.<sup>5</sup> The occupation number of an orbital is

$$5.17) \quad n_i = \frac{1}{e^{\epsilon_i - \epsilon_F / k_B T} + 1}$$

with  $\epsilon_F$  the Fermi energy,  $T$  the temperature, and  $k_B$  Boltzmann's constant. We are interested in the ground state at  $T = 0$ , where  $n_i = 1$  for  $\epsilon_i < \epsilon_F$ ,  $n_i = 0$  for  $\epsilon_i > \epsilon_F$ , and  $n_i = n_j$  for  $\epsilon_i = \epsilon_j = \epsilon_F$ , the case of degenerate one electron energies at the Fermi level. Such degenerate orbitals occur, for example, when the  $nl$  quantum numbers are the same in an atom, or when electrons belong to the same irreducible representation in a molecule. The occupation numbers  $q_i$  of individual shells are integral for the eigenstates of the system, but in the case of a partially filled shell of degeneracy  $q_{i0}$ , this leads to fractional orbital occupation numbers  $n_i = \frac{q_i}{q_{i0}}$  for all orbitals in the shell.

An important advantage of the use of Fermi statistics in  $X_\alpha$  theory is that the molecular total energy goes to the sum of the free atom total energies in the limit of infinite internuclear separation.<sup>8</sup> This is in contrast to the Hartree-Fock determinantal wave function which in this limit goes to a linear combination of free atom and ionic wave functions.

This leads to an incorrect value for the total energy. We consider the lithium ( $\text{Li}_2$ ) molecule as a typical example of a homonuclear system. The  $X_\alpha$  theory leads to the proper theoretical separated atom limit (which is very close to the true separated atom total energy) because the electron-electron interactions may be expressed in the form of a density functional. The choice of  $\alpha$  to agree with the Hartree-Fock atomic total energy then automatically results in the proper separated atom limit. The Hartree-Fock method leads to an equal probability for free atom  $\text{LiLi}$  and ionic  $\text{Li}^+\text{Li}^-$  configurations, and a total energy significantly above the true value. As we might expect, the  $X_\alpha$  theory yields potential energy curves which are generally better than the results of Hartree-Fock theory. In the  $\text{Li}_2$  case, the total energy at equilibrium separation is  $-29.81$  Rydbergs (exact),  $-29.79$  Rydbergs ( $X_\alpha$  theory), and  $-29.74$  Rydbergs (Hartree-Fock).<sup>8</sup> The Hartree-Fock method in this case predicts a dissociation energy only 15% of the experimental value, as opposed to about 75% for the  $X_\alpha$  method.

In addition to giving accurate ground state properties, we are, of course, interested in the description of excitations. Ideally, we would want a theory which describes the details of the multiplet structure found in atomic and molecular spectra. However, the nature of the multiplets depends on the explicit coupling of spins and electronic motions in partially filled shells. This is beyond the range of any one

electron theory like  $X_{\alpha}$  or Hartree-Fock.<sup>5</sup> The spin polarized  $X_{\alpha}$  theory (spin unrestricted) we have described in this section does give some information about the spin multiplets. The net spin occupancy  $q_i^{\uparrow} - q_i^{\downarrow}$  of a shell is related to  $M_S$  (the Z component of the total spin S) by  $M_S = \frac{q_i^{\uparrow} - q_i^{\downarrow}}{2}$ , since each electron has spin  $\frac{1}{2}$ . The state is then a mixture of spin multiplets with S values,  $S \geq M_S$ . In the high spin case (all electron spins parallel), the state has a unique spin  $S = M_S$ , but in general the spin state is not unique. We should then expect that excitation energies in the  $X_{\alpha}$  method represent a weighted average of multiplet excitations.

## THE TRANSITION STATE CONCEPT

Our next problem is to understand the relationship between excitation energies in the theory and the one electron energies  $\epsilon_i$  we have defined.<sup>5</sup> An excitation energy is simply the total energy difference between a ground and an excited eigenstate, so we may begin by relating the  $\epsilon_i$  to the total energy. The change in the total energy  $\delta E_{x\alpha}$  resulting from a small change in occupation number  $\delta n_i$  of orbital  $u_i$  is

$$5.18) \quad \frac{\delta E_{x\alpha}}{\delta n_i} = \frac{\partial E_{x\alpha}}{\partial n_i} + \left( \frac{dE_{x\alpha}}{dn_i} \right)_{\text{Implicit}}$$

The first term is the explicit change in  $E_{x\alpha}$  found by taking  $\frac{\partial}{\partial n_i}$  and holding the orbitals  $u_i$  fixed. However, the orbitals  $u_i$  implicitly depend on the occupation numbers  $n_i$  since these determine the self-consistent field. Straight-forward differentiation of the first term yields

$$5.19) \quad \frac{\partial E_{x\alpha}}{\partial n_i} = \xi_i$$

For the second term one obtains

$$5.20) \quad \left( \frac{dE_x}{dn_i} \right)_{\text{Implicit}} = \frac{1}{dn_i} \sum_{j=1}^N \frac{dE_{x\alpha}}{du_j} du_j + \text{c.c.} = \frac{1}{dn_i} \delta E_{x\alpha} = 0$$

(with c.c. meaning complex conjugate). Here  $E_{x\alpha}$  is the same variation of the total energy which is 0 as a consequence of the minimum principle. We therefore conclude that

$$5.21) \quad \frac{\delta E_{x\alpha}}{\delta n_i} = \epsilon_i, \quad \delta E_{x\alpha} = \epsilon_i \delta n_i$$

The lowest total energy is then obtained when levels of

minimum  $\epsilon_i$  are occupied subject to the exclusion principle  $0 \leq n_i \leq 1$ . This is consistent with Fermi statistics. Also, the meaning of the one electron energies  $\epsilon_i$  in  $X_\alpha$  theory is that of a differential ionization potential, or of a differential electron affinity.<sup>5</sup> The true ionization potential from orbitals  $u_i$  is not given by  $-\epsilon_i$ , since ionization corresponds to the removal of one electron from orbital  $u_i$ , not a small fraction of an electron as described in equation 5.21.

From equation 5.21 it can be shown that the ionization potential from orbital  $u_i$  is given by  $-\bar{\epsilon}_i^T$ , where  $\bar{\epsilon}_i^T$  is the eigenvalue of orbital  $i$  not for the ground state configuration but rather for a configuration having  $\frac{1}{2}$  an electron removed from shell  $i$ . Similarly, optical excitation energies are given to a good approximation by  $\epsilon_j^T - \epsilon_i^T$ . Here  $\epsilon_i^T$  and  $\epsilon_j^T$  are one electron eigenvalues for a configuration having  $\frac{1}{2}$  an electron removed from shell  $i$  and  $\frac{1}{2}$  an electron added to shell  $j$ . (These states are called the transition states of the system.)

To prove this, we compute the excitation energy by making a Taylor series expansion of the total energy as a function of occupation number.<sup>5</sup> The total energy is uniquely defined if for any set of occupation numbers the variational principle is assumed to hold. The derivatives in the expansion  $\frac{dE_{x\alpha}}{dq_i}$  include the implicit dependence of  $u_j$  on  $q_i$ . Let  $q_j = q_j - q_{j1}$ , where  $q_{j1}$  is the set of shell (level) occupation numbers taken as a reference point for the total energy.

$$5.22) \quad E_{x\alpha}(q_1 \dots q_k) = E_{x\alpha} | 0^+ \sum_j \frac{dE_{x\alpha}}{dq_j} \Big|_0 \Delta q_j + \frac{1}{2!} \left( \sum_j \Delta q_j \frac{d}{dq_j} \right)^2 E_{x\alpha} | 0 \\ + \frac{1}{3!} \left( \sum_j \Delta q_j \frac{d}{dq_j} \right)^3 E_{x\alpha} | 0^+ \dots$$

with the subscripts 0 referring to the reference state. Let the transition be from an initial level  $i$  to a final level  $j$ . Let  $q_i$  (initial),  $q_j$  (initial),  $q_i$  (final),  $q_j$  (final) be the level occupation numbers for the initial and final eigenstates. Then using the transition state configuration as our reference state

$$5.23) \quad q_i \text{ (final)} = q_i \text{ (initial)} - 1 \\ q_j \text{ (final)} = q_j \text{ (initial)} + 1 \\ q_{i1} = q_i \text{ (initial)} - \frac{1}{2} \\ q_{j1} = q_j \text{ (initial)} + \frac{1}{2}$$

Since only two levels are effected all other  $\Delta q_j = 0$ . The resultant excitation energy is

$$5.24) \quad E_{x\alpha} \text{ (final)} - E_{x\alpha} \text{ (initial)} = \frac{dE_{x\alpha}}{dq_j} \Big|_0 - \frac{dE_{x\alpha}}{dq_i} \Big|_0 = \\ \xi_j^T - \xi_i^T + 3\text{rd order terms}$$

from the definition of the reference state we gave previously. The reference state of equation 5.23 is called the transition state of the system. In the next chapter we will find that in addition to giving the approximate excitation energies of the molecule  $\xi_j^T - \xi_i^T$ , the transition state orbitals  $u_i^T$  provide a useful basis set for the calculation of optical intensities.



## THE SCATTERED WAVE METHOD

In order to solve the self-consistent equations 5.15 for the spin orbitals  $n_i$  and one electron energies  $\epsilon_i$ , it is necessary to make further approximations. In the scattered wave method, developed by Johnson, we partition the molecule into three adjacent regions I) atomic, II) interatomic, and III) extramolecular. The potential  $V = V_c + V_{x\alpha}$  is approximated by its spherical average in each of the atomic regions (I), by a volume averaged potential (a constant) in the interatomic region (II), and by a spherical average about the center of the molecule in the extramolecular region (III).

The initial potential for the self-consistent field (SCF) calculation is found from the superposition

$$5.25) \quad V(\vec{x}) = \sum_g V_g(|\vec{x} - \vec{R}_g|)$$

of free atom or free ion SCF- $X_\alpha$  potentials centered at positions  $R_g$ . These potentials and the related charge densities are generated by a program by Herman and Skillman, modified for the use of selected  $X_\alpha$  parameters.<sup>88</sup> The  $\alpha$  parameter is determined in the manner discussed in the  $X_\alpha$  theory section. The appropriate parameters have been calculated by Schwarz using Mann's Hartree-Fock values.<sup>89</sup>

This form of potential is called the muffin tin approximation when the atomic regions do not overlap each other or the extramolecular region. The use of overlapping spheres has been found to yield a generally superior description of

molecular properties for a modest degree of overlap, although the mathematical formulation of this theory is less clearcut.<sup>90</sup> The muffin tin approximation appears as well in the augmented-plane-wave (APW) and Korringa-Kohn-Rostoker (KKR) methods of crystal band theory, where it has proven quite successful.<sup>7,91,92</sup>

The spherically symmetric potentials in the atomic and extramolecular regions imply that the spin orbitals may be written as linear combinations of real spherical harmonics times radial functions  $R_{\ell}^g(\epsilon, r)$  with the appropriate coefficients  $C_L^g$  to be determined by the boundary conditions.<sup>6</sup> The index  $g$  designates each atomic region of radius  $b_g$ . The orbital inside each atomic sphere is then

$$5.26) \quad u_i^I(\vec{r}_g) = \sum_L C_L^g R_{\ell}^g(\epsilon, r_g) Y_L(\vec{r}_g) \quad (0 \leq r \leq b_g)$$

where  $L = (\ell, m)$  is the partial-wave (angular momentum) index. The position  $\vec{r}_g$  is measured with respect to the origin of the atomic region  $g, \vec{r}_g = 0$ . Similarly, the extramolecular region is designated by  $g = 0$  and the corresponding orbital is

$$5.27) \quad u_i^{III}(\vec{r}_0) = \sum_L C_L^0 R_{\ell}^0(\epsilon, r_0) Y_L(\vec{r}_0) \quad (b_0 \leq r < \infty)$$

with the origin at the center of the molecule. The functions  $R_{\ell}^g(\epsilon, r)$  satisfy the radial Schrodinger equation

$$5.28) \quad \left( -\frac{1}{r^2} \frac{d}{dr} r^2 \frac{d}{dr} + \frac{\ell(\ell+1)}{r^2} + V^g(r) - \epsilon \right) R_{\ell}^g(\epsilon, r) = 0$$

for the spherically averaged potential  $V^g(r)$ . The radial functions are finite at the origin of each atomic sphere and

are generated by outward numerical integration for trial values of  $\epsilon$  for each given  $\ell$ . The orbital in the extramolecular region decays exponentially at large distances from the molecule, and is obtained by numerically integrating the radial equation inward for given values of  $\epsilon$  and  $\ell$ .

In the interatomic region, the potential  $\bar{V}_{II}$  is constant, and the wave function satisfies the ordinary wave equation

$$5.29) \quad (\nabla^2 + \epsilon - \bar{V}_{II}) u_i^{II}(\vec{r}) = 0$$

The solution may be written as a sum of "outgoing" spherical waves scattered by the spherically averaged potentials in the atomic regions and an "incoming" wave scattered by the spherically averaged potential in the extramolecular region.

$$5.30) \quad u_i^{II}(\vec{x}) = \sum_g \sum_L A_L^g K_\ell^{(1)}(Kr_g) Y_L(\vec{r}_g) + \sum_L A_L^0 i_\ell(Kr_0) Y_L(\vec{r}_0) \text{ for } \epsilon < \bar{V}_{II}$$

where

$$5.31) \quad i_\ell(r) = i^{-\ell} j_\ell(ir)$$

is a modified spherical Bessel function,

$$5.32) \quad K_\ell^{(1)}(r) = -i h_\ell^{(1)}(ir)$$

is a modified spherical Hankel function of the first kind,

$$5.33) \quad K = (\bar{V}_{II} - \epsilon)^{\frac{1}{2}}$$

is the wave vector, and  $\vec{r}_g = \vec{x} - \vec{R}_g$ .

For  $\epsilon > \bar{V}_{II}$ , the solution is

$$5.34) \quad u_i^{II}(\vec{x}) = \sum_g \sum_L A_L^g n_\ell(Kr_g) Y_L(\vec{r}_g) + \sum_L A_L^0 j_\ell(Kr_0) Y_L(\vec{r}_0)$$

where

$$K = (\epsilon - \bar{V}_{II})^{\frac{1}{2}}$$

and  $n_\ell$  ( $Kr_g$ ) and  $j_\ell$  ( $Kr_g$ ) are ordinary spherical Neumann and Bessel functions.

Physically, we see that the wave functions for the levels lying lower in energy than the constant interatomic potential should decay exponentially in the interatomic region. This explains the imaginary argument of the spherical Bessel and Hankel functions of equations 5.31 and 5.32. The wave functions for the higher lying levels ( $\epsilon > \bar{V}_{II}$ ) should appear as standing waves in the intersphere region, decaying only when they reach the extramolecular region.

Because the model potential has only finite jump discontinuities at the sphere boundaries and is continuous elsewhere, both the wave functions and their first derivatives must be continuous everywhere. In particular, the wave functions and their first derivatives must be continuous across the sphere boundaries. This condition is only satisfied for certain values of  $\epsilon$ , the one electron eigenvalues  $\epsilon_i$ , which then leads to unique values of the eigenvectors  $\{C_L^g, C_L^0\}$  and  $\{A_L^g, A_L^0\}$ , and of the radial functions  $\{R_\ell^g, R_\ell^0\}$  for each orbital  $u_i$ . Degenerate orbitals have the same radial functions  $\{R_\ell^g, R_\ell^0\}$ , with the eigenvectors,  $\{C_L^g, C_L^0\}$  and  $\{A_L^g, A_L^0\}$  related by symmetry. The calculations are done via the scattered wave formalism described by Johnson.<sup>6</sup>

The use of group theory further simplifies the problem, and allows a solution for the eigenstates and eigenvalues of the model potential in a moderate amount of computer time.

The occupied eigenstates are then used to construct a new potential, and the calculation is carried to self-consistency.

For excitations, a separate self-consistent calculation is done for each transition state (one calculation per transition). However, in complex systems the scattered wave procedure is sufficiently quick so that this does not become a serious hindrance, unlike a separate determinantal calculation in Hartree-Fock theory. In addition, a one electron energy difference  $\epsilon_j^T - \epsilon_i^T$  will yield a far better excitation energy than a direct total energy difference in a complex system, since one is talking about excitation energies of a few electron volts out of total energies of typically a thousand Rydbergs.

Although the muffin tin approximation yields a fairly accurate description of electronic structure in many systems, a further improvement of the physical realism of the model may be obtained by using overlapping atomic spheres. In this way, one obtains a more realistic representation of the potential in the interatomic region.

## THE USE OF OVERLAPPING ATOMIC SPHERES

In the last section, we showed that the use of non-overlapping spheres led to a well defined mathematical formulation of the scattered wave theory. The overlapping sphere method may be looked at in two ways: 1) as a truncation at the  $\ell=0$  potential term (about each nuclear center) of a precise cellular multiple scattering theory, plus some additional approximations, or 2) as an approximate method for solving Schrodinger's equation in spherical overlapping regions with central field potentials in each region.<sup>90,93</sup> Following a recent discussion by Herman and co-workers, we will adopt the second approach.<sup>90</sup>

There are two separate problems involved in the scattered wave method. First, we must find the electrostatic and exchange-correlation potentials,  $V_C + V_{X\alpha}$ . Second, we must solve Schrodinger's equation for this potential. To obtain the electrostatic potential, we must solve Poisson's equation

$$5.35) \quad \nabla^2 V_C = -4\pi\rho$$

which we may convert to integral form

$$5.36) \quad V_C(x_1) = \int \rho(x_2) \frac{2}{|\vec{x}_1 - \vec{x}_2|} dv_2$$

where we now include the nuclear charge densities in  $\rho$ . We may expand this result in spherical harmonics about a particular nuclear center for any charge distribution<sup>94</sup>

$$5.37) \quad \rho(\vec{r}) = \sum_{\ell, m} Y_{\ell m}(\theta, \phi) \rho_{\ell m}(r)$$

$$5.38) \quad V_C(\vec{r}) = \sum_{\ell, m} Y_{\ell m}(\theta, \phi) \frac{4\pi}{2\ell+1} \left[ \frac{1}{r^{\ell+1}} \int_0^r (r')^{\ell+2} \rho_{\ell m}(r') dr' + r^\ell \int_r^\infty (r')^{-\ell+1} \rho_{\ell m}(r') dr' \right]$$

The first term is the potential from the charge inside radius  $r$ ; the second term arises from the charge outside  $r$ . The charge distribution within an atom, even when it is part of a molecule, is still basically spherically symmetric. The surrounding atoms are neutral and also have approximately spherical charge distributions. One should then expect that the primary term in  $V_C(r)$  would be the  $\ell=0$  potential  $V_{00}^C(r)$ , with some correction from the higher order harmonics.

Before proceeding to a discussion of Schrodinger's equation, it is necessary to consider the form of  $\rho$  used in the actual computational procedure, which differs from the precise  $\rho$  we have just defined.<sup>90</sup> The exact electronic charge density  $\rho_e(\mathbf{x})$  is defined by

$$5.39) \quad \rho_e(\vec{x}) = \sum_{i=1}^N |u_i(\vec{x})|^2$$

However, before solving Poisson's equation,  $\rho_e(\mathbf{x})$  is approximated by

$$5.40) \quad \rho_e(\vec{x}) \cong \bar{\rho} + \sum_g \tilde{\rho}_g(r_g); |\vec{x} - \vec{R}_0| \equiv r_0 < b_0, \rho_e(\vec{x}) \cong \rho_0^S(r_0); r_0 > b_0$$

This expression is in overlapping spherical form which must be explained further. Consider an arbitrary function  $F(\mathbf{x})$  which is approximated by another function  $f(\mathbf{x})$

$$5.41) \quad F(\vec{x}) \cong f(\vec{x}) \equiv \bar{f} + \sum_{g=1}^{\bar{M}} \tilde{f}_g(r_g); \quad |\vec{x} - \vec{R}_0| \equiv r_0 < b_0 \\ \equiv f_0^s(r_0); r_0 > b_0$$

where  $\bar{M}$  is the number of atoms in the system.  $\bar{f}$  is a constant, and  $\tilde{f}_g(r_g)$ , which is spherically symmetric, is assumed to vanish for  $r_g > b_g$  (the atomic sphere radius  $b_g$  in general overlaps other atomic spheres). The spherical average of the exact function  $F(\vec{x})$  about center  $g$  is given by

$$5.42) \quad f_g^s(r_g) = (4\pi)^{-1} \int d\hat{r}_g F(\vec{x}); r_g < b_g$$

with  $d\hat{r}_g$  denoting the element of solid angle. The prescription for finding  $\tilde{f}_g(r_g)$  is simply  $\tilde{f}_g(r_g) = f_g^s(r_g) - \bar{f}$ . We can see that in the region of overlap of atoms  $g$  and  $g'$ ,  $f^s$  is counted twice in the sense that

$$5.43) \quad f(\vec{x}) = f_g^s(r_g) + f_{g'}^s(r_{g'}) - \bar{f} \quad (\text{In the region of overlap of } g \text{ and } g')$$

This is clearly an undesirable feature. However, let us define  $\bar{f}$  so that at least the average value of  $f(\vec{x})$  is the same as the average value of  $F(\vec{x})$  inside the outer sphere

$$5.44) \quad \int_{W_0} d^3x F(\vec{x}) = \int_{W_0} d^3x f(\vec{x})$$

where  $\int_{W_g}$  indicates  $\int_0^{b_g} r_g^2 dr_g \int d\hat{r}_g$ , integrating over the interior of the atomic or outer sphere. The resulting value of  $\bar{f}$  is

then

$$5.45) \quad \bar{f} = \bar{W}^{-1} \left[ \int_{W_0} d^3x F(\vec{x}) - \sum_{g=1}^{\bar{M}} \int_{W_g} d^3x F(\vec{x}) \right]$$



where

$$5.46) \quad \bar{W} = \frac{4\pi}{3} \left( b_0^3 - \sum_{g=1}^{\bar{M}} b_g^3 \right)$$

Now we may simply identify  $f(\vec{x})$  with the approximated form of  $\rho_e$ . The quantity conserved by the definition of  $\bar{\rho}$  is the total number of electrons  $N$ .

$$5.47) \quad \bar{\rho} = \bar{W}^{-1} \left[ N - \sum_{g=0}^{\bar{M}} Q_g \right]$$

where

$$5.48) \quad Q_g \equiv 4\pi \int_0^{b_g} r_g^2 dr_g \rho_g^s(r_g)$$

$$Q_0 \equiv 4\pi \int_{b_0}^{\infty} r_0^2 dr_0 \rho_0^s(r_0)$$

$$\bar{W} \equiv \frac{4\pi}{3} \left[ b_0^3 - \sum_{g=1}^{\bar{M}} b_g^3 \right]$$

$Q_g$  is the total number of electrons inside atomic sphere  $g$ , and  $Q_0$  is the total number of electrons in the extramolecular region. The various  $\rho$  quantities simply correspond to the definitions we made for  $f(x)$ . The definitions for  $\rho$  we have made are equivalent to the way  $\rho$  is used in the computer program for either overlapping or non-overlapping spheres. In particular, for zero overlap, these formulae reduce to the muffin tin approximation.

From the overlapping spherical form of  $\rho_e(x)$  and the distribution of nuclear charge, we may evaluate the potentials  $V_{00}(\vec{r}_g)$  and  $\bar{V}_{II}$  by a straight-forward procedure.<sup>90</sup> Since the evaluation of the exchange potential  $V_{x\alpha}$  is no problem, let  $V_{00}(\vec{r}_g) = V_{00}^C(\vec{r}_g) + V_{00}^{x\alpha}(\vec{r}_g)$ , the latter being the spherically averaged exchange potential. The potentials

$V_{00}(r_g)$  are defined out to the respective sphere boundaries  $b_g$ , which exceed the muffin tin radii.

We may solve the Schrodinger equation on atom  $g$  in the potential  $V_{00}(\vec{r}_g)$  as a single center problem out to the radius  $b_g$ . We then match the solutions across the sphere boundaries to those in the intersphere region. The mathematical formulation is the same as in the muffin tin case, and leads to a solution which is continuous (with continuous first derivative) everywhere except in the overlap region of atoms  $g$  and  $g'$ . Beyond the muffin tin radius,  $V_{00}(\vec{r}_g)$  replaces the constant potential  $\bar{V}_{II}^{MT}$  of the non-overlapping sphere case as the model potential. Since  $\bar{V}_{II}^{MT}$  samples a much larger region of space (which is also less characteristic of the true potential) than  $V_{00}(\vec{r}_g)$ , the use of  $V_{00}(\vec{r}_g)$  results in a significant increase in the physical realism of the model. This is particularly apparent in open structures, where the fraction of intersphere volume is very large for zero overlap.

The remaining difficulty is that the wave function is not single valued in the overlap region of atoms  $g$  and  $g'$ .<sup>94</sup> We would particularly want to require continuity across a plane through the intersection of the atomic sphere boundaries. Johnson has found empirically that the wave function is approximately continuous and single value for modest overlap ( $b_g = 1.0 - 1.3 \times$  the muffin tin radius).<sup>95</sup> This is understandable, since for the wave function to be approximately single valued,  $V_{00}(r_g)$  and  $V_{00}(r_{g'})$  must be similar in the

overlap region. For excessive overlap, this condition and the resultant continuity of the wave function do not hold.

Occasionally, the approximations involved in the overlapping sphere method result in a negative intersphere charge  $\bar{\rho}\bar{w}$ .<sup>90</sup> This is not a serious problem if the charge is small, but it should be set to zero if the amount of charge becomes significant.

The overlapping sphere method has been applied to several systems with uniformly good results. Ionization potentials in good agreement with experiment have been obtained for  $H_2O$ ,  $CO$ , and  $N_2$ <sup>96</sup> as well as in larger systems like  $Cr(CO)_6$ <sup>97</sup> and  $TCNQ$ .<sup>90</sup> The method also yields substantial improvement in molecular total energies and potential curves.<sup>96</sup>

Another indication that the solution is close to the solution for the true  $X_\alpha$  potential  $V_c(\vec{x}) + V_{x\alpha}(\vec{x})$  comes from the virial theorem. The virial theorem says that the total potential energy of a molecule  $V_{Tot}$  (including nuclear-nuclear repulsion) is equal to the negative of twice the total kinetic energy  $T_{Tot}$ ,  $V_{Tot} = -2T_{Tot}$ . Alternatively, the molecular total energy  $E_{Tot}$  is given by  $E_{Tot} = -T_{Tot}$ . The theorem is satisfied exactly in atoms, molecules, and solids. Slater has also proved that the theorem is satisfied in  $X_\alpha$  theory if all regions of space are assigned the same  $\alpha$  value, which is approximately true in most calculations.<sup>74</sup> The introduction of the muffin tin approximation causes the virial coefficient to differ from the exact value of -2. However, with

overlapping spheres, the theorem may be satisfied exactly for the proper choice of  $b_g$ , generally about 1.3 x the muffin tin radius.<sup>90</sup> This is another sign that a modest amount of overlap yields an optimal solution to the  $X_\alpha$  Schrodinger equation.

As we have previously mentioned, a precise solution of the  $X_\alpha$  equations 5.15 is in principle possible. One can divide the molecular volume into a set of polyhedral cells (for example, of the Wigner-Seitz type), expand the potential in each cell in spherical harmonics about the nearest nucleus as is done in equation 5.38, solve the resulting Schrodinger equation in the various cells, and then match the solution across the boundaries.<sup>93</sup> In practice, one must truncate the angular momentum expansions of the potential and of the radial functions at a certain point, usually at about  $\ell=4$  for both. (In the  $\ell=0$  potential case, the radial functions are also generally truncated at no more than  $\ell=4$  on any center. The  $\ell=2$  term is generally sufficient for atoms with no d electrons). In the cellular method, one finds that the radial equations are coupled, in contrast to the separability found for spherically averaged potentials. The solutions are then more difficult to obtain, and require significantly more computer time. Williams and Morgan have completed such a calculation for the  $\Gamma$  point ( $k=0$ ) of the Brillouin zone of crystalline silicon.<sup>93</sup> Their results indicate that about two-thirds of the error in the muffin tin method may be

eliminated by employing overlapping spheres with modifications to eliminate double counting of charge in the overlap region. Even in its present form, however, the overlapping sphere approximation yields a fairly accurate solution of Schrodinger's equation without unnecessary complications.<sup>94</sup>

## CHAPTER VI

THE DEVELOPMENT OF A NEW APPROACH TO CALCULATING  
OPTICAL INTENSITIES BASED ON THE  $X_{\alpha}$  SCATTERED WAVE METHOD

## APPLICATION OF DENSITY MATRICES TO OPTICAL ABSORPTION

We approach the optical absorption problem through the use of density matrices, employing the single particle Liouville equation as the equation of motion for the density matrix.<sup>98,99</sup> Transitions between states arise from the  $\vec{A} \cdot \vec{p}$  term of the perturbing electromagnetic field of vector potential  $\vec{A}$ . Density matrix language allows us to discuss optical absorption within the context of the  $X_{\alpha}$  method, without invoking determinants which have no foundation within the theory, and without using many particle wave functions which imply a more comprehensive solution of the problem than is accessible. Such an approach does require us to make several plausible, though unproven, assumptions. After obtaining the theoretical optical coefficient, the real part of the conductivity tensor  $\text{Re} \sigma_{ij}$ , we relate this to the more phenomenological constants. Finally, in the next section on degeneracy and symmetry, we derive the general optical

constants for open shell and spin unrestricted systems as well as the more restricted cases.

Let  $\psi = \psi(1,2,\dots,N)$  be the many particle wave function for an N electron system. In general,  $(1) = (\vec{x}_1, \sigma_1)$  the complete coordinate includes the two valued spin coordinate  $\sigma_1$ , as well as the space coordinate  $\vec{x}_1$ . Then we define the first order density matrix by

$$6.1) \quad \rho(1,1') = N \int \psi^*(1',2,\dots,N) \psi(1,2,\dots,N) dv_2 \dots dv_N$$

which includes sums over spin coordinates as well as integrations over the space coordinates.<sup>5,87</sup> As in equations 5.1 and 5.2 the charge density is defined as  $\rho(1) = \rho(1,1)$  so when  $\sigma_1 = +1$ ,  $\rho(1) = \rho \uparrow(x_1)$  and  $\sigma_1 = -1$ ,  $\rho(1) = \rho \downarrow(x_1)$ . If the set of  $u_i$  is any complete orthonormal set of spin orbitals, then neglecting spin

$$6.2) \quad \rho(x_1, x_1') = \sum_{i,j} \gamma_{ij} u_i(x_1) u_j^*(x_1')$$

(In the following treatment of optical intensities, spin up and spin down excitations may be treated separately, each exactly along the lines we will follow). We can see that equation 6.2 differs from the diagonal density matrix of equation 5.2 by the presence of off-diagonal terms. However,  $\gamma_{ij}$  in equation 6.2 is Hermitean  $\gamma_{ij} = \gamma_{ji}^*$ ; this follows from the fact that the charge density  $\rho(x_1, x_1)$  must be real. Therefore,  $\rho(x_1, x_1')$  may be diagonalized by a unitary transformation, by standard methods.<sup>87</sup> Let  $U_{ij}$  be a unitary matrix, and  $v_1, v_2, \dots, v_N$  be a complete orthonormal set of orbitals related to

the original orbitals  $u_i$  by

$$6.3) \quad u_i = \sum_k v_k U_{ki}$$

Then

$$\begin{aligned} 6.4) \quad \rho(x_1, x_1') &= \sum_{i,j} \sum_{k,l} \gamma_{ij} v_k(x_1) U_{ki} v_l^*(x_1') U_{lj}^* \\ &= \sum_{k,l} \left( \sum_{i,j} U_{ki} \gamma_{ij} U_{jl}^+ \right) v_k(x_1) v_l^*(x_1') \\ &= \sum_{k,l} \gamma'_{kl} v_k(x_1) v_l^*(x_1') \quad \text{where } \gamma'_{kl} \\ &= \sum_{i,j} U_{ki} \gamma_{ij} U_{jl}^+ \end{aligned}$$

Since  $\gamma_{ij}$  is Hermitean,  $U_{ki}$  may be chosen so that  $\gamma'_{kl}$  is diagonal

$$6.5) \quad \gamma'_{kl} = n_k \delta_{kl}$$

with the resulting diagonal density matrix

$$6.6) \quad \rho(x_1, x_1') = \sum_i n_i v_i(x_1) v_i^*(x_1')$$

For a given state of the many electron system, the  $v_i$  are called the natural spin orbitals of the system, and equation 6.6 is called the natural orbital expansion. Unfortunately, the natural orbital expansion is prohibitively difficult to find in all but the simplest systems.<sup>87,100</sup> In addition, the sets of natural orbitals for the various states of a system are in general different, which again complicates the problem of evaluating properties.

We approach the problem by assuming that the diagonal density matrix of equation 5.2 representing a self-consistent set of orbitals, is a good approximate solution to the true



density matrix of equation 6.2. It is important to remember that the  $n_i$  of the natural orbitals are, in general, fractional even for closed shell systems in contrast to the  $X_\alpha$  rules for shell filling. The reasons for this are discussed in Dahl's article.<sup>87</sup> We should expect, therefore, that the appropriate  $n_i$  for the self-consistent orbitals at the Fermi energy or below should be smaller than those dictated by Fermi statistics at  $T = 0$ . In the absence of explicit formulae for the occupation numbers of such a pseudo-natural orbital expansion, we will employ  $X_\alpha$  occupation numbers in our calculations. The  $X_\alpha$  occupation numbers will later be seen as resulting from ensemble averaging over states with integral occupation numbers.

The use of self-consistent field (SCF) orbitals and occupation numbers from Fermi statistics has been employed previously by Ehrenreich and Cohen in their paper on the many electron problem.<sup>98</sup> In this paper, they show that their approach is equivalent to the random phase approximation (RPA) of many body theory.

The Ehrenreich and Cohen paper dealt specifically with the electromagnetic properties of crystals. We are dealing with molecules which makes the problem quite different. They considered an extended system with lattice periodicity, in which the orbitals are Block waves. When electrons make transitions between Block type states, the orbitals are sufficiently diffuse not to perturb the self-consistent field.

In the case of electronic transitions in atoms and molecules, however, the initial and final state self-consistent fields are different.

In the case of optical absorption, we may write the single particle Liouville equation<sup>98,99</sup>

$$6.7) \quad i\hbar \frac{\partial \rho(x, x', t)}{\partial t} = [H, \rho] = H(x, t) \rho(x, x', t) - \rho(x, x', t) H(x', t)$$

where

$$6.8) \quad H = H_{\text{SCF}} + \frac{e}{mc} \vec{A}_0 \cdot \vec{p} e^{-i\omega t}$$

$\vec{A}(t) = \vec{A}_0 e^{-i\omega t}$  is the vector potential of the electromagnetic field which induces the perturbation. The term in  $\vec{A} \cdot \vec{p}$  appears because of the modification of the kinetic energy term in the Hamiltonian due to the presence of the electromagnetic field

$\frac{\vec{p}^2}{2m} \rightarrow \frac{(\vec{p} + \frac{e\vec{A}}{c})^2}{2m}$ . Equation 6.7 is the equation of motion for the density matrix, with  $[H, \rho]$  being the expression which determines how  $\rho(x, x', t)$  evolves in time. As we have already pointed out  $H_{\text{SCF}}$  is ambiguous, since we do not know at what stage of the excitation process to evaluate  $H_{\text{SCF}}$ . Similarly, for a given transition, it is advantageous to use a single set of orthonormal basis orbitals. For  $H_{\text{SCF}}$ , we shall use the transition state Hamiltonian  $H_{\text{T}}$  for the given transition. This is equivalent to putting into the driving term of the Liouville equation a knowledge of both the initial and final states for the transition. This is plausible if we remember that the transition probability for a system depends on both its initial and final states. We let the system be initially in

its ground state, so we are describing absorption. We expand the ground state density operator in transition state orbitals  $u_i^T$ , and make the assumption that the density operator is still approximately diagonal. Essentially, we have chosen a basis set which is a compromise between the basis sets of the ground state and excited state self-consistent fields.

The ground state density operator is then

$$6.9) \quad (\rho_{op})_0 = \sum_i |u_i^T\rangle n_i \langle u_i^T|$$

in Dirac notation. The density operator  $\rho$  of equation 6.7 is given by the ground state operator  $\rho_0$ , plus a first order correction  $\rho_1$  due to the perturbing electromagnetic field

$$6.10) \quad \rho = \rho_0 + \rho_1$$

Letting  $H_T$  be the zeroth order Hamiltonian, with  $H_1 =$

$\frac{e}{mc} \vec{A}_0 \cdot \vec{p} e^{-i\omega t}$  the first order correction, we find a zero and a first order equation<sup>99</sup>

$$6.11) \quad i\hbar \frac{\partial \rho_0}{\partial t} = H_0 \rho_0 - \rho_0 H_0$$

$$i\hbar \frac{\partial \rho_1}{\partial t} = H_1 \rho_0 - \rho_0 H_1 + H_0 \rho_1 - \rho_1 H_0 - i\hbar \beta \rho_1$$

The zeroth order equation just says the matrix element  $(\rho_0)_{kl}$  is constant as we expect with  $(\rho_0)_{kk} = n_k$  and  $(\rho_0)_{kl} = 0$  for  $k \neq l$ . The equation for  $\rho_1$  contains the additional term  $-i\hbar\beta\rho_1$ , which was added to take into account the dissipative forces which cause de-excitation of the excited state. The lifetime of the excited state is then  $t = \frac{1}{\beta}$  and the width of the absorption line is  $2\hbar\beta$ . The finite lifetime of an excited state in a molecule is due to the spontaneous emission

probability, and to molecular collisions and interactions which cause changes in the vibrational sublevels of the excited state. Also contributing to the width of spectral lines is Doppler broadening.<sup>20</sup> While the latter effects are far more important than the spontaneous emission mechanism in accounting for the observed width of spectral lines, they are not simply describable by the additional term  $-i\hbar\beta\rho_1$ . This term is characteristic of the spontaneous emission mechanism and will yield a Lorentzian line shape. The other mechanisms will yield a superposition of such Lorentzians resulting in a broader band having a Voigt shape.<sup>101</sup> A further discussion of vibrational effects will be given later.

For simplicity, however, we will retain the form of equation 6.11, and take matrix elements of the first order equation

$$6.12) \quad i\hbar \frac{\partial(\rho_1)}{\partial t} k\ell = (H_1 \rho_0)_{k\ell} - (\rho_0 H_1)_{k\ell} + (H_0 \rho_1)_{k\ell} - (\rho_1 H_0)_{k\ell} \\ -i\hbar\beta(\rho_1)_{k\ell} = (n_\ell - n_k) \langle u_k^T | H_1 | u_\ell^T \rangle + \epsilon_k^T(\rho_1)_{k\ell} - \epsilon_\ell^T(\rho_1)_{k\ell} \\ -i\hbar\beta(\rho_1)_{k\ell}$$

Since  $H_1 = \frac{e}{mc} \vec{A}_0 \cdot \vec{p} e^{-i\omega t}$ ,  $\rho_1$  will have the same time dependence leading to

$$6.13) \quad (\rho_1)_{k\ell} = \frac{n_k - n_\ell}{\epsilon_k^T - \epsilon_\ell^T - \hbar\omega - i\hbar\beta} \langle u_k^T | \frac{e}{mc} \vec{A}_0 \cdot \vec{p} | u_\ell^T \rangle e^{-i\omega t}$$

Since the expectation value of an observable (for a one particle operator) may be written as<sup>99</sup>

$$6.14) \quad \langle O \rangle = \sum_k O_{k\ell} \rho_{\ell k} = \text{Tr}(O\rho)$$

and the current density operator is  $-\frac{1}{\Omega} \frac{e\hbar\vec{\nabla}}{im}$  (to lowest order in the vector potential), with  $\Omega$  the volume containing  $M$  absorbing molecules, we obtain

$$\begin{aligned}
 6.15) \quad \langle j \rangle &= \frac{1}{\Omega} \sum_{\mathbf{k}, \ell} \rho_{\mathbf{k}\ell} \langle u_{\ell}^T | \frac{-e\hbar\vec{\nabla}}{im} | u_{\mathbf{k}}^T \rangle \\
 &= \frac{-ie^2\hbar^2}{m^2\omega} \frac{M}{\Omega} \sum_{\mathbf{k}, \ell} \frac{n_{\mathbf{k}} - n_{\ell}}{\epsilon_{\mathbf{k}}^T - \epsilon_{\ell}^T - \hbar\omega - i\hbar\beta} \langle u_{\mathbf{k}}^T | \vec{\nabla} | u_{\ell}^T \rangle \\
 &\quad \langle u_{\ell}^T | \vec{\nabla} | u_{\mathbf{k}}^T \rangle \cdot \vec{E}_0 e^{-i\omega t}
 \end{aligned}$$

where  $\vec{E}$  is the electric field vector  $\vec{E} = E_0 e^{-i\omega t}$  and  $\vec{\dot{E}} = -\frac{1}{c} \cdot \frac{\partial \vec{A}}{\partial t}$  so that  $\vec{E}_0 = +i\omega \vec{A}_0$ . We notice that  $\frac{M}{\Omega}$  is simply the molecular density  $\bar{N}$ , and that the entire expression to the left of  $\vec{E}_0 e^{-i\omega t}$  constitutes the conductivity tensor as a function of angular frequency  $\omega$ ,  $\sigma_{ij}(\omega)$ . As we shall show later, the real part of  $\sigma_{ij}$ ,  $\text{Re}\sigma_{ij}$  leads to absorption.

The conductivity may be converted from the matrix element of  $\vec{\nabla}$  form to a matrix element of the dipole moment operator form by noting the commutator relation

$$6.16) \quad \frac{1}{i\hbar} [\vec{x}, H_T] = \frac{\vec{p}}{m}, \quad \vec{p} = -i\hbar\vec{\nabla}, \quad \frac{m}{\hbar^2} [\vec{x}, H_T] = \vec{\nabla}$$

with  $H_T$  again the one electron Hamiltonian for the states in question. The local character of the  $X_{\alpha}$  potential allows this identity, which is only approximate with a non-local Hartree-Fock potential. A detailed discussion of this issue will be given in Chapter VI Section C. Substituting into equation 6.15 we derive the formula for the conductivity

$$\begin{aligned}
 6.17) \quad \text{Re } \sigma_{ij} &= \Pi e^2 \omega \bar{N} \sum_{\mathbf{k}, \ell} (n_{\ell} - n_{\mathbf{k}}) \langle u_{\mathbf{k}}^T | x_i | u_{\ell}^T \rangle \langle u_{\ell}^T | x_j | u_{\mathbf{k}}^T \rangle \\
 &\quad \cdot \delta(\epsilon_{\mathbf{k}}^T - \epsilon_{\ell}^T - \hbar\omega)
 \end{aligned}$$

taking the spectral line width to be small for convenience. Notice that our assumptions have led to an excitation energy of  $\Delta E = \hbar\omega = \epsilon_k^T - \epsilon_l^T$  in accordance with the results of Chapter VB.

Now, if we consider the light to be unpolarized, only the diagonal matrix elements of  $\text{Re}\sigma_{ij}$  will contribute to the transition rate for absorption. The true time dependent electric field in the  $x$  direction is given by  $\vec{E}_x(t) = \text{Re} \vec{E}_{0x} e^{-i\omega t} = E_{0x} \cos\omega t$ . Similarly, the physically meaningful current is  $\vec{J}(t) = \text{Re} \vec{J}_0 e^{-i\omega t}$ . Since the fields in the  $x$ ,  $y$ , and  $z$  directions have equal magnitude,  $|E_{0x}|^2 = |E_{0y}|^2 = |E_{0z}|^2$ . The time averaged rate of energy absorption per unit volume is  $\frac{1}{2}\text{Re}(\vec{J}_0 \cdot \vec{E}_0^*)$ , and the time averaged energy flux or Poynting's vector is  $\text{Re}(\vec{E}_0 \times \vec{H}_0^*) = \text{Re}(\vec{E}_0 \times \vec{B}_0^*)$  for non-magnetic materials.<sup>80</sup> The ratio of these two quantities is the absorption coefficient.<sup>83,101</sup>

$$6.18) \quad \eta = \frac{\frac{1}{2}\text{Re}(\vec{J}_0 \cdot \vec{E}_0^*)}{\frac{c}{8\pi} \text{Re}(\vec{E}_0 \times \vec{B}_0^*)} = \frac{4\pi}{c} \frac{\text{Re}\left(\sum_{j=1}^3 \sigma_{jj}\right) |E_{0x}|^2}{3|E_{0x}|^2}$$

The numerator  $\frac{1}{2}\text{Re}(\vec{J}_0 \cdot \vec{E}_0^*)$  must then be integrated over wave number to eliminate the  $\delta$  function of equation 6.17.

Before going further, we notice that two assumptions were made in obtaining the last expression of equation 6.18. The assumptions are: 1) that the effective electric field at the absorbing molecule which produces the current  $\vec{J}_0$  is the same as the average macroscopic electric field  $\vec{E}_0$ , and 2) that the Poynting's vector is given in terms of the average

macroscopic electric field  $E_0$  by the free space expression,  $\frac{3c}{8\pi} |E_{0x}|^2$  (where the factor of 3 arises from the random polarization of the Poynting's vector). Neither of these assumptions is fundamentally correct. These points were previously discussed in the section on local field corrections (Chapter IV D).

In Appendix C, we will demonstrate that equation 6.18 coincides with the phenomenological definition of the absorption constant.<sup>101</sup>

$$6.19) \quad I(\nu) = I_0(\nu) e^{-\eta \ell}$$

giving the attenuation of the intensity  $I(\nu)$  ( $\nu$  is the ordinary frequency), with penetration depth  $\ell$  in the material.  $I_0(\nu)$  is the intensity at zero penetration (the reflected intensity is not counted in  $I_0(\nu)$ ). We shall relate  $\eta$  to the integrated molar extinction coefficient  $\int \epsilon_m d(\frac{1}{\lambda})$ , which (aside from local field effects) depends only on the intrinsic properties of the absorbing molecules, and to the oscillator strength  $f$  of a transition. The results are<sup>23,101</sup>

$$6.20) \quad \int \epsilon_m d(\frac{1}{\lambda}) = \frac{A}{10^3 \ell n 10} \frac{2\pi e^2 \Delta E}{3\hbar^2 c^2} \sum_{k=\text{degenerate}} \sum_{\ell=\text{degenerate}} (n_\ell - n_k) \left| \langle u_K^T | \vec{x} | u_\ell^T \rangle \right|^2$$

$$6.21) \quad f = \frac{2m\Delta E}{3\hbar^2} \sum_{k=\text{deg.}} \sum_{\ell=\text{deg.}} (n_\ell - n_k) \left| \langle u_K^T | \vec{x} | u_\ell^T \rangle \right|^2$$

$$6.22) \quad f = \frac{10^3 \ell n(10) mc^2}{A\pi e^2} \int \epsilon_m d(\frac{1}{\lambda}) = 4.319 \times 10^{-9} \int \epsilon_m d(\frac{1}{\lambda})$$

Here  $\frac{1}{\lambda}$  = wave number,  $\Delta E = \epsilon_K^T - \epsilon_\ell^T$  = excitation energy,  $A$  = Avogadro's number =  $6.02 \times 10^{23}$ . The label "degenerate" means that all initial state orbitals  $u_\ell^T$  (with occupation numbers

$n_\ell$ ) summed over have a single one electron transition energy, all  $\epsilon_\ell^T = \epsilon_1^T$ , and similarly for final states, all  $\epsilon_k^T = \epsilon_2^T$ . Then  $\Delta E = \epsilon_2^T - \epsilon_1^T$ . In practice, measurements are made of  $\epsilon_m$  which is then converted to  $f$ , which has the simple theoretical form of equation 6.21.  $f$  is also dimensionless. These equations are, in fact, correct as they stand if one assigns the orbital occupation numbers  $n_\ell$ ,  $n_k$  the  $X_\alpha$  values for the initial state of the molecule. However, this point could stand further elaboration which is provided in the next section.



## SYMMETRY AND DEGENERACY

The generally fractional occupation numbers of equation 6.21 are difficult to interpret physically. It is easy to understand that if orbital  $u_{\ell}^T$  is occupied,  $n_{\ell} = 1$ , and orbital  $u_k^T$  is unoccupied,  $n_k = 0$ , then a transition may occur with a probability governed by equation 6.21. We, therefore, take the  $X_{\alpha}$  occupation numbers to represent an ensemble average of the initial configurations possible with different sets of integral occupation numbers  $\{n_{\ell}\}$ ,  $\{n_k\}$ .

Specifically, let each orbital be labeled by  $(\Gamma_1, p_1, s_1)$  and  $(\Gamma_2, p_2, s_2)$  for initial and final state orbitals respectively, with  $(\Gamma, p, s) = (\text{irreducible representation, partner, spin})$ . As before, by an initial state orbital we mean any orbital with a transition energy  $\epsilon_1^T$ ; final state orbitals have energy  $\epsilon_2^T$ , and the excitation energy  $\Delta E = \epsilon_2^T - \epsilon_1^T$ . Then for a given configuration,  $n = n(\Gamma, p, s)$  and  $n = 0$  or  $1$ . We take the ensemble average in the following manner. A transition from partner  $p_1$  to partner  $p_2$  with a specified spin  $s_1 = s_2 = 1$  (for example), will occur if  $n(\Gamma_1, p_1, 1) = 1$  and  $n(\Gamma_2, p_2, 1) = 0$ . We must count the number of times  $T$  this occurs in  $K$  possible initial state configurations and then divide by  $K$ . Let  $q_1$  electrons occupy the  $q_{10}$  initial state orbitals, and let there be  $q_2$  electrons in the  $q_{20}$  final state orbitals (with spin index  $s$ ).

$$6.23) \quad K = \begin{pmatrix} q_{10} \\ q_1 \end{pmatrix} \cdot \begin{pmatrix} q_{20} \\ q_{20}-q_2 \end{pmatrix}, \quad T = \begin{pmatrix} q_{10}^{-1} \\ q_1^{-1} \end{pmatrix} \cdot \begin{pmatrix} q_{20}^{-1} \\ q_{20}-q_2^{-1} \end{pmatrix},$$

$$\text{with } \binom{a}{b} = \frac{a!}{(a-b)!b!}$$

$$\frac{T}{K}(s) = \begin{pmatrix} q_1 \\ q_{10} \end{pmatrix} \cdot \begin{pmatrix} 1 - \frac{q_2}{q_{20}} \end{pmatrix}$$

$q_{10}$  and  $q_{20}$  as defined here are simply the orbital degeneracies of the levels. Since this analysis applies to each set of partners,  $p_1$ ,  $p_2$  and both spin indices  $s = 1, 2$ , we find

$$6.24) \quad f = \frac{2m\Delta E}{3\hbar^2} \sum_{s=1,2} n_1(s)(1-n_2(s))$$

$$\cdot \sum_{p_1, p_2} \left| \langle u^T(\Gamma_1, p_1, s) | \vec{x} | u^T(\Gamma_2, p_2, s) \rangle \right|^2$$

Here  $n_1(s) = \frac{q_1}{q_{10}}(s)$ ,  $n_2(s) = \frac{q_2}{q_{20}}(s)$ , so  $n_1(s)$  and  $n_2(s)$  are

simply the appropriate  $X_\alpha$  occupation numbers for each initial and final state orbital respectively. For the ground state of a system, there are two possibilities. Either 1)  $n_2(s) = 0$ , or 2)  $n_2(s) \neq 0$  and  $n_1(s) = 1$ . In either case,  $n_1(s)(1-n_2(s)) = n_1(s) - n_2(s)$ . Consequently,

$$6.25) \quad f = \frac{2m\Delta E}{3\hbar^2} \sum_{s=1,2} (n_1(s) - n_2(s))$$

$$\cdot \sum_{p_1, p_2} \left| \langle u^T(\Gamma_1, p_1, s) | \vec{x} | u^T(\Gamma_2, p_2, s) \rangle \right|^2$$

which is identical to equation 6.21. Either equation 6.24 or 6.25 may be used subsequently since we will always deal with the ground state as the initial state of the system. The use

of the spin index preserves the selection rule that the net spin remain unchanged during the transition. This is required for an electric dipole transition since the perturbation  $A \cdot p$ , producing the excitation, is spin independent and orbitals having different spin indices are orthogonal.

It will be useful to consider some particular cases. For example, consider a system treated within the spin restricted framework. Such a system is assumed to have no net spin. Then  $u^T$  is spin independent as are  $n_1$  and  $n_2$  yielding

$$6.26) \quad f = \frac{2m\Delta E}{3\hbar^2} \cdot 2(n_1 - n_2) \sum_{p_1, p_2} \left| \langle u^T(\Gamma_1, p_1) | \vec{x} | u^T(\Gamma_2, p_2) \rangle \right|^2$$

The case of a system with net spin (spin unrestricted) brings out other features. Here the transition state orbitals and energies are spin dependent (remember that the one electron equations for the orbitals and energies are spin dependent -- see equation 5.15; as are the occupation numbers  $n_1(s)$  and  $n_2(s)$ , with the lowest energy levels being filled first. In this case, the  $f$  value of equation 6.25 becomes two different oscillator strengths with some separation between the spectral peaks. This spin dependence of the line positions and intensities furnishes the rough equivalent of a multiplet theory in  $X_\alpha$ .

Going back to equation 6.25, notice that it is necessary to evaluate  $3q_{10} \cdot q_{20}$  matrix elements to find  $f$ . For any molecular point group, these matrix elements are related by

symmetry, and the respective ratios of the amplitudes  $\langle u^T(\Gamma_1, p_1) | x | u^T(\Gamma_2, p_2) \rangle$  (and similarly with  $y$  and  $z$ ) are called vector coupling coefficients. Tables of vector coupling coefficients for several point groups, including the tetrahedral group ( $T_d$ ) are available in Koster's "Properties of the 32 Crystallographic Point Groups."<sup>102</sup> We list the squares of the vector coupling coefficients for the tetrahedral  $T_d$  group in Table 1. This table is based on Koster's book and our own calculations. (Our computer programs are set up so that the vector coupling coefficients may be easily generated. The  $O_h$  group values may be obtained in this way. See Appendix A).

Finally, it is important to connect the definition of an oscillator strength, such as equation 6.25 with definitions based on the full many electron wave functions for initial and final states  $\psi_m$  and  $\psi_n$  (following Herzberg's notation).<sup>7,15</sup>

If the full many electron wave function  $\psi_m$  has degeneracy  $d_m$  with the individual degenerate wave functions labeled as  $\psi_{m_k}$ , and similarly with  $\psi_{n_i}$  being the partners of  $\psi_n$ , then

$$6.27) \quad f = \frac{2m\Delta E}{3\hbar^2 d_m} \sum_{i,k} \left| \langle \psi_{m_k} | \sum_{j=1}^N \vec{x}_j | \psi_{n_i} \rangle \right|^2$$

Simply, one averages over initial state many electron wave functions and sums over final state many electron wave functions. Such a method represents a generalization of equation 6.24. For example, if one takes an ensemble of determinants for  $\psi_m$  and a set of final state determinants for

$\psi_n$ , the numerical factors  $n_1(s)$  and  $n_2(s)$  appear exactly as in equation 6.24. If one considers a singlet to singlet transition (the final state must be a linear combination of 2 determinants to yield total spin  $S = 0$  and  $M_S = 0$ ), the numerical factor  $2(n_1 - n_2)$  of equation 6.26 results.

COMMUTATION RELATIONS, LOCAL FIELDS, AND THE  $\vec{V}V$  FORMALISM

We have previously mentioned the desirability of converting between the different oscillator strength forms  $f(\vec{x})$ ,  $f(\vec{V})$ ,  $f(\vec{x}, \vec{V})$  and  $f(\vec{V}V)$ . The different oscillator strength forms are equivalent in the framework of an exact theory.<sup>25</sup> We will prove in this section that the oscillator strength forms are also equivalent in any theory having a local one electron potential ( $V_{\text{eff}}$ ) which is common to the orbitals involved in the transition, a criterion which is met by the  $X_\alpha$  theory. Conversely, the oscillator strength forms are not equivalent in the Hartree-Fock theory which has a non-local effective potential  $V_{\text{eff}}$ . From these results, we will give the equation for  $f(\vec{V}V)$  in the  $X_\alpha$  scattered wave method, and discuss the physical implications of this equation.

First we consider the commutator relations<sup>75</sup>

$$\begin{aligned}
 6.28) \quad \frac{1}{i\hbar} [\vec{x}, H_{\text{eff}}] &= \frac{\vec{p}}{m} \\
 \frac{1}{i\hbar} [\vec{p}, H_{\text{eff}}] &= -\vec{V}_{\text{eff}}
 \end{aligned}$$

We now show that these relations are not true for the Hartree-Fock effective Hamiltonian  $H_{\text{eff}}$  defined previously (equation 4.4). First, the Hartree-Fock exchange term

defined in equation 4.9 is

$$6.29) \quad \int d\mathbf{v}_2 \sum_{\substack{\text{occupied} \\ \mathbf{k}}} w_i^*(1) w_k^*(2) \frac{-2}{|\vec{x}_1 - \vec{x}_2|} \frac{w_i(2) w_k(1)}{w_i(1) w_i^*(1)}$$

This has the form of a non-local potential, ... different for each orbital  $w_i(1)$ , acting on  $w_i(1)$ . Now consider the matrix element  $\langle w_i | \frac{1}{i\hbar} [\vec{x}, H_{\text{eff}}] | w_j \rangle = \langle w_i | \frac{1}{i\hbar} (\vec{x} H_{\text{eff}} - H_{\text{eff}} \vec{x}) | w_j \rangle$ . Using the adjoint property of the Hermitean operator  $H_{\text{eff}}$ , we obtain

$$6.30) \quad \langle w_i | \frac{1}{i\hbar} [\vec{x}, H_{\text{eff}} - H_{\text{eff}} \vec{x}] | w_j \rangle = \frac{1}{i\hbar} (\epsilon_j - \epsilon_i) \langle w_i | \vec{x} | w_j \rangle$$

$\epsilon_j - \epsilon_i$  is the Hartree-Fock energy difference between the occupied orbital  $i$  and the virtual orbital  $j$ . But  $H_{\text{eff}}$ , as applied to the left, is different from  $H_{\text{eff}}$  as applied to the right since the exchange potentials of equation 6.29 are different for orbitals  $w_i(1)$  and  $w_j(1)$ . Let  $H_{\text{eff}}^j = \frac{p^2}{2m} + V_1$ ,  $H_{\text{eff}}^i = \frac{p^2}{2m} + V_2$ . Then we find

$$6.31) \quad \begin{aligned} \frac{1}{i\hbar} (\vec{x} H_{\text{eff}}^j - H_{\text{eff}}^i \vec{x}) &= \frac{1}{i\hbar} (\vec{x} (\frac{p^2}{2m} + V_1) - (\frac{p^2}{2m} + V_2) \vec{x}) = \\ \frac{1}{i\hbar} (\vec{x} \frac{p^2}{2m} + \vec{x} V_1 - (\frac{-i\hbar\vec{p}}{m}) - \vec{x} \frac{p^2}{2m} - V_2 \vec{x}) &= \\ \frac{1}{i\hbar} (\frac{+i\hbar\vec{p}}{m} + \vec{x} (V_1 - V_2)) &= \frac{\vec{p}}{m} + \frac{\vec{x}}{i\hbar} (V_1 - V_2) \end{aligned}$$

Here  $V_1 - V_2$  is the difference in Hartree-Fock potentials for the orbitals  $j$  and  $i$ , which is just the difference in the respective exchange terms of equation 6.29. It is evident that, if the effective Hamiltonian were the same for both orbitals, only the first term of equation 6.31 would remain and the first commutator relation in equation 6.28 would hold. Similar considerations yield the second commutator relation of equation 6.28 in this case. The resulting equations would be

$$6.32) \quad \frac{1}{m} \langle w_i | \vec{p} | w_j \rangle = \frac{1}{i\hbar} (\epsilon_j - \epsilon_i) \langle w_i | \vec{x} | w_j \rangle$$

$$6.33) \quad \langle w_i | -\vec{\nabla} V_{\text{eff}} | w_j \rangle = \frac{1}{i\hbar} (\epsilon_j - \epsilon_i)^2 \langle w_i | \vec{p} | w_j \rangle$$

$$6.34) \quad \langle w_i | -\vec{\nabla} V_{\text{eff}} | w_j \rangle = \frac{-m}{\hbar^2} (\epsilon_j - \epsilon_i)^2 \langle w_i | \vec{x} | w_j \rangle$$

In the  $X_\alpha$  theory, we may take  $H_{\text{eff}} = H_T$ , the transition state Hamiltonian for an excitation between orbitals  $u_i^T$  and  $u_j^T$ . This Hamiltonian is the same for the two transition state orbitals  $u_i^T$  and  $u_j^T$  involved in the excitation so

$$6.35) \quad \langle u_i^T | -\vec{\nabla} V_T | u_j^T \rangle = \frac{-m}{\hbar^2} (\epsilon_j^T - \epsilon_i^T)^2 \langle u_i^T | \vec{x} | u_j^T \rangle$$



where  $V_{\text{eff}} = V_T$ , the transition state potential for the excitation. From the oscillator strength formula 6.24, we find

$$f = \frac{2m\Delta E}{3\hbar^2} \sum_{s=1,2} n_1(s) (1-n_2(s)) \sum_{p_1, p_2} |\langle u^T(\Gamma_1, p_1, s) |$$

$$| \vec{x} | u^T(\Gamma_2, p_2, s) \rangle|^2$$

$$6.36) \quad f = \frac{2\hbar^2}{3m(\Delta E)^3} \sum_{s=1,2} n_1(s) (1-n_2(s)) \sum_{p_1, p_2} |\langle u^T(\Gamma_1, p_1, s) |$$

$$| -\vec{\nabla} V_T | u^T(\Gamma_2, p_2, s) \rangle|^2$$

In Rydberg units,  $\frac{\hbar^2}{2m} = (1 \text{ Rydberg}) (1 \text{ bohr radius})^2 = 1$ .

We, therefore, obtain

$$6.37) \quad f = \frac{\Delta E}{3} \sum_{s=1,2} n_1(s) (1-n_2(s)) \sum_{p_1, p_2} |\langle u^T(\Gamma_1, p_1, s) |$$

$$| \vec{x} | u^T(\Gamma_2, p_2, s) \rangle|^2$$

$$6.38) \quad f = \frac{4}{3(\Delta E)^3} \sum_{s=1,2} n_1(s) (1-n_2(s)) \sum_{p_1, p_2} |\langle u^T(\Gamma_1, p_1, s) |$$

$$| -\vec{\nabla} V_T | u^T(\Gamma_2, p_2, s) \rangle|^2$$

The advantage of the second form lies in the particular character of  $-\vec{\nabla}V$  in the scattered wave method.  $V$  is radially symmetric in the atomic and outer sphere regions, and constant in the intersphere region. Thus,  $-\vec{\nabla}V_{\text{T}} = 0$  in region II, resulting in a matrix element which is a simple sum of terms over the atomic and extramolecular regions. The gradient takes the simple form

$$6.39) \quad \vec{\nabla}V = [\hat{i} \sin \theta \cos \phi + \hat{j} \sin \theta \sin \phi + \hat{k} \cos \theta] \frac{\partial V}{\partial r_g}$$

in each atomic region  $g$ , including the extramolecular region.

Here  $\hat{i}$ ,  $\hat{j}$ , and  $\hat{k}$  are unit vectors in the  $x$ ,  $y$ , and  $z$  directions, with  $(\theta, \phi)$  the cone and polar angles respectively referred to the atomic origin  $g$ . The  $\vec{\nabla}V$  matrix element is (suppressing the superscript T)<sup>103</sup>

$$6.40) \quad \langle u_i | +\nabla_x V | u_j \rangle = \sum_{gLL'L'} C_{LL'}^g C_{L'L}^g [ \int R_{\ell}^g(\epsilon_i, r_g) R_{\ell'}^g(\epsilon_j, r_g) \cdot \frac{\partial V}{\partial r_g} r_g^2 dr_g + R_{\ell}^g(\epsilon_i, b_g) b_g^2 (\Delta V) ] \cdot I_{11}(L; L')$$

$$\langle u_i | \nabla_y V | u_j \rangle = [ \quad ] \cdot I_{1-1}(L; L')$$

$$\langle u_i | \nabla_z V | u_j \rangle = [ \quad ] \cdot I_{10}(L; L')$$

It is necessary to describe this result more completely. The unprimed quantities refer to orbitals  $u_i$ , the primed quantities to  $u_j$ . (The forms of the orbitals  $u_i$  and  $u_j$  are specified in Chapter V C.) The open brackets [ ] mean that the same expressions precede  $I_{1+1}(L;L')$ ,  $I_{1-1}(L;L')$ , and  $I_{10}(L;L')$ . The range of integration is  $\int_0^{bg}$  for atomic spheres, and  $\int_{bo}^{\infty}$  for the extramolecular region. The quantity  $\Delta V$  is  $\bar{V}_{II} - V$  (inside sphere  $g$  on surface) for the atomic spheres  $g \neq 0$ , and  $V$  (outside on surface) -  $\bar{V}_{II}$  for the outer sphere,  $g = 0$ . The quantities  $I(L;L')$  are the Gaunt integrals

$$\begin{aligned}
 6.41) \quad I_{11}(L;L') &= \int \tilde{Y}_{11}(\hat{r}) Y_L(\hat{r}) Y_{L'}(\hat{r}) d\Omega \\
 I_{1-1}(L;L') &= \int \tilde{Y}_{1-1}(\hat{r}) Y_L(\hat{r}) Y_{L'}(\hat{r}) d\Omega \\
 I_{10}(L;L') &= \int \tilde{Y}_{10}(\hat{r}) Y_L(\hat{r}) Y_{L'}(\hat{r}) d\Omega
 \end{aligned}$$

where  $d\Omega$  denotes integration over solid angle,  $Y_L, Y_{L'}$  are the normalized real spherical harmonics, and  $\tilde{Y}_{11}(\hat{r}), \tilde{Y}_{1-1}(\hat{r}),$  and  $\tilde{Y}_{10}(\hat{r})$  are unnormalized  $\ell = 1$  harmonics defined by

$$\begin{aligned}
 6.42) \quad \tilde{Y}_{11}(\hat{r}) &= \sin \theta \cos \phi \\
 \tilde{Y}_{1-1}(\hat{r}) &= \sin \theta \sin \phi \\
 \tilde{Y}_{10}(\hat{r}) &= \cos \theta
 \end{aligned}$$

(Our Gaunt integrals, therefore, differ in normalization from those conventionally defined). The  $I(L;L')$  may be expressed as products of Clebsch-Gordon coefficients, and this is how they are generated within our computer program<sup>104</sup>. The detailed derivation of the  $\vec{V}V$  matrix elements, as well as the construction of the  $I(L;L')$  are described in Appendix B. The computer program for calculating intensities is listed and described in Appendix A.

As previously mentioned, the  $\vec{V}V$  matrix elements do not explicitly depend on the intersphere wave functions,  $u_i^{II}$  and  $u_j^{II}$ . This is in contrast with the matrix elements of  $\vec{x}$ , which require an explicit integration over this region. These integrations may either be done by putting the wave function in numerical form and carrying out a numerical 3-dimensional integration, or by putting the wave function in approximate one-center form in the intersphere region.<sup>56,69</sup> The  $\vec{V}V$  method, on the other hand, requires only one dimensional, numerical integrations, the angular integrations being performed combinatorially via the Clebsch-Gordon coefficients.

The equation 6.40 may be given an interesting physical interpretation. The total transition amplitude  $\langle u_i | \vec{V}V | u_j \rangle$  is a sum of transition amplitudes for the

various atomic regions and for the extramolecular region. On each center, a non-zero amplitude results only if  $I(L;L') \neq 0$  for the respective partial waves involved in coupling the initial to the final state. By the properties of the Gaunt integrals,  $I_{lm}(L;L') \neq 0$  only if  $\Delta l = |l' - l| = 1$ .<sup>6</sup> But this is just the dipole selection rule for atomic transitions in a central field.<sup>2</sup> The total transition amplitude is, therefore, a sum of atomlike transitions. The atomic amplitudes may have either sign, and so they can add either constructively or destructively. The transformation properties of the  $\vec{V}$  operator are the same as for  $\vec{x}$ , so the complete cluster obeys dipole selection rules. One can then tell from the symmetry of the irreducible representations when a zero total amplitude will result from the calculation.

Another important issue is the appearance of surface terms  $R_l^g(\epsilon_i, b_g) R_{l'}^g(\epsilon_j, b_g) b_g^{-2} \Delta V I_{lm}(L, L')$  in the amplitude equation. These arise from the finite jump in potential at each sphere boundary.  $\frac{dV}{dr}$  becomes a delta function at each sphere boundary, which then yields a finite surface term on integration. The terms, in effect, compensate for the absence of an integration over the intersphere region. The finite jump in potential may be regarded as an idealization of the more gradual rise in potential

expected as the electron moves away from the central field of a particular nucleus.

Finally, we should mention the issue of the intrinsic accuracy of the  $f(\vec{\nabla}V)$  form for the oscillator strength.  $f(\vec{\nabla}V)$  contains a factor  $\frac{1}{(\Delta E)^3}$  which becomes very large for small excitation energies. To obtain a reasonable oscillator strength in this case, the total transition amplitude  $\langle u_i | \vec{\nabla}V | u_j \rangle$  must be small. But since the transition amplitude is generally a small difference of atomic amplitudes, errors in these amplitudes can produce a large error in the final result<sup>18</sup>. In practice, one should expect failure of the  $\vec{\nabla}V$  form of  $f$  for sufficiently small excitation energies, and we will explore this issue further in Chapter 7B.

CHAPTER VII  
 APPLICATIONS OF THE  $\vec{V}$  FORM OF THE  
 OSCILLATOR STRENGTH IN THE  $X_\alpha$  SCATTERED WAVE METHOD  
 TEST CASES

Hydrogen Molecular Ion

As an initial test of the optical intensities program, we have calculated intensities for the  $1\sigma_g \rightarrow 1\sigma_u$  and  $1\sigma_g \rightarrow 1\Pi_u$  transitions in  $H_2^+$  at interatomic spacings  $R$  from 1.0 to  $5.0a_0$  (Bohr radii). The oscillator strengths and energy eigenvalues are presented in Tables 4, 5, and 6, and compared with the exact results of Bates and co-workers as well as with the approximate Gaussian basis set results of Lamb, Young, and LaPaglia<sup>54-56</sup>.

At  $R \leq 2.0a_0$ , the equilibrium nuclear separation, the scattered wave intensities are in good agreement with the exact values. The typical error is about 10% for the  $1\sigma_g \rightarrow 1\sigma_u$  transition, and 1% to 2% for the  $1\sigma_g \rightarrow 1\Pi_u$  transition. However, when the outer sphere is allowed to overlap the atomic spheres, the error in the calculated intensity increases to 22% for the  $1\sigma_g \rightarrow 1\sigma_u$  transition, and to 11% for the  $1\sigma_g \rightarrow 1\Pi_u$  ( $R \leq 2.0a_0$ , Case 1). This should not be surprising since the spherical averaging of the potential in the outer sphere region is probably

not much better than volume averaging in the vicinity of the atomic spheres. When combined with the approximations inherent in overlapping regions, a less reliable model results. At  $R = 2.0a_0$ , we may also compare the energy eigenvalues for the muffin tin model and the two overlapping sphere models (overlapping outer sphere and tangent outer sphere, respectively) in Table 5. While both overlapping sphere models yield better energy eigenvalues than the muffin tin models, overlapping the outer sphere produces only a very small change in energy compared with the tangent sphere.

For  $R = 3.0a_0$ , calculations were done with the atomic sphere radius  $b_1 = 1.35$  and  $1.5 \times b_N$  ( $b_N$  is the non-overlapping radius). For the larger overlap, the  $1\sigma_g \rightarrow 1\sigma_u$  intensity is much worse, while the  $1\sigma_g \rightarrow 1\Pi_u$  intensity improves a little. Our viewpoint is that  $b_1 = 1.5b_N$  constitutes excessive overlap, which is supported by the computed intensities. The scattered wave intensities are too low with either model, the most important discrepancy being in the  $1\sigma_g \rightarrow 1\sigma_u$  transition. By  $R = 5.0a_0$ , the scattered wave intensity is practically zero for  $1\sigma_g \rightarrow 1\sigma_u$  compared with the exact  $f = 0.175$ , while the scattered wave intensity for the  $1\sigma_g \rightarrow 1\Pi_u$  excitation is in



good agreement with the exact value, scattered wave  $f = 0.398$  and exact  $f = 0.430$ .

These results are intelligible in terms of the atomic orbital compositions of the states. The  $1\sigma_g$  and  $1\sigma_u$  states consist mostly of s and  $p_z$  functions on the atomic sites, while the  $1\Pi_u$  state is primarily composed of  $p_x$  atomic functions. In the large separation limit,  $1\sigma_g$  and  $1\sigma_u$  become  $H(1s) + \text{proton}$ , so for  $R \rightarrow \infty$ ,  $f = 0$  ( $1\sigma_g \rightarrow 1\sigma_u$ ), as we have found for  $R = 5.0a_0$ . The trouble is that at intermediate distances the proton polarizes the  $H(1s)$  state producing  $H(1s) + H(p_z)$ , and our spherical averaging at the atomic sites eliminates this polarization. For the  $1\Pi_u$  state, the polarization does not affect the intensity (asymptotically, the transition is  $s \rightarrow p_x$ ), and the scattered wave  $f$  value remains accurate.

Subsequent to these calculations, the optical intensities program was incorporated into the scattered wave computer programs. Certain variables, especially the energy eigenvalues and radial functions, were transferred more accurately to the optical intensity subroutine. We then recalculated the two transition intensities for  $R = 2.0a_0$ ,  $b_1 = 1.35b_N$ , and a tangent outer sphere, obtaining  $f(1\sigma_g \rightarrow 1\sigma_u) = 0.284$  and  $f(1\sigma_g \rightarrow 1\Pi_u) = 0.438$ . These results are about as accurate as before, but the

intensities are smaller by 21% and 5.5%. Our conclusions on the accuracy of the overlapping sphere  $f$  values should remain valid, though the muffin tin results may be less satisfactory with the improved computer program. (The last conclusion is based on the assumption that the muffin tin  $f$  values will decrease with the modified computer program, as we found for the overlapping sphere  $f$  values).

Finally, we should mention the issue of partial wave convergence, which is important in all the systems we shall treat. The truncation of the partial wave expansion in the scattered wave method will induce errors, and cause discrepancies between the different oscillator strength forms. For this reason, convergence of the  $f$  values must be insured by including a sufficient number of partial waves. For  $H_2^+$ , we include through  $\ell = 2$  on the hydrogen atoms, and  $\ell = 4$  on the outer sphere. Generally, it is necessary to include  $d$  functions on atoms where  $s$  and  $p$  functions are chemically important, and  $f$  functions on transition metal atoms. Sometimes convergence problems still persist, as we will describe further in the section on  $CO^+$ .

Table 4

 $H_2^+$  Optical Properties -- Oscillator Strengths

(R = internuclear distance,  $b_1$  = atomic sphere radius,  $b_N$  = non-overlapping atomic sphere radius,  $b_o$  = outer sphere radius, may be either tangent to or overlapping the atomic spheres,  $a_o$  = Bohr radius).

R	$\frac{b_1}{b_N}$	$b_o$	Scattered Wave f ( $\bar{V}V$ )	Exact f <sup>a,b</sup>
$1\sigma_g \rightarrow 1\sigma_u$				
1.0 $a_o$				
2.0 $a_o$				
	1.35	overlapping ( $b_o = 2.0 a_o$ )	0.247	0.319 Case 1
	1.35	tangent	0.358	0.319 Case 2
3.0 $a_o$	1.35	tangent	0.175	0.289 Case 3
	1.5	tangent	0.108	0.289 Case 4
5.0 $a_o$	1.35	tangent	$3.5 \times 10^{-4}$	0.175
$1\sigma_g \rightarrow 1\Pi_u$				
1.0 $a_o$	1.35	tangent	0.385	0.392
2.0 $a_o$	1.0	tangent	0.452	0.460
	1.35	overlapping ( $b_o = 2.0 a_o$ )	0.410	0.460 Case 1
	1.35	tangent	0.464	0.460 Case 2
3.0 $a_o$	1.35	tangent	0.412	0.479 Case 3
	1.5	tangent	0.430	0.479 Case 4
5.0 $a_o$	1.35	tangent	0.398	0.430

Table 4  
(continued)

(The various cases designate the different overlapping sphere models (1), (2), (3), and (4) at  $R = 2.0 a_0$  and  $R = 3.0 a_0$ ).

In all the calculations, partial waves through  $l = 2$  were used on each atomic center, and through  $l = 4$  on the outer sphere.

<sup>a</sup> Reference 54.

<sup>b</sup> Reference 55.

Table 5

 $H_2^+$  Energy Eigenvalues

(All Energies Measured in Rydbergs)

R = 1.0  $a_0$ 

<u>State</u>	<u>Overlapping Spheres</u>	<u>Exact</u> <sup>a</sup>
$1\sigma_g$	-2.8366	-2.9036
$1\sigma_u$	-1.1043	-1.1296
$1\Pi_u$	-0.9668	-0.9482

R = 2.0  $a_0$ 

<u>State</u>	<u>Muffin-Tin</u>	<u>Overlapping Spheres (1) &amp; (2)</u>	<u>Exact</u>
$1\sigma_g$	-2.072	-2.157 -2.155	-1.105
$1\sigma_u$	-1.288	-1.360 -1.366	-1.335
$1\Pi_u$	-0.889	-0.865 -0.860	-0.858

R = 3.0  $a_0$ 

<u>State</u>	<u>Overlapping Spheres (3) &amp; (4)</u>	<u>Exact</u>
$1\sigma_g$	-1.7939 -1.8689	-1.8218
$1\sigma_u$	-1.4312 -1.4476	-1.4028
$1\Pi_u$	-0.7651 -0.7539	-0.7729

R = 5.0  $a_0$ 

<u>State</u>	<u>Overlapping Spheres</u>	<u>Exact</u>
$1\sigma_g$	-1.4427	-1.4488
$1\sigma_u$	-1.3619	-1.3546
$1\Pi_u$	-0.6134	-0.6428

<sup>a</sup> Reference 55.

Table 6

$H_2^+$  Optical Properties -- Comparison of Oscillator Strengths by Scattered Wave Method with Gaussian results

(Overlapping sphere results with  $b_1 = 1.35b_N$ )

R Gaussian <sup>a</sup>	$f(x, \nabla)$	$f(x)$	$f(\nabla)$	Scattered Wave $f(\vec{\nabla})$	Exact $f^{b,c}$
$1\sigma_g \rightarrow 1\sigma_u$					
1.0 $a_0$	0.283	0.290	0.276	0.251	0.269
2.0 $a_0$	0.318	0.328	0.309	0.358	0.319
3.0 $a_0$	0.273	0.305	0.245	0.175	0.289
5.0 $a_0$	0.116	0.191	0.071	$3.5 \times 10^{-4}$	0.175
$1\sigma_g \rightarrow 1\Pi_u$					
1.0 $a_0$	0.359	0.368	0.350	0.385	0.392
2.0 $a_0$	0.433	0.426	0.440	0.464	0.460
3.0 $a_0$	0.425	0.390	0.463	0.412	0.479
5.0 $a_0$	0.338	0.270	0.423	0.398	0.430

<sup>a</sup> Reference 56.

<sup>b</sup> Reference 54.

<sup>c</sup> Reference 55.

## HYDROGEN MOLECULE

The scattered wave results for the  ${}^1\Sigma_g \rightarrow {}^1\Sigma_u$ ,  ${}^1\Sigma_g \rightarrow {}^3\Sigma_u$ , and  ${}^1\Sigma_g \rightarrow {}^1\Pi_u$  excitations are given in Table 7. The results are compared with the experimental excitation energies and with the CI oscillator strengths of Wolniewicz<sup>57</sup>. (The less accurate CI oscillator strength of Ehrenson and Phillipson is also included)<sup>33</sup>. The  ${}^1\Sigma_g \rightarrow {}^3\Sigma_u$  excitation is spin forbidden, and, therefore, the  ${}^3\Sigma_u$  energy eigenvalue was originally obtained by measuring the  $H_2$  emission spectrum from a higher lying  ${}^3\Sigma_g$  state.<sup>15</sup> All theoretical  $f$  values are given at the equilibrium nuclear separation  $R = 1.4 a_0$ , in accordance with the Franck-Condon principle.

The experimental singlet-triplet splitting of the  ${}^3\Sigma_u$  and  ${}^1\Sigma_u$  states is fairly large,  $\Delta E_{ST} = 1.6 - 1.7$  ev., so spin effects must be taken into account in the scattered wave calculations.<sup>15</sup> There are two possible approaches to this. As we have discussed before, in the spin unrestricted  $X_\alpha$  method, the  $M_s$  (z component of total spin) value for a shell is  $(M_s)_i = \frac{q_i\uparrow - q_i\downarrow}{2}$ , with total  $M_s = \sum_i (M_s)_i$ . Therefore, a state with  $M_s = 0$  is a simple mixture of a singlet and a triplet state, and a state with  $M_s = 1$  is a pure triplet for a two-electron

system. For excitation from a ground state singlet  $^1\Sigma_g$ , the excited state may have the same spin  $M_S = 0$ , or a flipped spin  $M_S = 1$ , with corresponding excitation energies  $\Delta E_{UN}$  and  $\Delta E_T$ . The singlet excitation energy  $\Delta E_S$  is then determined by  $E_{UN} = \frac{\Delta E_S + \Delta E_T}{2}$ , which implies  $\Delta E_S^{(1)} = 2\Delta E_{UN} - E_T$ . Alternatively, the spin restricted excited state may be considered as a mixture of a singlet with all three possible triplet states. The spin restricted excitation energy is  $\Delta E_{RES} = \frac{\Delta E_S + 3\Delta E_T}{4}$ , resulting in a singlet excitation energy  $\Delta E_S^{(2)} = 4 \Delta E_{RES} - 3\Delta E_T$ . Bagus and Bennett have derived these results by analogy with averages over spin states in Hartree-Fock theory.<sup>105</sup> They conclude that the singlet-triplet splitting  $\Delta E_{ST} = \Delta E_S - \Delta E_T$  by either method is an upper bound to the true value. Since  $\Delta E_S^{(1)} \neq \Delta E_S^{(2)}$ , one should use the least upper bound for  $\Delta E_{ST}$ .

For the  $^1\Sigma_g \rightarrow ^1\Sigma_u$  and  $^1\Sigma_g \rightarrow ^3\Sigma_u$  transitions, both the excitation energies and the oscillator strength are given quite accurately by the spin unrestricted formalism. This holds for both overlapping and non-overlapping spheres. The most accurate results are from the overlapping sphere calculations,  $\Delta E_T = 10.88$  ev.,  $\Delta E_S^{(1)} = 13.1$  ev.,  $\Delta E_{ST}^{(1)} = 2.33$  ev., and  $f = 0.296$  compared with the experimental values  $\Delta E_T = 10.6 - 10.7$  ev.,  $\Delta E_S = 12.27$  ev.,  $\Delta E_{ST} = 1.6 - 1.7$



eV., and  $f = 0.300$  (the Kolos-Wolniewicz value).

By contrast, the spin restricted formalism (with overlapping spheres) yields inaccurate values for  $\Delta E_S$  and  $\Delta E_{ST}$ , but the  $f$  value is of reasonable accuracy. The results are  $\Delta E_S^{(2)} = 19.5$  eV.,  $\Delta E_{ST}^{(2)} = 8.6$  eV., and  $f = 0.335$ . The result  $\Delta E_{ST}^{(1)} < \Delta E_{ST}^{(2)}$  was previously found for  $X_\alpha$  calculations in large molecules by Bagus and Bennett.<sup>105</sup> In addition,  $\Delta E_{ST}^{(1)}$  does form the least upper bound to the experimental  $\Delta E_{ST}$ .

The calculated oscillator strength and excitation energy for the  ${}^1\Sigma_g \rightarrow {}^1\Pi_u$  transition is in much poorer agreement with the experimental results, as shown in Table 7. The calculation was done only in the spin restricted form with overlapping spheres (no triplet was computed). Since  $\Delta E_S^{(2)} \geq \Delta E_{RES}$  the excitation energy error in spin restricted form is larger than 1.3 eV. result in the table. The state is particularly high lying in energy and diffuse (98% of the  $1\Pi_u$  charge is in the extra-molecular region), and is probably not well represented by the model. We notice, however, that use of the experimental  $\Delta E_S$  value in the intensity formula yields an improved value of  $f = 0.296$ . The  ${}^1\Pi_u$  wave function may, therefore, be of fair accuracy. The total spin restricted intensity for the Lyman and Werner bands of  $f = 0.555$  is

in reasonable agreement with the experimental value  $f = 0.65$ .

It is clear that the spin unrestricted results in  $H_2$  are superior to the spin restricted results for both intensities and excitation energies. In this regard, the self-consistent fields for the  $X_\alpha$  states are multiplet averaged fields. We may therefore postulate that the best states are achieved by averaging over the least number of multiplets, a condition satisfied in this case by the spin unrestricted formalism. Before accepting this conclusion, however, further comparisons with experiment in other systems are necessary.

Table 7  
H<sub>2</sub> Optical Properties

(Excitation Energies are  $\Delta E_{UN}$  = spin unrestricted,  $\Delta E_{RES}$  = spin restricted,  $\Delta E_T$  = triplet,  $\Delta E_S$  = singlet from the formulae  $\Delta E_S^{(1)} = 2\Delta E_{UN} - \Delta E_T$ ,  $\Delta E_S^{(2)} = 4\Delta E_{RES} - 3\Delta E_T$ . Overlapping sphere radius  $b_1 = 1.35 \times$  the muffin tin radius. The singlet-triplet splitting is  $\Delta E_{ST} = \Delta E_S - \Delta E_T$ ).

$1_{\Sigma_g} \rightarrow 1_{\Sigma_u}$  and  $1_{\Sigma_g} \rightarrow 3_{\Sigma_u}$

Non-overlapping Spheres, Spin Unrestricted

$$\Delta E_{UN} = 11.75 \text{ ev.}$$

$$\Delta E_T = 10.44 \text{ ev.}$$

$$\Delta E_S^{(1)} = 13.07 \text{ ev.}$$

$$\Delta E_{ST}^{(1)} = 2.63 \text{ ev.}$$

Oscillator Strength = 0.290

Overlapping Spheres, Spin Unrestricted

$$\Delta E_{UN} = 11.99 \text{ ev.}$$

$$\Delta E_T = 10.88 \text{ ev.}$$

$$\Delta E_S^{(1)} = 13.10 \text{ ev.}$$

$$\Delta E_{ST}^{(1)} = 2.33 \text{ ev.}$$

Oscillator Strength = 0.2956

Table 7  
(continued)

$1_{\Sigma_g} \rightarrow 1_{\Sigma_u}$  and  $1_{\Sigma_g} \rightarrow 3_{\Sigma_u}$

Overlap Spheres, Spin restricted

$$\Delta E_{RES} = 12.98 \text{ ev.}$$

$$\Delta E_T = 10.88 \text{ ev.}$$

$$\Delta E_S^{(2)} = 19.5 \text{ ev.}$$

$$\Delta E_{ST}^{(2)} = 8.6 \text{ ev.}$$

Oscillator Strength = 0.335

Experimental Results<sup>a</sup>

$$\Delta E_T = 10.6 \text{ ev. (based on indirect measurements)}$$

$$\Delta E_S = 12.27 \text{ ev.}$$

$$\Delta E_{ST} = 1.6 - 1.7 \text{ ev.}$$

Oscillator Strength = 0.27 (based on CI calculation of Ehrenson and Phillipson)<sup>b</sup>

Oscillator Strength = 0.300 (based on CI calculation of Kolos and Wolniewicz)<sup>c</sup>

$1_{\Sigma_g} \rightarrow 1_{\Pi_u}$

Overlapping Spheres, Spin Restricted

$$\Delta E_{RES} = 14.18 \text{ ev.}$$

Oscillator Strength = 0.222

Experimental Results

$$\Delta E_S = 12.9 \text{ ev.}$$

Table 7  
(continued)

Oscillator Strength = 0.356 (based on CI calculation of Kolos and Wolniewicz)<sup>c</sup>

$1\Sigma_g$  Ground State Energy

Non-Overlapping Spheres

E = 2.137 Rydbergs

Overlapping Spheres

E = 2.235 Rydbergs

Experimental Results<sup>c</sup>

E = 2.349 Rydbergs

<sup>a</sup> Reference 15.

<sup>b</sup> Reference 33.

<sup>c</sup> Reference 57.

## CARBON MONOXIDE POSITIVE ION

The  $X_\alpha$  theory  $f(\vec{V})$  values for the  $1\pi \rightarrow 5\sigma$  and  $5\sigma \rightarrow 2\pi$  transitions in  $\text{CO}^+$  were computed by the author. In Table 8, we compare these results with the corresponding Hartree-Fock  $f$  values (uncorrected), with the  $X_\alpha$  theory  $f(\vec{x})$  values (from the work of Messmer and Salahub), and with the experimental  $f$  value for the  $1\pi \rightarrow 5\sigma$  transition (there are no experimental intensities for the  $5\sigma \rightarrow 2\pi$  transition).<sup>22,59</sup> The important point here is that the  $f(\vec{V})$  values differ significantly from the  $f(\vec{x})$  values, although both sets of values were determined using the  $X_\alpha$  theory. Also, in the  $1\pi \rightarrow 5\sigma$  case, the  $f(\vec{V})$  intensity is about 5.4 times the experimental intensity, versus about 1.6 times the experimental intensity for the  $f(\vec{x})$  form.

The discrepancy may be understood in terms of basic theory. In the  $X_\alpha$  scattered wave theory, the  $f(\vec{x})$  and  $f(\vec{V})$  intensities are identical only if the model one electron Schrodinger equation is solved precisely. In practice, however, it is necessary to truncate the partial wave expansions in the various regions for a given orbital  $u_i$  to obtain a tractable secular problem. It is this basis set truncation that leads to the discrepancy

between the  $f(\vec{\nabla}V)$  and  $f(\vec{x})$  forms. The two oscillator strength forms become identical only in the limit of a large number of partial waves on all centers. An indication of this relationship is given by the  $1\Pi \rightarrow 5\sigma$  intensities in Table 8.  $f(\vec{\nabla}V)$  is slowly converging to a lower value as we increase the number of partial waves on the different centers. The  $f(\vec{\nabla}V)$  value is therefore approaching both the  $f(\vec{x})$  value and the experimental  $f$  value. The  $f(\vec{\nabla}V)$  value (at  $\ell = 4$  on all centers) is not of quantitative accuracy, but this value does clearly indicate that the  $1\Pi \rightarrow 5\sigma$  transition has a low intensity. In Chapter VI, we proved that the total transition amplitude for a molecule in the  $f(\vec{\nabla}V)$  method is a sum of atomiclike amplitudes. Generally, there is a great deal of cancellation between these atomic amplitudes, so that the total amplitude is a small difference of much larger amplitudes. Under these circumstances, the slow convergence of  $f(\vec{\nabla}V)$  particularly in the case of low intensity transitions is not surprising.

In conclusion, it seems that  $f(\vec{x})$  has better partial wave convergence properties than does  $f(\vec{\nabla}V)$  in the  $x_\alpha$  scattered wave theory. The  $f(\vec{x})$  intensity for the  $1\Pi \rightarrow 5\sigma$  transition is very good considering the problems involved

in evaluating both the theoretical and the experimental intensities. A general conclusion on whether the  $f(\vec{x})$  form is to be preferred to the  $f(\vec{V})$  form can only be obtained after more extensive comparisons of the two methods.



Table 8  
CO<sup>+</sup> Oscillator Strengths

Transition	Hartree-Fock $f^a$	X <sub>α</sub> Theory		Experimental $f$
		$f(\vec{x})^b$	$f(\vec{V}V)$	
1Π→5σ	0.0177	0.0088	0.030	0.0056
5σ→2Π	0.105	0.0476	0.081	

Convergence of  $f(\vec{V}V)$

	f with $\ell = 2$	$\ell = 4$ on all centers
1Π→5σ	0.064	0.030

<sup>a</sup> Reference 22.

<sup>b</sup> Reference 59.

## TRANSITION METAL COMPLEXES

The transition metal complexes treated in this work were chosen to exemplify the wide variety of possible excitations in complex molecules.  $\text{MnO}_4^{-1}$  has a closed shell electronic structure; transitions in this complex are dipole allowed ligand to metal charge transfer in nature.<sup>9</sup>  $\text{FeCl}_4^{-1}$  was chosen as an example of an open shell system in which spin effects would be important (total spin  $S = +\frac{5}{2}$ ).<sup>4</sup> The electronic structure of this system is sufficiently close to that in  $\text{MnO}_4^{-1}$  so that comparisons of analogous transitions in the two systems would be meaningful. In both cases, the molecular structure is tetrahedral.  $\text{CoCl}_4^{-2}$ , also with a tetrahedral structure, has an  $e \rightarrow t_2$  (metal 3d  $\rightarrow$  metal 3d) crystal field transition in addition to ligand to metal charge transfer transitions closely analogous to those in  $\text{FeCl}_4^{-1}$ .<sup>4,47</sup> We are interested in the ability of the  $X_\alpha$  theory to predict the average over multiplets of the  $e \rightarrow t_2$  crystal field transition energy. We are also interested in the usefulness of the  $\vec{V}V$  method in predicting the intensity of the  $e \rightarrow t_2$  transition which occurs at low energy, about 0.5 eV.<sup>48-50</sup> The  $\vec{V}V$  method

becomes less reliable for low excitation energies, as we have discussed previously.  $\text{Cr}(\text{CO})_6$  is the largest cluster we will consider. The primary dipole allowed transitions in this system have a metal to ligand charge transfer character in contrast to the previous cases.<sup>51</sup>  $\text{Cr}(\text{CO})_6$  has an octahedral structure. Vibronic transitions can therefore occur in this complex when an odd normal mode vibration destroys the molecular inversion center.<sup>7,51</sup> Although we will not predict vibronic intensities, we will compare the corresponding excitation energies with our theory for vibronic coupling. We have predicted that vibronic excitation energies lie below the Franck-Condon value. Finally, we will see to what extent the theoretical line intensities determine spectral assignments which are ambiguous from energetic considerations alone. Through the examples above, we will have considered most types of spin allowed excitations found in transition metal complexes.

PERMANGANATE

As previously mentioned  $\text{MnO}_4^{-1}$  is a tetrahedrally coordinated molecule, which may appear either as a component of an ionic crystal or as an anion in solution. The complex has been extensively studied with previous theoretical methods, but the experimental data is less adequate.<sup>12,41-43,63-66</sup>

The  $X_{\alpha}$  ground state orbital energies from the work of Johnson and Smith for  $\text{MnO}_4^{-1}$  are presented in Table 9, and a diagram of the levels is given in Figure 1.<sup>9</sup> These calculations were done with non-overlapping spheres, as were most of the intensity calculations we shall present. Calculations on several systems indicate that the non-overlapping sphere approximation yields accurate results in most metal oxide systems.<sup>106,107</sup> (Although we have found it necessary to include partial waves through  $\ell = 2$  on O and through  $\ell = 4$  on Mn and the outer sphere for the intensity calculations, the energy eigenvalues are basically unchanged from the earlier results).

$\text{MnO}_4^{-1}$  has a closed shell electronic structure.<sup>9</sup> As indicated in Table 9, the lowest lying levels are chemically shifted  $\text{Mn}(1s)^2(2s)^2(2p)^6(3s)^2(3p)^6$  and

$O(1s)^2(2s)^2$  free atom levels. The occupied valence orbitals may be classified as follows. The  $5t_2$  and  $1e$  states are  $\sigma$  and  $\Pi$  bonding combinations of O 2p and Mn 3d orbitals. The  $6a_1$  and  $6t_2$  orbitals are composed mostly of O 2p orbitals, with some hybridization to the Mn 4s and Mn 3d orbitals respectively. The highest occupied orbital, the  $1t_1$  level, is primarily a non-bonding O 2p state.

The unoccupied  $2e$  and  $7t_2$  levels constitute the final states for the optical transitions. These are primarily Mn 3d states in the tetrahedral crystal field of the surrounding oxygen atoms. The higher lying  $8t_2$  (Mn 4p) and  $7a_1$  (Mn 4s) states are not involved in absorption at optical or near ultraviolet (u.v.) frequencies.

The (non-overlapping sphere)  $X_\alpha$  scattered wave results for the optical properties of  $MnO_4^{-1}$  are presented in Table 10. Our analysis of the permanganate spectrum indicates that all transitions are dipole allowed ligand to metal charge transfer in type. Table 10 shows excellent agreement between the theoretical and experimental excitation energies in  $MnO_4^{-1}$ . The relative theoretical intensities for the various transi-

tions are in agreement with the corresponding experimental values, but the absolute intensities differ between theory and experiment by about a factor of 17. A similar scale factor will appear in many of our results, and reflects a combination of local field and correlation effects. In particular, correlation causes a decrease in the occupation numbers of the transition state orbitals for the initial level. (This is a consequence of the fact that the natural orbital occupation numbers are smaller than the  $X_\alpha$  theory occupation numbers for those levels lying at or below the Fermi energy. See Chapter 6A for a further discussion of this subject.) As a result, the theoretical intensities are often uniformly too large, though the scale factor is generally much smaller than the  $\text{MnO}_4^{-1}$  value. The experimental  $\text{MnO}_4^{-1}$  intensities are also unusually small compared with analogous transitions in similar tetrahedral complexes. In the isoelectronic chromate ion  $\text{CrO}_4^{-2}$ , the oscillator strength for the  $1t_1 \rightarrow 2e$  transition is  $f = 0.08$  compared with  $f = 0.03$  for the same transition in  $\text{MnO}_4^{-1}$ . The other optical intensities in  $\text{CrO}_4^{-2}$  are similarly larger than the corresponding  $\text{MnO}_4^{-1}$  intensities. Since  $\text{CrO}_4^{-2}$  has a very similar electronic structure to  $\text{MnO}_4^{-1}$ , these results

indicate that the permanganate intensities must be very sensitive to the form of the wave functions. In the following section, we will also compare the intensities in  $\text{MnO}_4^{-1}$  with those in  $\text{FeCl}_4^{-1}$ .

Our spectral assignments are: first band  $1t_{1 \rightarrow 2e}$  (2.3 eV.) second band (weak shoulder)  $6t_{2 \rightarrow 2e}$  (3.5 eV.), third band  $1t_{1 \rightarrow 7t_2}$  (4.0 eV.), and fourth band  $5t_{2 \rightarrow 2e}$  and  $6a_{1 \rightarrow 7t_2}$  (5.5 eV.). This assignment coincides with that of Johnson and Smith except for the  $6a_{1 \rightarrow 7t_2}$  contribution to the fourth band system which they did not consider.<sup>9</sup>

In Chapter III C, we discussed in detail the many spectral assignments and intensity results that have been given for  $\text{MnO}_4^{-1}$ . In Table 11, we compare the best of these earlier calculations (the results of Mortola and co-workers) with the  $X_\alpha$  results for  $\text{MnO}_4^{-1}$ . In contrast to the intensities of Mortola and co-workers, the  $X_\alpha$  values are in relative agreement with the corresponding experimental intensities. Nonetheless, the large scale factor found between the  $X_\alpha$  theory oscillator strengths and the experimental values is very unsatisfactory. It is therefore necessary to establish the cause of this problem.

In Table 12, we show the respective atomic amplitude contributions to the total intensity for the  $1t_{1 \rightarrow 2e}$  excitation in  $\text{MnO}_4^{-1}$ . The overall intensity is a consequence

of destructive interference between the various atomic amplitudes. This is a general characteristic of electronic transitions in molecules. This feature suggests that the theoretical intensities could be sensitive to changes in various computational parameters.

We have examined this in several ways. First, we varied the manganese-oxygen distance from  $1.54 \text{ \AA}$  to  $1.63 \text{ \AA}$ . These are the limiting values of the experimental Mn-O distance from X-ray diffraction measurements.<sup>38-40</sup> The excitation energy increases with decreasing manganese-oxygen distance, with the intensity slowly decreasing. The behavior of the excitation energy is expected. As the ligands are brought closer to the central manganese, the anti-bonding  $2e$  state is pushed up by the increased interaction with the crystal field. The non-bonding  $1t_1$  state is relatively stable in energy. The intensity effects are small and unimportant, except for supporting the validity of the Franck-Condon principle in this system.

Second, a test was made of the effect of changing the position of the stabilizing electrostatic sphere (total charge  $+1e$ ). Changing the sphere radius from  $4.3 a_0$  to  $6.5 a_0$  was found to have a negligible effect on the intensity and to contribute only a constant shift to the energy eigenvalues.



Third, a calculation was done of the  $1t_{1 \rightarrow 2e}$  intensity with a sphere overlap of 30% ( $\frac{b_g}{b_N} = 1.30$  for all atoms). The oscillator strength decreased to  $f = 0.252$ . However, this decrease is caused almost entirely by the new excitation energy  $\Delta E = 3.0$  eV, which contains a large error. We do not, therefore, regard this result as significant.

Despite the inconclusive results of the preceding test cases for  $\text{MnO}_4^{-1}$ , there is strong evidence that a change in the boundary condition on the cluster could yield substantially different intensities. (A new boundary condition on the cluster must, of course, be justified from physical considerations.) This view is substantiated by Table 12. In this table, the outer sphere amplitudes, while small compared with the individual atomic amplitudes, are still very significant with respect to the total amplitude  $A_T$  because the various atomic contributions cancel almost precisely. In fact, if the outer sphere contribution were ignored, the resulting intensity of the  $1t_{1 \rightarrow 2e}$  transition would be  $f = 0.0028$ , less than the experimental intensity. There is no justification for this procedure, but an alternate outer sphere boundary condition could reduce the outer sphere amplitudes resulting in a much smaller theoretical intensity. Of all the transition metal complexes we shall treat, only  $\text{MnO}_4^{-1}$  displays this extreme

sensitivity to the outer sphere transition amplitude. This arises through the larger outer sphere contribution to the molecular orbitals, about 3-6%. (In  $\text{FeCl}_4^{-1}$ , for example, omitting the outer sphere amplitude for the  $2t_1 \rightarrow 3e$  transition decreases the intensity by a factor of 1.54, compared with a reduction factor of 142 for the  $1t_1 \rightarrow 2e$  transition in  $\text{MnO}_4^{-1}$ .) It is then no coincidence that  $\text{MnO}_4^{-1}$  has the largest scale factor of the transition metal systems we shall study.

We postulate that  $\text{MnO}_4^{-1}$  interacts covalently via the oxygen ligands with the surrounding aqueous or crystalline environment. It is likely that an interaction of this type would substantially reduce the outer sphere amplitudes, and would also reduce the atomic amplitudes as well. This hypothesis will have to be tested by further calculations on the  $\text{MnO}_4^{-1}$  cluster.

Table 9  
 $\text{MnO}_4^{-1}$  Energy Levels by the  $X_\alpha$  Scattered Wave Method  
 with Non-Overlapping Spheres<sup>a</sup>

<u>Level</u>	<u>One Electron Energy (Rydbergs)</u>
1a <sub>1</sub> (Mn 1s)	-468.584
2a <sub>1</sub> (Mn 2s)	- 54.105
1t <sub>2</sub> (Mn 2p)	- 46.513
3a <sub>1</sub> (O 1s)	- 37.738
2t <sub>2</sub> (O 1s)	- 37.738
4a <sub>1</sub> (Mn 3p)	- 6.435
3t <sub>2</sub> (Mn 3s)	- 4.259
5a <sub>1</sub> (O 2s)	- 1.813
4t <sub>s</sub> (O 2s)	- 1.785
5t <sub>2</sub>	- 0.915
1e	- 0.901
6a <sub>1</sub>	- 0.775
6t <sub>2</sub>	- 0.761
1t <sub>1</sub>	- 0.682
<hr/>	
2e	- 0.526
7t <sub>2</sub>	- 0.350
8t <sub>2</sub>	- 0.020
7a <sub>1</sub>	- 0.006

<sup>a</sup> Reference 9.

Table 10  
 $\text{MnO}_4^{-1}$  Optical Properties

<u>Transition</u>	<u>Intensity</u>		<u>Excitation Energy</u>	
	Theory	Experiment <sup>a, b</sup>	Theory	Experiment <sup>a</sup>
$1t_1 \rightarrow 2e$	0.5406	0.032	2.29 ev.	2.3 ev.
$6t_2 \rightarrow 2e$	0.2620	0.025	3.25 ev.	3.5 ev.
$1t_1 \rightarrow 7t_2$	0.5988	0.045	4.75 ev.	4.0 ev.
$6a_1 \rightarrow 7t_2$	1.2132	0.04-0.07	5.37 ev.	5.45 ev.
$5t_2 \rightarrow 2e$	0.2970		5.19 ev.	
$6t_2 \rightarrow 7t_2$	0.6336		5.72 ev.	

<sup>a</sup> Reference 41.

<sup>b</sup> Reference 42.

Table 11

Comparison of  $X_{\alpha}$  Theory  $f(\nabla V)$  Intensities with the  $f$  Values  
of Mortola and Co-Workers for  $MnO_4^{-1}$

Transition	Intensities of Mortola <sup>a</sup>			$X_{\alpha}$ Theory	Experiment <sup>b,c</sup>
	$f(x)$	$f(\nabla)$	$f(x, \nabla)$	In- tensities $f(\nabla V)$	
$1t_1 \rightarrow 2e$	0.426	0.128	0.233	0.541	0.032
$6t_2 \rightarrow 2e$	0.199	0.097	0.139	0.262	0.025
$1t_1 \rightarrow 7t_2$	0.101	0.083	0.079	0.600	0.045
$6a_1 \rightarrow 7t_2$			0.668	1.213	0.04-0.07

<sup>a</sup> Reference 66.

<sup>b</sup> Reference 41.

<sup>c</sup> Reference 42.

Table 12

Amplitude for  $1t_{1 \rightarrow 2e}$  (col. 1  $\rightarrow$  col. 2) in  $\text{MnO}_4^{-1}$  (Internuclear Distance  $R = 1.59 \text{ \AA}$ , Non-Overlapping Spheres).

Amplitudes for transitions between partial wave components:

Outer Sphere

$$A(f \rightarrow d) = 0.011237$$

$$A(f \rightarrow g) = 0.005200$$

Manganese

$$A(f \rightarrow d) = -0.142030$$

$$A(f \rightarrow g) = 0.002478$$

Oxygen

$$A(p \rightarrow d) = 0.131458$$

$$A(d \rightarrow p) = 0.009593$$

(The initial state partial waves are given first).

Total Amplitude

$$\sum_{i=\text{atoms}} A_i = 0.001499$$

$$\sum_{i=\text{outer sphere}} A_i = 0.016437$$

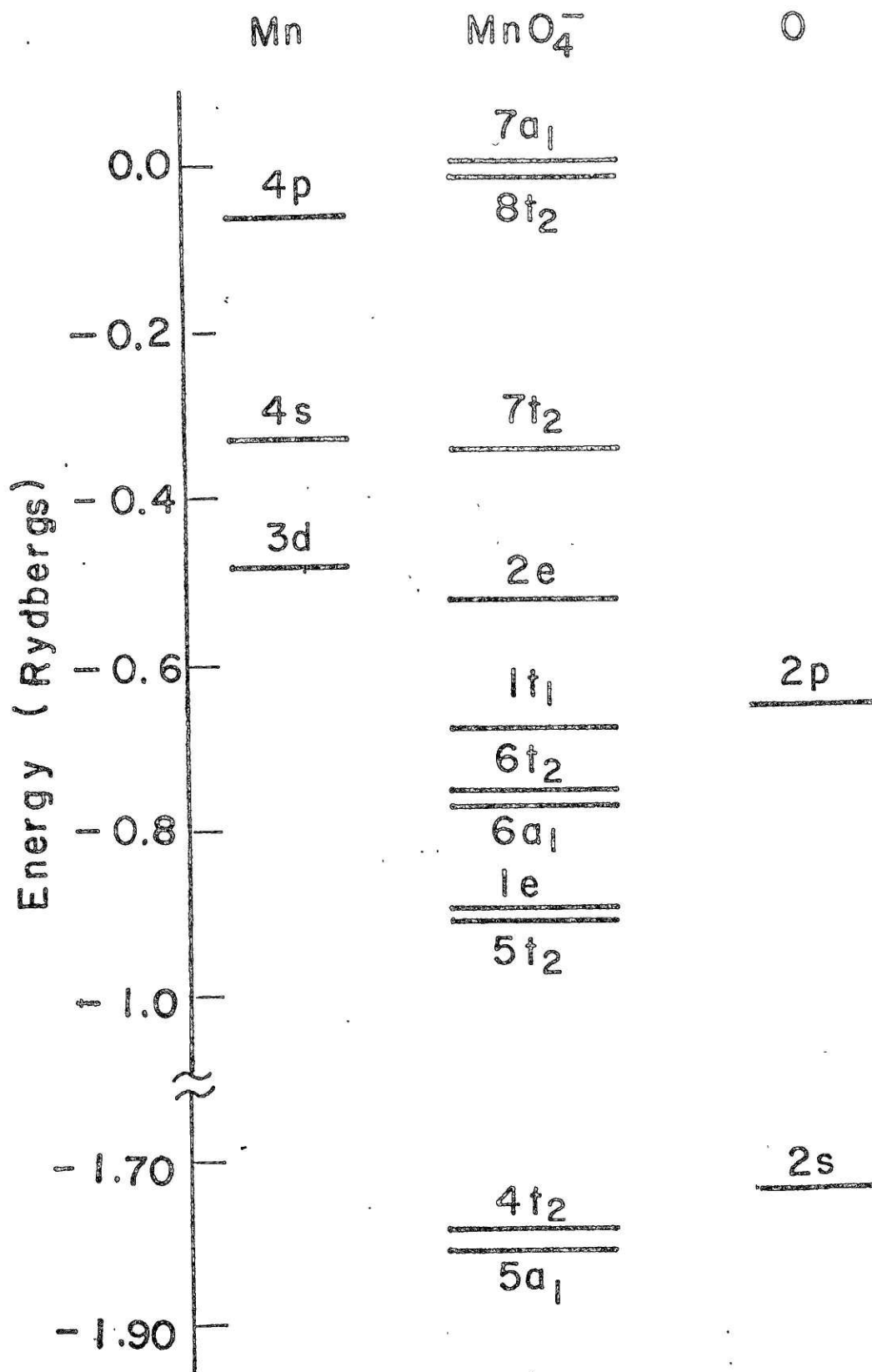
$$A_T = \text{Total Amplitude} = 0.017936$$

$$f = \frac{4}{3} \frac{G}{(\Delta E)^3} |A_T|^2 \quad G = \text{degeneracy factor} = 6 = 2$$

(for spin)  $\times$  3 (orbital)

$$\Delta E = (0.168216), \quad (\Delta E)^3 = (0.004760), \quad \text{Oscillator Strength}$$

$$f = 0.540672$$

Figure 1. MnO<sub>4</sub><sup>-</sup> energy levels

## IRON TETRACHLORIDE

The tetrahedral complex  $\text{FeCl}_4^{-1}$  has an open shell electronic structure with high net spin  $S = \frac{+5}{2}$ .<sup>4</sup>  $\text{FeCl}_4^{-1}$  has a greater ionicity than  $\text{MnO}_4^{-1}$  due to the greater electronegativity of the chlorine ligands as opposed to the oxygens. This is borne out by the larger band gap in  $\text{FeCl}_4^{-1}$ , 3.2 ev. versus 2.3 ev. in  $\text{MnO}_4^{-1}$ , and by a smaller separation between the bonding (beginning with the  $8a_1^\uparrow$  level) and non-bonding (ending with the  $2t_1^\downarrow$  level) states in  $\text{FeCl}_4^{-1}$ . The valence level ordering in the two complexes is similar, except that the  $8a_1$  state appears at the bottom of the valence band in  $\text{FeCl}_4^{-1}$  while the analogous  $6a_1$  state in  $\text{MnO}_4^{-1}$  occurs near the top of the valence band (only weakly bonding). A summary of the energy level structure in  $\text{FeCl}_4^{-1}$  from our  $X_\alpha$  calculations is given in Table 13 and Figure 2. A 20% overlap factor ( $\frac{b_g}{b_N} = 1.20$ , for all atoms) was used in the calculation because the atomic radius of chlorine is known to be large. The high spin  $S = \frac{+5}{2}$  makes it imperative that the  $X_\alpha$  calculation on this system be spin unrestricted. This is the high spin case mentioned earlier in which the spin unrestricted formalism yields a pure  $S = \frac{+5}{2}$  multiplet. The levels through the  $2t_1$  state are completely filled, with the higher Fe 3d crystal field states assuming the configuration  $(3e^\uparrow)^2 (10t_2^\uparrow)^3$ . All transitions below 4.6ev. are from bonding or non-bonding states concentrated mostly on the chlorines to the unoccupied  $3e^\downarrow$  and  $10t_2^\downarrow$  levels concentrated



on the iron atom. At higher energies (above 5.0 ev., experimentally) transitions to the unoccupied  $9a_1$  state occur as well. The latter is a diffuse hybrid s state with most of its charge in the intersphere and extramolecular regions. The atomic orbital compositions of the occupied states in  $\text{FeCl}_4^{-1}$  are indicated in Table 13.

In Table 14, we present a comparison of the theoretical and experimental optical properties for  $\text{FeCl}_4^{-1}$ .<sup>4</sup> Both theoretical excitation energies and relative intensities are in excellent agreement with the experimental values. The scale factor between the  $X_\alpha$  intensities and the experimental intensities is a very reasonable 1.7, which is fairly constant ( $\pm 0.2$ ) throughout the different transitions. The advantages of carrying out the calculation in spin unrestricted form are apparent from our spin restricted results in Table 14. While the intensities are surprisingly stable (especially in view of the large changes in  $\Delta E$ ), the excitation energies are too low by 1.1-1.5 ev. In a system having the complexity of  $\text{FeCl}_4^{-1}$ , spectral assignments then become particularly treacherous. The use of the spin restricted form of the  $X_\alpha$  method was also a major source of error in the work of Ellis and Averill discussed earlier.<sup>69</sup>

Returning to the spin unrestricted results for  $\text{FeCl}_4^{-1}$ , there is a close connection between the calculated spectral intensities in this system and the calculated  $\text{MnO}_4^{-1}$  intensities. Consider the first three bands for the two systems. In each case,

the calculated  $\text{MnO}_4^{-1}$  intensity is just about 2 times the analogous theoretical intensity in  $\text{FeCl}_4^{-1}$ . This would follow as a consequence of the Pauli exclusion principle if  $\text{MnO}_4^{-1}$  and  $\text{FeCl}_4^{-1}$  have similar wave functions for those states involved in the transitions. Transitions to the filled  $3e^\uparrow$  and  $10t_2^\uparrow$  levels are prohibited by the Pauli principle in  $\text{FeCl}_4^{-1}$ , but the analogous  $2e^\uparrow$  and  $7t_2^\uparrow$  levels in  $\text{MnO}_4^{-1}$  are unoccupied making transitions to the latter states allowed. The valence states in  $\text{MnO}_4^{-1}$  and  $\text{FeCl}_4^{-1}$  are for the most part quite similar using the present scattered wave cluster model. This model is based, however, on a purely electrostatic boundary condition (that is, on a purely ionic interaction between the molecule and the surrounding medium). The experimental intensities for the two systems suggest that an ionic boundary condition is fairly accurate for  $\text{FeCl}_4^{-1}$ , but that a mixed ionic and covalent boundary condition is required to represent the bonding of  $\text{MnO}_4^{-1}$  to the surrounding medium.

The agreement of the  $\text{FeCl}_4^{-1}$  calculated intensities with the experimental results must be considered very good, especially in view of the uncertainties in the experimental values.

Table 13  
Energy Levels in  $\text{FeCl}_4^{-1}$

Valence Levels		One Electron Energy (Rydbergs)	
		Spin-Up	Spin-Down
6a <sub>1</sub>	(Fe3s)	-6.679	-6.467
6t <sub>2</sub>	(Fe3p)	-4.327	-4.120
7a <sub>1</sub>	(Cl3s)	-1.442	-1.423
7t <sub>2</sub>	(Cl3s)	-1.419	-1.400
8a <sub>1</sub>	(Cl3p + Fe4s)	-0.682	-0.656
8t <sub>2</sub>	(Cl3p + Fe3d)	-0.661	-0.600
2e	(Cl3p + Fe3d)	-0.603	-0.540
9t <sub>2</sub>	(Cl3p + F 3d)	-0.558	-0.529
2t <sub>1</sub>	(Cl3p)	-0.483	-0.467
3e	(Fe3d)	-0.436	unoccupied
10t <sub>2</sub>	(Fe3d)	-0.386	unoccupied
9a <sub>1</sub>	(diffuse Fe4s)	unoccupied	unoccupied
<u>Core Levels (Chemically Shifted)</u>			
Fe 1s		-509.20	
Fe2s		- 59.10	
Fe 2p		- 51.10	
Cl 1s		-201.11	
Cl 2s		- 18.41	
Cl 2p		- 14.10	

Table 14

$\text{FeCl}_4^{-1}$  Optical Properties -- Spin Unrestricted --  
net Spin Up +  $\frac{5}{2}$

<u>Transition</u>	<u>Intensity</u>		<u>Excitation Energy</u>	
	Theory	Experiment <sup>a</sup>	Theory	Experiment <sup>a</sup>
$2t_1 \rightarrow 3e$	0.194	0.11	3.2 ev. 25,800 $\text{cm}^{-1}$	3.4 ev. 27,480 $\text{cm}^{-1}$
$2t_1 \rightarrow 10t_2$	0.276	0.16	3.7 ev. 29,800 $\text{cm}^{-1}$	3.9 ev. 31,520 $\text{cm}^{-1}$
$9t_2 \rightarrow 3e$	0.123	0.07	4.0 ev. 32,200 $\text{cm}^{-1}$	4.6 ev. 37,000 $\text{cm}^{-1}$
$9t_2 \rightarrow 10t_2$	0.009		4.3 ev. 34,700 $\text{cm}^{-1}$	
$2e \rightarrow 10t_2$	0.077		4.62 ev. 37,200 $\text{cm}^{-1}$	
$8t_2 \rightarrow 3e$	0.009		4.78 ev. 38,600 $\text{cm}^{-1}$	
$10t_2 \uparrow \rightarrow 9a_1 \uparrow$	0.126		4.94 ev. 39,800 $\text{cm}^{-1}$	
$8t_2 \rightarrow 10t_2$	0.201	0.28	5.25 ev. 42,250 $\text{cm}^{-1}$	5.1 ev. 44,250 $\text{cm}^{-1}$
$9t_2 \downarrow \rightarrow 9a_1 \downarrow$	0.268		6.1 ev. 49,700 $\text{cm}^{-1}$	
$9t_2 \downarrow \rightarrow 9a_1 \downarrow$	0.117		6.7 ev. 54,000 $\text{cm}^{-1}$	

Table 14  
(continued)

Spin Restricted

<u>Transition</u>	<u>Intensity</u>		<u>Excitation Energy</u>	
	Theory	Experiment <sup>a</sup>	Theory	Experiment <sup>a</sup>
$2t_1 \rightarrow 3e$	0.189	0.11	2.3 ev. 18,550 cm <sup>-1</sup>	3.4 ev. 27,480 cm <sup>-1</sup>
$2t_1 \rightarrow 10t_2$	0.276	0.16	2.74 ev. 22,100 cm <sup>-1</sup>	3.9 ev. 32,520 cm <sup>-1</sup>
$9t_2 \rightarrow 3e$	0.116	0.07	3.09 ev. 25,000 cm <sup>-1</sup>	4.6 ev. 37,000 cm <sup>-1</sup>
$9t_2 \rightarrow 10t_2$	0.023		3.66 ev. 29,500 cm <sup>-1</sup>	

<sup>a</sup>Reference 4.

Table 15  
Optical Properties of  $\text{FeCl}_4^{-1}$  from the Work  
of Averill and Ellis.

The Spin Restricted  $X_\alpha$  method was used, and the Dipole Length form for  $f$ .

<u>Transition</u>	<u>Intensity</u>			<u>Excitation Energy</u>	
	Theory <sup>a</sup>	Corrected Value	Experiment <sup>b</sup>	Theory <sup>a</sup>	Experiment <sup>b</sup>
$2t_1 \rightarrow 3e$	0.05	0.15	0.11	$17400\text{cm}^{-1}$	$27480\text{cm}^{-1}$
$2t_1 \rightarrow 10t_2$	0.06	0.18	0.16	$26800\text{cm}^{-1}$	$31520\text{cm}^{-1}$
$9t_2 \rightarrow 3e$	0.05	0.15	0.07	$28400\text{cm}^{-1}$	$37000\text{cm}^{-1}$
$9t_2 \rightarrow 10t_2$	0.06	0.18		$37900\text{cm}^{-1}$	
$2e \rightarrow 10t_2$	0.04	0.08		$41100\text{cm}^{-1}$	
$8t_2 \rightarrow 3e$	0.01	0.03		$33200\text{cm}^{-1}$	
$8t_2 \rightarrow 10t_2$	0.09	0.27	0.28	$42600\text{cm}^{-1}$	$41250\text{cm}^{-1}$
$8a_1 \rightarrow 10t_2$	0.44	0.44		$48900\text{cm}^{-1}$	
$10t_2 \rightarrow 9a_1$	0.003	0.009		$33200\text{cm}^{-1}$	

(The spectral assignments in this Table are our own, not Averill and Ellis's).

<sup>a</sup> Reference 69.

<sup>b</sup> Reference 4.

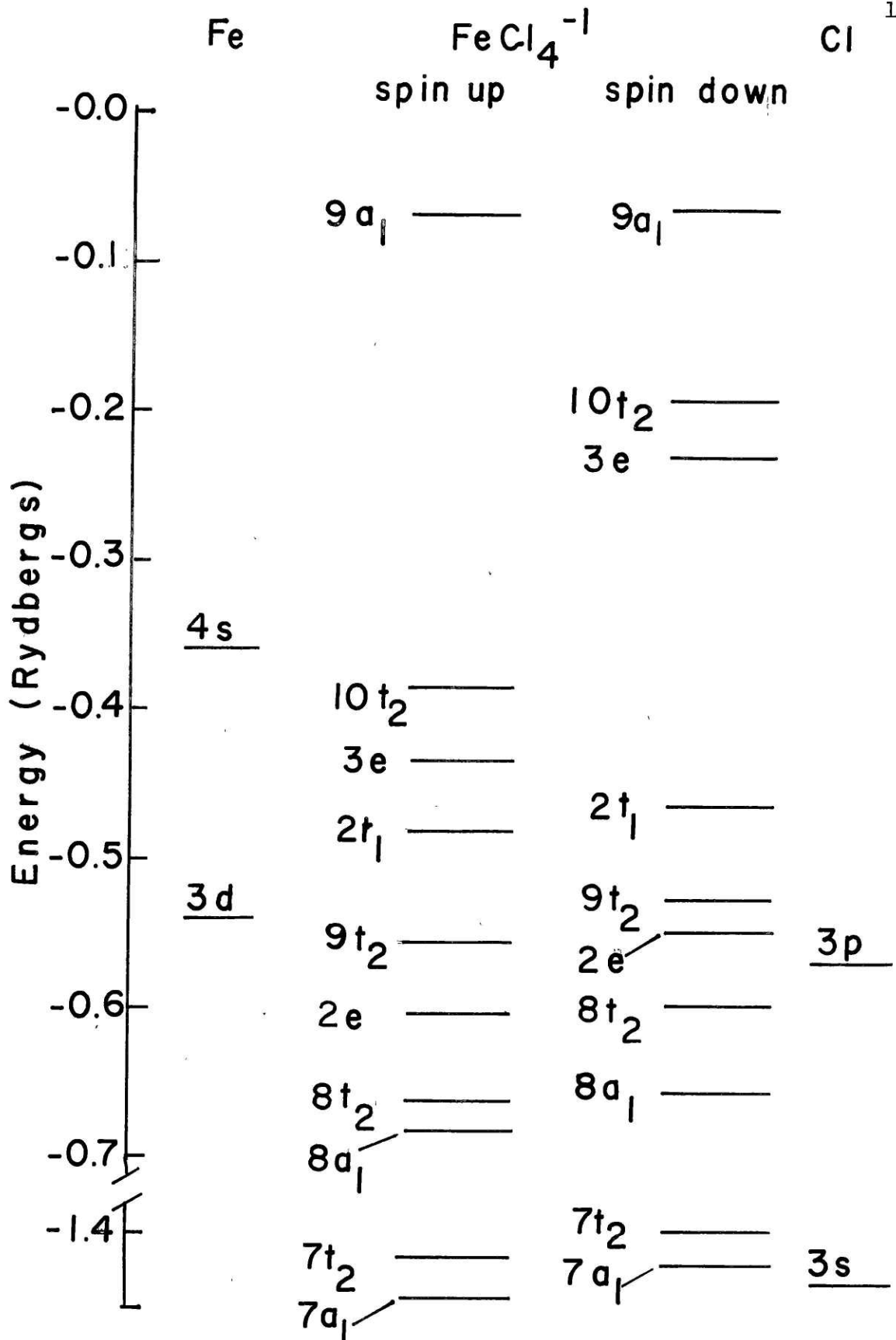


Figure 2.  $\text{FeCl}_4^{-1}$  energy levels.

## COBALT TETRACHLORIDE

The electronic structure of  $\text{CoCl}_4^{-2}$  is quite similar to the  $\text{FeCl}_4^{-1}$  structure, except for the additional filling of the  $3e\downarrow$  orbitals producing a net configuration  $(3e\uparrow)^2(10t_2\uparrow)^3(3e\downarrow)^2$ .<sup>49</sup> The chlorine tetrahedron in the  $\text{CoCl}_4^{-2}$  case is distorted although we will use a regular tetrahedron for our calculations. The details of the calculation are as found in the  $\text{FeCl}_4^{-1}$  work. There are two transitions to be considered, the crystal field  $3e\downarrow \rightarrow 10t_2\downarrow$  excitation at low energy  $\Delta E = 0.37 - 0.74 \text{ ev.}$ , and the first charge transfer transition  $2t_1\downarrow \rightarrow 10t_2\downarrow$  at  $\Delta E = 5.3 \text{ ev.}$  In addition, there is another crystal field multiplet transition at  $\Delta E = 1.8 \text{ ev.}$ <sup>48,49</sup> The results are summarized in Table 16.

We will treat the crystal field transition first. As indicated in the table, the first two multiplet transitions  ${}^4A_2 \rightarrow {}^4T_2$ ,  ${}^4A_2 \rightarrow {}^4T_1(F)$  correspond to the allowed one electron transition  $(3e\downarrow)^2 \rightarrow (3e\downarrow)^1(10t_2\downarrow)^1$  in the strong field limit.<sup>49</sup> However, only the  ${}^4A_2 \rightarrow {}^4T_1(F)$  excitation is dipole allowed in multiplet language. Our calculated excitation energy  $\Delta E = 0.408 \text{ ev.}$  should be an average of the two multiplet excitation energies, and this is roughly the case, although we are closer to the lower multiplet.<sup>5</sup> The  ${}^4A_2 \rightarrow {}^4T_1(P)$  transition is multiplet allowed, but corresponds to the forbidden  $(3e\downarrow)^2 \rightarrow (10t_2\downarrow)^2$  transition in the strong field limit.<sup>49</sup> The transition is allowed because the  ${}^4T_1(P)$  state is really a mixture of two configurations, approximately  $65\% (10t_2\downarrow)^2 + 35\% (3e\downarrow)^1(10t_2\downarrow)^1$ . (The lower lying levels in this discussion are unchanged for all the multiplets



considered.) Because the primary configuration of  ${}^4T_1(P)$  is  $(10t_2\uparrow)^2$ , this state should not be included in our multiplet average to obtain  $\Delta E(X_{\text{O}} \text{ theory})$ . This idea is in agreement with the energies we have found.

The theoretical intensity for the  $3e\downarrow \rightarrow 10t_2\downarrow$  transition is completely wrong, and provides the first example of the failure of the  $\vec{V}V$  method. The calculated excitation energy  $\Delta E = 0.408 \text{ ev.}$  is so small that errors in the transition amplitude entirely dominate the result. The computer program was then put into double precision form, but the intensity did not change significantly. To relate this error to our previous results, let us consider that in the present case the total transition amplitude should be 0 to obtain the experimental intensity. This is very nearly true. Let this amplitude error be  $\Delta A$ . We would like to find the fractional error induced in a similar system by the amplitude error  $\Delta A$ . As an example, we will take the  $2t_1 \rightarrow 3e$  transition in  $\text{FeCl}_4^{-1}$ . Let the  $\text{FeCl}_4^{-1}$  amplitude be  $\bar{A}$ . Then there are two different ways to find the error.

$$\text{Random error} = 1 - \left( \frac{\bar{A}^2 - (\Delta A)^2}{\bar{A}^2} \right) = \frac{(\Delta A)^2}{\bar{A}^2}$$

$$\text{Systematic error} = 1 - \left( \frac{\bar{A} - \Delta A}{\bar{A}} \right)^2$$

The random error formula means that the phase of the amplitude error  $\Delta A$  is arbitrary. This would be the case with computational

inaccuracies, and probably applies to errors developed by truncating the partial wave expansions as well. The systematic error means that one is consistently underestimating or overestimating certain atomic amplitudes or the outer sphere amplitude. Consequently, the predicted error can take on different values depending on our assumptions as to the source of the problem. The two results in  $\text{FeCl}_4^{-1}$  for the  $2t \rightarrow 3e$  transition are random error = 4.3%, systematic error = 37%. This is a crude estimate of the error limits in  $\text{FeCl}_4^{-1}$ . For higher energy transitions, both errors decrease roughly as  $\frac{1}{(\Delta E)^3}$ .

For the charge transfer transition in  $\text{CoCl}_4^{-2}$ , the results are very reasonable, with the scale factor equal to 2.8, somewhat larger than in the  $\text{FeCl}_4^{-1}$  case. Both the theoretical and the experimental results predict a substantial decrease in the  $2t_{1\downarrow} \rightarrow 10t_{2\downarrow}$  intensity in going from  $\text{FeCl}_4^{-1}$  to  $\text{CoCl}_4^{-2}$ . The larger scale in  $\text{CoCl}_4^{-2}$  may simply reflect the larger error in the computed excitation energy in this case as contrasted with  $\text{FeCl}_4^{-1}$ .

Table 16  
 $\text{CoCl}_4^{-2}$  Optical Properties

<u>Transition</u>	<u>Excitation Energy</u>		<u>Intensities</u>	
	Theory	Experiment	Theory	Experiment
$3e\uparrow \rightarrow 10t_2\downarrow$	0.408ev.	0.370-0.435ev.	5.6	
		${}^4A_2 \rightarrow {}^4T_2$ <sup>d</sup>		
		0.62-0.745ev.		$7.2 \times 10^{-4}$ <sup>b</sup>
		${}^4A_2 \rightarrow {}^4T_1$ (F) <sup>b, c</sup>		
$2t_1\downarrow \rightarrow 10t_2\downarrow$	4.54ev.	1.75-1.85ev.	0.184	$5.09 \times 10^{-3}$ <sup>b</sup>
		${}^4A_2 \rightarrow {}^4T_1$ (P) <sup>b, c</sup>		
$2t_1\downarrow \rightarrow 10t_2\downarrow$	4.54ev.	5.3ev. <sup>a</sup>	0.184	0.065 <sup>a</sup>

Observed d→d transitions

${}^4A_2 \rightarrow {}^4T_2$  forbidden

${}^4A_2 \rightarrow {}^4T_1$  (F) allowed

${}^4A_2 \rightarrow {}^4T_1$  (P) allowed

Strong Field Limit Configurations

${}^4A_2$  (3e↑)

${}^4T_2$  (3e↑) (10t<sub>2</sub>↓)

${}^4T_1$  (F) (3e↑) (10t<sub>2</sub>↓)

${}^4T_1$  (P) (10t<sub>2</sub>↓)

In all cases above the levels are filled through  $(3e\uparrow)^2(10t_2\uparrow)^3$  as well.

<sup>a</sup> Reference 47.

<sup>b</sup> Reference 48.

<sup>c</sup> Reference 49.

<sup>d</sup> Reference 50.

## CHROMIUM HEXACARBONYL

The electronic structure of  $\text{Cr}(\text{CO})_6$  is summarized in Table 17 and Figure 3. These results were obtained from the unpublished work of Klemperer and co-workers using the overlapping sphere  $X_\alpha$  model spin restricted including an overlapping outer sphere.<sup>92</sup> (Early  $X_\alpha$  work on  $\text{Cr}(\text{CO})_6$  with the muffin tin potential was carried out by the author and Dr. K. H. Johnson.)<sup>108</sup> For consistency, we will adopt Klemperer's model including the overlapping outer sphere, since we have found from additional calculations that the optical properties of the complex are not substantially different with a tangent outer sphere. A sphere overlap of 18% was used.

Since  $\text{Cr}(\text{CO})_6$  is an octahedral complex, vibronic as well as dipole allowed transitions may appear in the spectrum. Table 18 gives a summary of the calculated optical properties in  $\text{Cr}(\text{CO})_6$ . The  $2t_{2g} \rightarrow 9t_{1u}$  and  $2t_{2g} \rightarrow 2t_{2u}$  are dipole allowed metal (3d) to ligand (CO  $2\pi$  anti-bonding) charge transfer transitions of large intensity, both in our model and in the experimental values. The  $2t_{2g} \rightarrow 2t_{2u}$  is particularly strong, the final state being a pure CO  $2\pi$  level. This corresponds to the view that a pure dipole allowed charge transfer excitation has a very large intensity. The  $2t_{2g} \rightarrow 10t_{1u}$  transition is also dipole allowed, but is less intense due to the diffuse Cr 4p character of the final state. The transition has an atomic character, Cr  $3d \rightarrow$  Cr 4p. Finally, we have assigned the two weak

transitions at 3.91 ev. and 4.83 ev. to the vibronically allowed transitions  $2t_{2g} \rightarrow 9a_{1g}$  (Cr 3d  $\rightarrow$  diffuse Cr 4s), and  $2t_{2g} \rightarrow 3t_{2g}$  (Cr 3d  $\rightarrow$  Cr 3d + CO  $2\pi$ , anti-bonding). The transition at 3.91 ev. shows a gradual increase in intensity with higher temperature, which is characteristic of a vibronic transition. The very weak spectral peak at 3.59 ev. is probably another vibrational component of the  $2t_{2g} \rightarrow 9a_{1g}$  excitation.

From Table 18, it is clear that the spectral assignments in this complex cannot be made from the calculated excitation energies alone, which are generally too low by about 1.1-1.2 ev. However, the calculated spectral intensities bear a sufficiently close correlation to the experimental intensities that an assignment can be made on this basis. The agreement between the experimental and theoretical intensities is not quantitative, but both sets of values predict  $f(2t_{2g} \rightarrow 2t_{2u}) > f(2t_{2g} \rightarrow 9t_{1u}) > f(2t_{2g} \rightarrow 10t_{1u})$ .

We must understand 1) why the calculated excitation energies are generally too low by 1.1-1.2 ev., 2) why the experimental  $2t_{2g} \rightarrow 9a_{1g}$  excitation energy lies below the  $2t_{2g} \rightarrow 9t_{1u}$  energy, while the calculated  $2t_{2g} \rightarrow 9a_{1g}$  energy is higher than the  $2t_{2g} \rightarrow 9t_{1u}$  energy, and 3) why the  $2t_{2g} \rightarrow 3t_{2g}$  calculated energy is too low by 0.7 ev., as compared with 1.1-1.2 ev. for the dipole allowed transitions. We will consider problem 1 first. It is known that the carbonyl complexes of Mo and W (both Group 6B elements like Cr),  $\text{Mo}(\text{CO})_6$  and  $\text{W}(\text{CO})_6$  have significant singlet-triplet splittings, about 0.4 ev.<sup>51</sup>

$\text{Cr}(\text{CO})_6$  should also have large singlet-triplet splittings, although the triplet states are difficult to find experimentally. A singlet-triplet splitting of 0.4 ev. in  $\text{Cr}(\text{CO})_6$  would mean that the singlet-singlet excitation energy would lie 0.3 ev. above our computed spin restricted value. Since the computed  $X_\alpha$  singlet-triplet splittings may be much larger than this (see, for example, our  $\text{H}_2$  singlet-triplet splittings in the spin restricted formulation), the  $X_\alpha$  singlet-singlet excitation energies may be much closer to the experimental values. For this purpose, additional spin unrestricted calculations are necessary on  $\text{Cr}(\text{CO})_6$ .

Let us now simply translate up the theoretical spectrum by 1.1 ev. The dipole allowed transitions are in good agreement with experiment, but the vibronically allowed  $2t_{2g} \rightarrow 9a_{1g}$  and  $2t_{2g} \rightarrow 3t_{2g}$  are too high by 1.0 ev. and 0.4 ev., respectively. In the section on molecular vibrations, we showed that the excitation energy for a vibronic transition lies below the Franck-Condon principle value by an average of one vibrational quantum  $\hbar\omega_q$ , with  $q$  the odd normal mode responsible for the vibronic coupling. Applying this result to a typical odd vibrational mode in  $\text{Cr}(\text{CO})_6$ , we would obtain an energy lowering of 0.1-0.3 ev. for the vibronic levels, bringing them into better agreement with experiment. Although quantitative results must await spin unrestricted calculations on  $\text{Cr}(\text{CO})_6$ , the preceding arguments on spin effects and vibronic coupling rules produce correct qualitative shifts in the spectrum.

Further evidence for the  $2t_{2g} \rightarrow 9a_{1g}$  assignment at 3.91 ev., comes from the experimentally observed photo-dissociation of neutral CO from  $\text{Cr}(\text{CO})_6$  at this energy.<sup>52</sup> This effect implies that the final state lies mostly on the metal atom. By contrast, a metal to ligand charge transfer transition would yield  $\text{CO}^-$  on photo-dissociation, ruling out the  $2t_{2g} \rightarrow 9t_{1u}$  transition. Beach and Gray have made the assignment  $2t_{2g} \rightarrow 6e_g$  for the 3.91 ev. excitation.<sup>51</sup> This also meets the criteria of being a metal to metal transition. However, since this assignment was used to parametrize their semi-empirical calculations on  $\text{Cr}(\text{CO})_6$ , it cannot be considered to have predictive value. At present, it is not possible to experimentally distinguish between the two assignments  $2t_{2g} \rightarrow 9a_{1g}$  (Cr 3d $\rightarrow$ Cr 4s) and  $2t_{2g} \rightarrow 6e_g$  (Cr 3d $\rightarrow$ Cr 3d). In the  $X_\alpha$  calculations, however, the  $6e_g$  level lies very high in energy.

The experimental results in Table 18 are the measured spectral intensities of Beach and Gray on  $\text{Cr}(\text{CO})_6$  vapor at 300°K.<sup>51</sup> Solution spectra of  $\text{Cr}(\text{CO})_6$  in EPA (a mixture of ethanol, isopentane, and ethyl ether) yields intensities which are lower by 40-50% at the same temperature. This contrasts with the Lorentz-Lorenz correction factor  $\frac{f_{\text{solution}}}{f_{\text{vapor}}} = \frac{1}{\gamma} > 1$ . It is likely that the carbonyl molecules interact covalently with the solvent producing a lower intensity. In this case, the experimental boundary condition on the carbonyl molecule has a large effect on the intensities

paralleling the sensitivity to boundary conditions we found theoretically in  $\text{MnO}_4^{-1}$ .



Table 17  
Energy Levels in  $\text{Cr}(\text{CO})_6$

Valence Levels		One Electron Energy (Rydbergs)
$5t_{1u}$	(CO $3\sigma$ )	-2.022
$6a_{1g}$	(CO $3\sigma$ )	-2.022
$3e_g$	(CO $3\sigma$ )	-2.021
$7a_{1g}$	(Cr-C, $\sigma$ bonding)	-1.141
$6t_{1u}$	(CO $4\sigma$ )	-1.060
$4e_g$	(CO $4\sigma$ )	-1.054
$8a_{1g}$	(CO $4\sigma$ )	-0.962
$5e_g$	(Cr-C, $\sigma$ bonding)	-0.886
$7t_{1u}$	(Cr-C, $\sigma$ bonding)	-0.854
$1t_{2g}$	(CO $1\Pi$ )	-0.770
$1t_{2u}$	(CO $1\Pi$ )	-0.735
$8t_{1u}$	(CO $1\Pi$ )	-0.729
$1t_{1g}$	(CO $1\Pi$ )	-0.721
$2t_{2g}$	(Cr d)	-0.417
Unoccupied		
$9t_{1u}$	(CO $2\Pi$ , Cr p)	-0.199
$9a_{1g}$	(Cr s diffuse)	-0.157
$2t_{2u}$	(pure CO $2\Pi$ )	-0.119
$3t_{2g}$	(CO $2\Pi$ + Cr 3d, antibonding)	-0.116
$10t_{1u}$	(CO $2\Pi$ + Cr p, diffuse)	-0.061

Table 17  
(continued)

Valence Levels		One Electron Energy (Rydbergs)
$6e_g$	(Cr $d_z^2, d_{x^2-y^2}$ )	-0.042
$2t_{1g}$	(pure CO $2\Pi$ )	-0.034

Core Levels (Chemically Shifted)

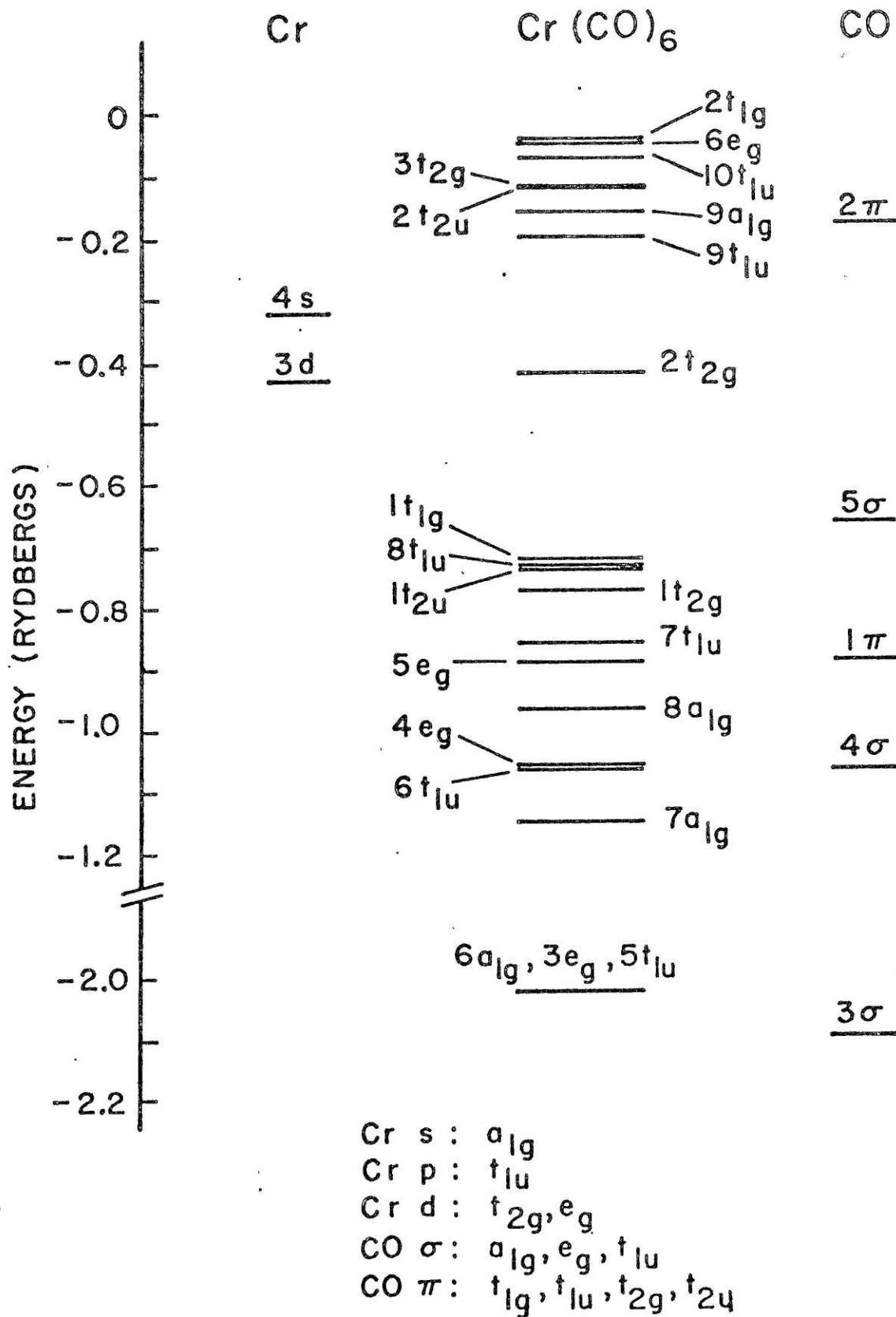
Cr 1s	-428.744
Cr 2s	- 48.624
Cr 2p	- 41.456
O 1s	- 37.526
C 1s	- 20.186

Table 18  
Cr(CO)<sub>6</sub> Optical Properties

Overlapping Spheres -- Including Outer Sphere

<u>Transition</u>	<u>Excitation Energy</u>		<u>Intensity</u>	
	Theory	Experiment <sup>a</sup>	Theory	Experiment <sup>a</sup>
$2t_{2g} \rightarrow 9a_{1g}$	3.83ev.	3.59ev. 3.91ev.	vibronically allowed	0.008 0.037
$2t_{2g} \rightarrow 9t_{1u}$	3.26ev.	4.44ev.	0.78	0.25
$2t_{2g} \rightarrow 3t_{2g}$	4.14ev.	4.83ev.	vibronically allowed	0.037
$2t_{2g} \rightarrow 2t_{2u}$	4.34ev.	5.48ev.	1.87	2.30
$2t_{2g} \rightarrow 10t_{1u}$	5.18ev.	6.31ev.	0.27	0.035

<sup>a</sup> Beach and Gray, Vapor Spectra at 300° K, see Reference 51.

Figure 3. Cr(CO)<sub>6</sub> energy levels.

## Figure Caption for Figure 4

The transition goes from  $1 \rightarrow 2'$  rather than  $1 \rightarrow 3'$  as indicated by the Franck-Condon principle and our calculations (see Figure 4a). The lowering of the excitation energy is  $\Delta E'$ . The overlap amplitudes for different vibrational transitions are determined by the overlap of state 2 with  $1', 2', 3', \dots$  which follows from

$$\phi_1^i(0)q_1 \approx \left(\frac{h}{8\pi^2cv_1}\right)^{\frac{1}{2}} \cdot \phi_1^i(1). \quad \text{The overlap of state 2}$$

with  $4'$  is small due to destructive interference. The latter is a consequence of the large kinetic energy of  $4'$  away from the classical turning point. Schematically, the resulting spectrum is given by Figure 4b.

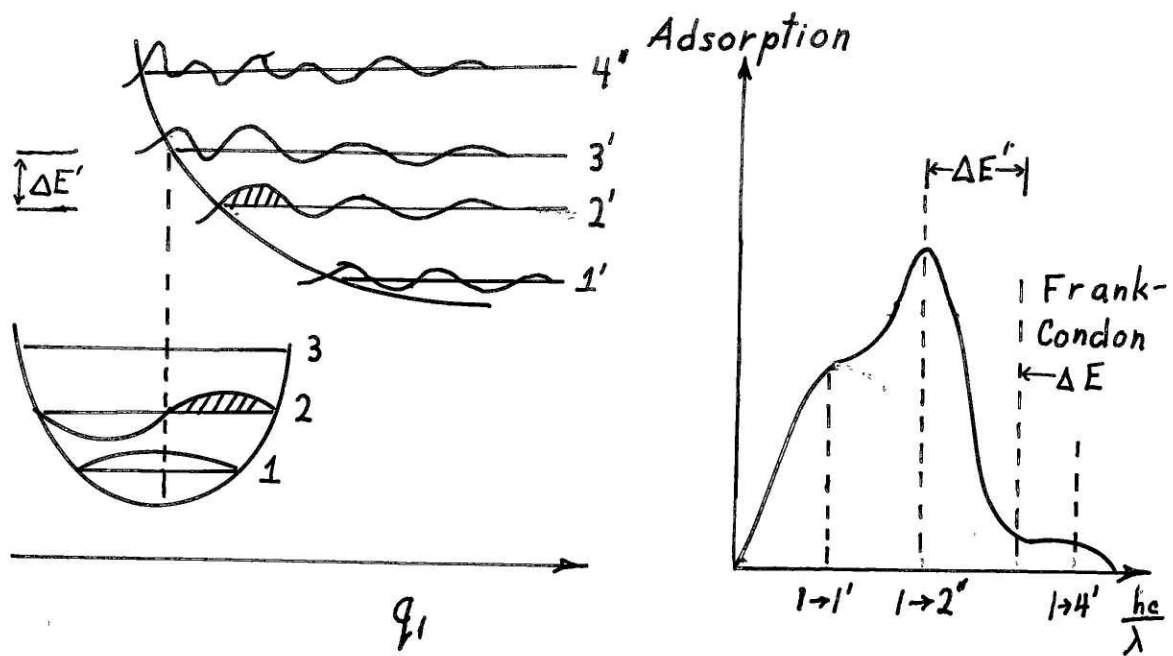


Figure 4. Vibrational Overlap in Vibronic Transitions

Table 19  
Symmetry Information for  $T_d$  Group

Irreducible representations:

$a_1$  one dimensional  
 $t_2$  (col. 1)  $x$   
 $t_2$  (col. 2)  $y$   
 $t_2$  (col. 3)  $z$   
 $t_1$  (col. 1)  $x(z^2 - y^2)$   
 $t_1$  (col. 2)  $-y(z^2 - x^2)$   
 $t_1$  (col. 3)  $z(x^2 - y^2)$   
 $e$  (col. 1)  $-(2x^2 - y^2 - z^2)$   
 $e$  (col. 2)  $z^2 - y^2$

Squares of Vector coupling coefficients for  $T_d$  Group

		col. 1	$\frac{t_1}{\text{col. 2}}$	col. 3
$\underline{e}$	col. 1	0	3/4	3/4
	col. 2	1	1/4	1/4

		col. 1	$\frac{t_2}{\text{col. 2}}$	col. 3
$\underline{t_2}$	col. 1	0	1/2	1/2
	col. 2	1/2	0	1/2
	col. 3	1/2	1/2	0

		col. 1	$\frac{t_2}{\text{col. 2}}$	col. 3
$\underline{e}$	col. 1	1	1/4	1/4
	col. 2	0	3/4	3/4

Table 19  
(continued)

	col. 1	$\frac{t_2}{\text{col. 2}}$	col. 3
$\underline{t_2}$	col. 1	0	1/2
	col. 2	1/2	0
	col. 3	1/2	0
		$\frac{t_2}{\text{col. 2}}$	
$\underline{a_1}$	col. 1	col. 2	col. 3
	col. 1	1	1



## CHAPTER VIII

## CONCLUSIONS

We have found that the  $\vec{V}V$  form of the oscillator strength is a very convenient form for evaluating intensities in the  $X_\alpha$  scattered wave method. The principle disadvantages of the  $\vec{V}V$  form of  $f$  lie in the relatively slow partial wave convergence of  $f$  (see the  $f(\vec{V}V)$  results for  $CO^+$ ) and in the failure of the  $\vec{V}V$  method at low excitation energies  $\Delta E < 1$  ev. (and perhaps somewhat higher.) The  $f(\vec{x})$  form seems to display better partial wave convergence. This is indicated by the results of Messmer and Salahub on  $CO^+$  using the  $\vec{x}$  form.<sup>59</sup> However, the  $f(\vec{x})$  method has not as yet been applied to transition metal complexes, so its full value cannot be assessed. It would be desirable to have the comparative results of the  $f(\vec{x})$ ,  $f(\vec{V})$ ,  $f(\vec{x}, \vec{V})$ , and  $f(\vec{V}V)$  forms for transition metal complexes to see if substantial improvements over the  $f(\vec{V}V)$  intensities are possible within the  $X_\alpha$  scattered wave framework.

Nonetheless, the  $f(\vec{V}V)$  method adopted in the present work has proven very valuable in understanding the optical properties of transition metal complexes. The relative intensities in  $FeCl_4^{-1}$  are in excellent agreement with the

experimental results.<sup>4</sup> The scale factor between the theoretical and the experimental intensities in this system is 1.7. These results must be considered very satisfactory in view of the possible errors in the experimental spectrum, and in view of the absence of an accurate theoretical treatment of local field and correlation effects. In addition, the good agreement between the theoretical and experimental intensities leads us to believe that an ionic boundary condition on the  $\text{FeCl}_4^{-1}$  cluster is physically accurate.

The calculated intensity of the charge transfer  $2t_1 \rightarrow 10t_2$  transition in  $\text{CoCl}_4^{-2}$  is 2.8 times the experimental value, which is also quite reasonable.<sup>47</sup> While this charge transfer intensity is fairly well described by the  $f(\vec{V})$  form, the crystal field  $3e \rightarrow 10t_2$  intensity is completely unreliable. The source of this error lies in the extreme sensitivity of the  $f(\vec{V})$  result at low excitation energies  $\Delta E < 1$  ev. Conversely, we should expect that the  $f(\vec{x})$  form of the oscillator strength should be most accurate at low excitation energies following the line of argument presented in Chapter VI C. The  $f(\vec{x})$  form would consequently be very useful in obtaining accurate intensities for crystal field transitions which generally occur at low energies.

In  $\text{Cr}(\text{CO})_6$  the calculated intensities provide a reasonable basis for making spectral assignments. The assignments are consistent both with our predicted intensities and with the calculated excitation energies. In addition, the assignments

are consistent with the photo-dissociation of neutral CO from  $\text{Cr}(\text{CO})_6$  at ultraviolet frequencies.<sup>52</sup> The most unsatisfactory features of the  $\text{Cr}(\text{CO})_6$  calculations are the inaccuracies in the calculated excitation energies. To obtain better quantitative results for this complex, spin unrestricted calculations on the system will be necessary.

In  $\text{MnO}_4^{-1}$ , the results are not as satisfactory as in the preceding examples. Although the relative intensities of the various spectral peaks are properly portrayed, a large scale factor of 17 was found between the theoretical and the experimental intensities.<sup>41-43</sup> On examination, we found that the  $\text{MnO}_4^{-1}$  intensities were highly dependent on the outer sphere amplitudes. This suggests that an alternate outer sphere boundary condition including covalent bonding between the  $\text{MnO}_4^{-1}$  and the surrounding environment could produce more reasonable intensities. Here two approaches are required. First, the  $\vec{x}$  form of the oscillator strength should be calculated to insure that the results we have found are not a peculiarity of the  $\vec{V}\vec{V}$  method. Second, a proper boundary condition must be found for the molecule to represent its interaction with the surrounding aqueous or crystalline environment. An understanding of the latter problem should have implications for other metal oxide systems as well (for example, in understanding the proper boundary conditions to use in clusters representing metal-oxide compounds).

The results on  $\text{H}_2^+$  and  $\text{H}_2$  are also very interesting.

In  $H_2^+$ , we found that non-spherical components of the potential did alter the spectral intensities. This effect should be expected as well in tetrahedral and octahedral complexes, although the effect should be less pronounced than in the case of diatomic systems. The  $H_2$  results suggest that multiplets are best calculated through the use of the spin unrestricted method above, rather than the combination of spin restricted and spin unrestricted methods currently in use.<sup>105</sup> This idea requires further study from both empirical (computational) and theoretical viewpoints.

Although we have not been able to calculate spectral intensities in transition metal complexes with quantitative accuracy, the calculated intensities are sufficiently accurate to obtain valuable information on spectral assignments and chemical bonding in these systems. In addition, the use of alternative forms of the oscillator strength (the  $f(\vec{x})$  and  $f(\vec{V})$  forms) should further improve the agreement between theory and experiment. We will then be better able to assess the importance of correlation, local field effects, and molecule-environment interactions in molecular spectra.

## CHAPTER IX

## SUGGESTIONS FOR FURTHER WORK

The methods developed in the present work may be applied to understanding spectral assignments and to evaluating spectral intensities in a wide variety of systems. Some examples are given below. In all cases, the  $f(\vec{\nabla}V)$  form of the oscillator strength should be checked against the  $f(x)$  form to insure the validity of one's conclusions.

We have already mentioned that further spin unrestricted  $X_{\alpha}$  theory calculations should be done on  $\text{Cr}(\text{CO})_6$  to obtain improved excitation energies and spectral intensities. A clear understanding of the character of the lowest excited state in  $\text{Cr}(\text{CO})_6$  (the  $9a_{1g}$  in our assignment versus the  $6e_g$  in Beach and Gray's assignment) is particularly valuable for understanding various photochemical reactions.<sup>51,52</sup> For example,  $\text{Cr}(\text{CO})_6$  is known to catalyze the hydrogenation of 1,3 dienes in the presence of u.v. light and  $\text{H}_2$ . Wrighton and Schroeder have found that the function of the u.v. light is to generate a thermally active catalyst through photo-dissociation of  $\text{Cr}(\text{CO})_6$ .<sup>52</sup> The subsequent hydrogenation

reaction then depends on the type of bonding between the  $\text{Cr}(\text{CO})_5$  excited state and the diene molecule.

The hydrogenation of ethylene on a metallic platinum surface is another important catalytic process.<sup>109</sup> It is known that the rate of this process is significantly reduced when the platinum surface is exposed to u.v. light of photon energy 4.2 eV.<sup>110</sup> It has been proposed that the reduction of catalytic activity is caused by platinum-to-ethylene charge transfer transitions which weaken the Pt- $\text{C}_2\text{H}_4$  bonds and therefore lead to photodesorption of  $\text{C}_2\text{H}_4$  from the platinum surface.  $X_\alpha$  scattered wave calculations for the excitation energies of the various transitions in this system are in progress.<sup>109</sup> Intensity calculations would be useful in fixing spectral assignments for the platinum-ethylene cluster. In addition, one could compare the calculated oscillator strengths to the observed reduction in the rate of catalytic activity to see if the oscillator strength values are of the correct magnitude.

In many transition metal compounds, localized excitations having large oscillator strengths can occur.<sup>111</sup> The optical properties (excitation energies and photoemission spectra) of NiO, for example, have been found to be well represented by  $X_\alpha$  scattered wave calculations on an  $\text{NiO}_6^{-10}$  cluster in a stabilizing electrostatic field. It would be

interesting to see to what extent the experimental oscillator strengths in NiO agree with the calculated intensities for the  $\text{NiO}_6^{-10}$  cluster. By analogy with our previous arguments, the scale factor between the theoretical and experimental  $f$  values should be related to the relative localization of the cluster model states versus the localization of the true states in bulk NiO.

Following the general philosophy of the example above, one may inquire to what extent the optical properties of other transition metal compounds such as  $\text{NiS}_2$  and  $\text{FeS}_2$  are determined by local molecular orbital-like states. Again, excitation energies and photoelectron spectra, calculated by the  $X_\alpha$  scattered wave method are in good agreement with experiment, but the theoretical oscillator strengths constitute a more critical test of the physical accuracy of the cluster models.

One type of system we have not treated are clusters containing metal-metal bonds. Many of the systems have optical spectra involving metal-metal charge transfer transitions. Dr. J. Norman is presently working on evaluating spectral intensities for this type of transition in the complex  $\text{Mo}_2\text{Cl}_8^{-4}$  using the author's optical properties computer program (see Appendix A).<sup>112</sup> Spectral assignments in this system are very controversial.

The theoretical evaluation of photoelectron emission intensities from molecules and clusters (the latter may be associated, for example, with the chemisorptive bond at a surface or with localized states in a semiconductor) would be an important addition to the field of photoelectron spectroscopy. Accurate theoretical intensities would lead to a better understanding of the character of the occupied states of the molecule or cluster.<sup>113</sup> However, previous theoretical methods for determining photoelectron emission intensities in these systems have been limited to simple cases.<sup>113,114</sup> Recently, Dill and Dehmer have developed a theoretical method (which has now been programmed for a computer) to evaluate photoelectron emission intensities based on the scattered wave method.<sup>115</sup> Preliminary applications of this method to diatomic molecules have already been completed, with work on complex systems in progress.<sup>116</sup> The approach of Dill and Dehmer is based on explicitly solving for the continuum eigenstates using the proper plane wave plus incoming wave boundary condition.

A less sophisticated approach to the photoemission problem has been developed by the author following a suggestion by Dr. K. H. Johnson. In this method, the continuum wave functions are confined to a large spherical box (one requires that the wave functions have a node at the sphere radius of the



box). A discrete set of positive energy eigenstates is then found which models the true continuum eigenstates. The photoelectron emission probabilities are then determined using the  $\vec{V}V$  method as in the optical absorption case. We have attempted to calculate photoemission intensities from  $\text{CH}_4$  using this method. The results of this work were unsatisfactory. A further description of the method and results is given in Appendix D.

Johnson and Messmer have suggested that in solving the photoemission problem the potential of all the molecular eigenstates be lowered in a fairly uniform way.<sup>117</sup> The positive energy eigenstates would then be bound for a sufficient change in the potential without the additional spherical box boundary conditions. This method has the advantage that the density of final states is small, so that less computer time is required than with the spherical box solutions.

The central problem in all these methods is to obtain a physically meaningful boundary condition for the continuum eigenstates which at the same time is computationally convenient. In this regard, the method of Dehmer and Dill is probably the most promising. Work on all three methods is continuing to resolve these issues.

Finally, further work is necessary on some basic theoretical issues. The relation of the spin restricted and spin unrestricted  $X_{\alpha}$  theory excitation energies and oscillator strengths to the multiplet structure of a system must be clarified. We must also obtain a better understanding of the significance of the transition state wave functions used in the intensity calculations.

## CHAPTER X

## APPENDIX A

## OPTICAL PROPERTIES PROGRAM

Input Description for Self Consistent Field Program

On the energy card, 3 new variables appear, NXGP(N), NWR(N), and SYMQR(N). For each state, EIGEN is called by MAIN to compute the state, then NRMLIZ (normalize routine) to normalize the state. Immediately after statement 4014, we set NXGO=NXGP(N), with N = state. If NXGO = 1, we compute the initial state for optical properties, NXGO = 2 = final state for optical properties, NXGO = 0 = passive state. SYMQR(N) is only used when NXGO = 2. When NXGO = 1, OPTIK is called, and the variables for the initial state are set up. For NXGO = 2, OPTIK is called, variables for the final state are set up, and optical intensities computed. For NXGO = 0, OPTIK is skipped. INPUT - ENERGY CARD - NXGP = 1 for initial state, 2 for final state, 0 otherwise. NWRIT = 1 means only the most important variables are output. SYMQR=XSVMF in OPTIK program; this variable takes spin and orbital degeneracy into account. The columns used are 50, 55 and 56-65 respectively.

Input Description for Non-Self Consistent Program

On the energy card, use the same variables as above. In addition, NIRREP appears in column 70. NIRREP = orbital degeneracy of the state if the program is used to compute the vector coupling coefficients. Follow this card by the other partners of the irreducible representation. The subsequent cards appear as usual. All partners of the irreducible representations appear for the initial state  $NXGP(N) = 1$  of the transition, and the final state  $NXGP(N) = 2$  of the transition. The program operates exactly analogous to the SCF program, except that additional temporary storage must be specified.

Optik Subroutine

The program may be divided into Sections. Section 1, extending through statement 2, initializes various quantities.  $NXGO = 1$  initial state, 2 final state.  $CI(KIT, MVNT, LNT, NUE)$  = initial state coefficients, and  $CF(KIT, MVNT, LNT, NUE)$  = final state coefficients of partial waves on various atomic centers.

$NUE$  = unique atom label,  $KIT$  = label of one of a set of equivalent atoms,  $LNT$  = total angular momentum + 1,  $MVNT$  = component of angular momentum label,

MVNT = 1 if MN = 0 and IN = 1.

MVNT = 2\*MN if MN  $\neq$  0 and IN = -1.

MVNT = 2\*MN + 1 if MN  $\neq$  0 and IN = 1.

CI and CF are initialized to 0 at the beginning of the program.

EI and EF are initial and final state energies, and NUATOM = number of unique atoms.

Section 2, beginning with DO 504, computes all the radial functions and radial integrals used in the program. This section extends through statement 30. Since such radial integrals require that both initial and final states be known, this section is skipped when NXGO = 1, the first time through the program. This is the purpose of IF(NXGO.EQ.1) GO TO 603. In section 2, the procedure is

1) Compute radial functions RI(LS, LVAL, NN), RF(LS, LVAL, NN) for the initial and final states, LS = mesh point, LVAL = angular momentum + 1, NN = unique atom label.

2) Compute radial integrals  $S(K,J,I) = \int_0^{b_I} RI(K,I) RF(J,I) r^2 \frac{dV(I)}{dr} dr$  where I = unique atom label

K, J = angular momenta of initial and final radial functions

$b_I$  = radius of atom I

3) Compute surface terms  $SUR(K,J,I) = RI(K,I) * RF(J,I) \Big|_{b_I} * b_I^2 * (VC - V(b_I)) = (\text{product of radial functions at sphere$

boundaries) \* (discontinuity of potential at sphere boundary) \* (radius of sphere)<sup>2</sup>

4) Sum radial integrals and surface terms

$$ST(K,J,I) = S(K,J,I) + SUR(K,J,I)$$

Section 3-- starts with statement 603.

1) Structural information on the molecule is set up from statement 603 to 601. For each atom  $N = 1, NAT$ , a unique atom label  $NU(N)$ , an equivalent atom label  $KI(N)$ , and a label for the total number of atoms of type  $I$ ,  $KB(I)$  are set up.

2) From 93 to statement 606, symmetry information for initial and final states  $KK = NXGO = 1, 2$  is set up. The partial wave coefficients as described on the first page of this Appendix are constructed as products of  $CN(K,N) * XC(N)$ , where  $K = \text{component}$  and  $N = \text{basis function}$ .  $CN(K,N)$  are the coefficients of the symmetry adapted basis functions as appearing in the symmetry input.  $XC(N)$  are the symmetry coefficients resulting from the solution of the secular problem.  $CN(K,N) * XC(N)$  are the coefficients for total angular momentum  $LNT$ ,  $m$  component  $MVNT$ , unique atom  $NU(KTA)$ , and atom out of a set of

equivalent atoms KI(KTA).

Section 4-- begins with statement 94 and ends with statement 20. This section does the symmetry calculations for the program. These include angular integrations as well as sums over sets of equivalent atoms and sums over angular momentum indices.

$$\langle \Psi_i, \nabla_x V \Psi_f \rangle = \sum_{\beta L L'} C_L^{\beta} C_{L'}^{\beta} \cdot \left[ \int_0^{b_B} R_{\ell}^{\beta}(E_i, r_B) R_{\ell'}^{\beta}(E_f, r_B) \frac{\partial V}{\partial r} r_B^2 dr_B + \right.$$

$$\left. \left( \text{when } \beta=0, \int_{b_0}^{\infty} \right) \right]$$

$$R_{\ell}^{\beta}(E_i, b_B) R_{\ell'}^{\beta}(E_f, b_B) \left[ \frac{b_B^2}{b_B} (V_c - V_{\text{inside on surface}}) \right] \cdot I_{11}(L; L')$$

$$\left[ \text{when } \beta=0, \text{ radius } b_0, \left( V_{\text{outside on surface}} - V_c \right) \right]$$

$$\langle \Psi_i, \nabla_y V \Psi_f \rangle = \quad (\text{Same expression}) \cdot I_{1-1}(L; L')$$

$$\langle \Psi_i, \nabla_z V \Psi_f \rangle = \quad (\text{Same expression}) \cdot I_{10}(L; L')$$

In these expressions,  $C_L, C_{L'}$ , are coefficients for initial and final states,  $R_{\ell}$  and  $R'_{\ell}$ , are radial functions

for initial and final states, B is simply the atom number, and  $L=(\ell, m)$ . The expression in brackets is the same for all equivalent atoms of type  $\alpha$ . Let the

$$[ \quad ] = A_{\ell\ell'}(E_i; E_f).$$

Let the equivalent atom label for an atom of type  $\alpha$  be  $k(\alpha)$ . Then

$$\left( \Psi_i, \left\{ \begin{array}{c} \nabla_x V \\ \nabla_y V \\ \nabla_z V \end{array} \right\} \Psi_f \right) = \sum_{\alpha} \sum_{\ell\ell'} A_{\ell\ell'}^{\alpha}(E_i; E_f) \cdot \left[ \sum_{m, m', k(\alpha)} C_{\ell m}^{k(\alpha)} C_{\ell' m'}^{k(\alpha)} \cdot \begin{pmatrix} I_{11}(\ell m; \ell' m') \\ I_{1-1}(\ell m; \ell' m') \\ I_{10}(\ell m; \ell' m') \end{pmatrix} \right]$$

$A_{\ell\ell'}(E_i; E_f)$  corresponds exactly to  $ST(K, J, I)$  discussed previously. Since  $I_{11}(\ell m; \ell' m')$  are independent of

1-1  
10

$k(\alpha)$ , one does the sum over  $k(\alpha)$  first. We define a variable  $B_{\ell\ell'}^{\alpha}(p)$  by

$$\sum_{m, m'} \begin{pmatrix} I_{11}(\ell m; \ell' m') \\ I_{1-1}(\ell m; \ell' m') \\ I_{10}(\ell m; \ell' m') \end{pmatrix} \cdot \left[ \sum_{k(\alpha)} C_{\ell m}^{k(\alpha)} C_{\ell' m'}^{k(\alpha)} \right] = B_{\ell\ell'}^{\alpha}(p)$$

$B_{\ell\ell'}^{\alpha}(p)$  corresponds exactly to  $ZUM(JP, J, I, IX)$  with  $p =$



electric field polarization = IX. As previously defined, J, JP are the total angular momentum indices for the initial and final states,

$$J = \ell + 1, \quad JP = \ell' + 1.$$

Finally, we obtain

$$\langle \Psi_i | \left\{ \begin{array}{l} \vec{\nabla}_x V \\ \vec{\nabla}_y V \\ \vec{\nabla}_z V \end{array} \right\} \Psi_f \rangle = \sum_{\alpha} \sum_{\ell \ell'} A_{\ell \ell'}^{\alpha}(E_i; E_f) B_{\ell \ell'}^{\alpha}(\rho)$$

This is done in the loop DO 23.

The oscillator strength f=XOSC is computed via

$$f = \frac{4}{3} \cdot \frac{1}{(E_i - E_f)^4} \left| \langle \Psi_i | \vec{\nabla} V \Psi_f \rangle \right|^2 \cdot (E_f - E_i)$$

$$f = \frac{4}{3} \cdot \frac{1}{(E_i - E_f)^3} \left| \langle \Psi_i | \vec{\nabla} \Psi_f \rangle \right|^2$$

The absolute transition probability (which is the important observable for photo-emission) is P=PABS

$$P = \frac{4}{3} \cdot \frac{1}{(E_i - E_f)^4} \left| \langle \Psi_i | \vec{\nabla} V \Psi_f \rangle \right|^2$$

Therefore, we have a simple relation between the oscillator strength and the absolute transition probability

$$f = P * (E_f - E_i) \quad \text{Physically, this says that } f = \frac{\text{amount of energy absorbed}}{\text{unit energy input}} = \frac{(\text{probability of transition } i \rightarrow f)}{\text{unit energy input}}$$

\*(amount of energy absorbed if transition occurs) , XSYMF is simply a multiplicative factor in the equation for XOSC = oscillator strength. It is an input parameter to the program used to take the spin degeneracy factor (or the orbital degeneracy factor as well) into account. The orbital degeneracy factor must either be known from vector coupling coefficient tables or computed from the ENERGY PROGRAM (the non-self consistent version) + the associated Optik routine which follows the NSCF ENERGY program in the preceding listing. We also compute the variables Q(I) and QAM(I,J) which are respectively the orbital charge in sphere I, and the orbital charge in sphere I with angular momentum index  $J = \ell + 1$ . The output variable JAKE =  $\ell$ .

	OPTICAL PROPERTIES PROGRAMS	SCF 0001
	SCATTERED WAVE SELF CONSISTENT FIELD PROGRAM	SCF 0002
C	SCATTERED-WAVE MODEL FOR POLYATOMIC MOLECULES AND CLUSTERS.	SCF 0003
C	PROGRAM WRITTEN BY F. C. SMITH, JR. AND K. H. JOHNSON, M.I.T.	SCF 0004
C	SELF-CONSISTENT SPIN-UNRESTRICTED MAIN PROGRAM.	SCF 0005
C	CALCULATES SCF-XALPHA ONE-ELECTRON ENERGIES, STATISTICAL TOTAL	SCF 0006
C	ENERGY, AND TOTAL KINETIC ENERGY -- ALL ELECTRONS OR FROZEN CORES.	SCF 0007
C	THIS VERSION DIMENSIONED FOR 18 CENTERS (INCLUDING ATOMS, OUTER OR	SCF 0008
C	WATSON SPHERE, AND INTERATOMIC SPHEPES), PARTIAL-WAVE LMAX=6 PER	SCF 0009
C	PAIR OF ATOMS, 10 DIFFERENT ATOMS (WITH A TOTAL OF 26 DIFFERENT L	SCF 0010
C	VALUES), 2 DIFFERENT INTERATOMIC POTENTIALS, A 28X28 SECULAR	SCF 0011
C	MATRIX, AND A MAXIMUM OF 24 COMPONENTS PER BASIS FUNCTION.	SCF 0012
	EQUIVALENCE (EINTEG (1), P (1, 1), (VN (1, 1), P (1, 2))	SCF 0013
	COMMON/STATE/CN (24, 28), MN (24, 28), IN (24, 28), NATCM (24, 28), LN (28),	SCF 0014
	1 NMS (28), IMIN (28, 18), IMAX (28, 18), NLEO (18), KTAU (18), NNS, ICORE,	SCF 0015
	2 NUATOM, NDG, NLS (18), NOL (18), NO (18), NTERMS (18), LMAXN (18), NDIM	SCF 0016
	COMMON/PARAM/VCON, XE, EV, IOUT, KONSW, NOUT, NAT, NDAT, NSPINS,	SCF 0017
	1 NACORE, RADION, QION, FAC1, EXFAC0, RS (18), XV (18), YV (18), ZV (18), Z (18)	SCF 0018
	2 , EXFACT (18), LMAXX (18), NZ (18), NSYMBL (18), NEQ (18), LCORE (18), KION	SCF 0019
	COMMON/FCNR/H (10), VCONS (2), R (200, 10), V (200, 20), ICHG (10, 10),	SCF 0020
	1 KPLACE (18), KMAX (18)	SCF 0021
	COMMON/SECULR/RHO (200, 11)	SCF 0022
	COMMON/CORE/ROCORE (200, 10)	SCF 0023
	COMMON/CP/NSPINA, NSPINB	SCF 0024
	DIMENSION P (200, 26), PS (26), DPS (26), XC (28), XA (28), RAMF (28)	SCF 0025
	DIMENSION Q (18), RHOTOT (200, 20), VN (200, 20), QITOT (2), VCN (2),	SCF 0026
	1 QE (18), QIOLD (2), EINTEG (200), STR (700), ISTR (5000)	SCF 0027
	DIMENSION ESTATE (55), OCUP (55), NSYM (55), DEST (55), NSFIX (55), NSFL (55)	SCF 0028
	1 , NSPIN (55), ISACOR (55), SYMQR (55)	SCF 0029
	INTEGER NXGP (55), NWRIT (55)	SCF 0030
	CALL ERRSET (208, 256, -1, 1)	SCF 0031
	CALL ERRSET (209, 256, -1, 1)	SCF 0032
	KCNSW=1	SCF 0033
140	CALL INPUT	SCF 0034
142	QNUC=0.	SCF 0035
	DO 141 N=1, NAT	SCF 0036

141	QNUC=QNUC+Z (N)		SCF 0037
	QNUC=2.0*QNUC		SCF 0038
	NSAT=NDAT*NSPINS		SCF 0039
	IF (IOUT.EQ.0) GO TO 302		SCF 0040
	IPR=3		SCF 0041
	IPU=0		SCF 0042
	IF (IOUT.EQ.2) IPU=3		SCF 0043
	CALL OUTPUT(XC,IPR,IPU,PS,DPS,P,E,EV)		SCF 0044
302	READ (5,100,END=302) NSTS,NITER,IPR,IPU,NTHR,NTOL,NAV,	NTYP,	SCF 0045
	1 NCORES,ALPH1		SCF 0046
100	FORMAT (9I5,5X,F10.5)		SCF 0047
	ECSUM=0		SCF 0048
	IF (NCORES.EQ.0) GO TO 303		SCF 0049
	WRITE (6,112)		SCF 0050
112	FORMAT (//35X,'CORE ENERGIES READ IN'/40X,' ENERGY	OCCUP')	SCF 0051
	DO 304 N=1,NCORES		SCF 0052
	READ (5,110) ECORE,OCORE		SCF 0053
110	FORMAT (2F10.0)		SCF 0054
	WRITE (6,111) ECORE,OCORE		SCF 0055
111	FORMAT (40X,2F15.7)		SCF 0056
304	ECSUM=ECSUM+ECORE*OCORE		SCF 0057
303	IF (NTYP.EQ.0) NTYP=1		SCF 0058
	IF (ALPH1.EQ.0) ALPH1=.5		SCF 0059
	ALPH2=1.-ALPH1		SCF 0060
	IPR=3*IPR		SCF 0061
	IEU1=0		SCF 0062
	IPU2=0		SCF 0063
	IF (IPU.GT.0) IPU2=3		SCF 0064
	IF (IPU.GT.1) IPU1=3		SCF 0065
	TCL=10.0**(-NTOL)		SCF 0066
	IF (NTOL.EQ.0) TOL=1.E-2		SCF 0067
	THRESH=10.**(-NTHR)		SCF 0068
	IF (NTHR.EQ.0) THRESH=1.E-5		SCF 0069
	WRITE (6,100) NSTS,NITER,IPR,IPU,NTHR,NTOL,NAV,	NTYP,	SCF 0070
	1 NCORES,ALPH1		SCF 0071
	IFL=1		SCF 0072

IFX=1	SCF 0073
OCEL=0.	SCF 0074
DC 311 N=1,NSTS	SCF 0075
READ (5,102) OCUP (N) ,ESTATE (N) ,DEST (N) ,NSYM (N) ,NSPIN (N) ,	SCF 0076
1 ISACOR (N) ,NXGP (N) ,NWRIT (N) ,SYMQR (N)	SCF 0077
102 FORMAT (3F10.0,5I5,F10.6)	SCF 0078
IF (NSPIN (N) .EQ.0) NSPIN (N) =1	SCF 0079
OCEL=OCEL+OCUP (N)	SCF 0080
DEST (N) = ABS (DEST (N) )	SCF 0081
WRITE (6,200) N,OCUP (N) ,ESTATE (N) ,DEST (N) ,NSYM (N) ,NSPIN (N) ,	SCF 0082
1 ISACOR (N)	SCF 0083
200 FORMAT (I5,F10.2,2F10.5,3I5)	SCF 0084
IF (NSYM (N) .NE.N) GO TO 311	SCF 0085
NSFIX (N) =IFX	SCF 0086
NSFL (N) =IFL	SCF 0087
CALL SYMM	SCF 0088
ISTR (IFX) =NDIM	SCF 0089
IFX=IFX+1	SCF 0090
ISTR (IFX) =NDG	SCF 0091
IFX=IFX+1	SCF 0092
ISTR (IFX) =NUATOM	SCF 0093
IFX=IFX+1	SCF 0094
DC 1 NN=1,NDIM	SCF 0095
NM=NMS (NN)	SCF 0096
ISTR (IFX) =LN (NN)	SCF 0097
IFX=IFX+1	SCF 0098
ISTR (IFX) =NM	SCF 0099
IFX=IFX+1	SCF 0100
DO 1 I=1,NM	SCF 0101
ISTR (IFX) =MN (I,NN)	SCF 0102
IFX=IFX+1	SCF 0103
ISTR (IFX) =IN (I,NN)	SCF 0104
IFX=IFX+1	SCF 0105
ISTR (IFX) =NATOM (I,NN)	SCF 0106
IFX=IFX+1	SCF 0107
STR (IFL) =CN (I,NN)	SCF 0108

1	IFL=IFL+1	SCF 0109
	DO 2 I=1,NAT	SCF 0110
	ISTR(IFX)=NLEQ(I)	SCF 0111
	IFX=IFX+1	SCF 0112
	ISTR(IFX)=NLS(I)	SCF 0113
	IFX=IFX+1	SCF 0114
	ISTR(IFX)=NOL(I)	SCF 0115
	IFX=IFX+1	SCF 0116
	ISTR(IFX)=NO(I)	SCF 0117
	IFX=IFX+1	SCF 0118
	ISTR(IFX)=NTERMS(I)	SCF 0119
	IFX=IFX+1	SCF 0120
	ISTR(IFX)=LMAXN(I)	SCF 0121
	IFX=IFX+1	SCF 0122
	DO 2 NN=1,NDIM	SCF 0123
	ISTR(IFX)=IMIN(NN,I)	SCF 0124
	IFX=IFX+1	SCF 0125
	ISTR(IFX)=IMAX(NN,I)	SCF 0126
2	IFX=IFX+1	SCF 0127
	IF(IFX.GT.5000) WRITE(6,104) IFX	SCF 0128
	IF(IFL.GT.700) WRITE(6,104) IFL	SCF 0129
311	CONTINUE	SCF 0130
104	FORMAT('       TEMPORARY STORAGE EXCEEDED - SUBSCRIPT=',I4)	SCF 0131
	CALL STRUCT	SCF 0132
	DO 312 ITER=1,NITER	SCF 0133
	NSC=1	SCF 0134
	NS=1	SCF 0135
	DO 324 ISPIN=1,NSPINS	SCF 0136
	QITOT(ISPIN)=0	SCF 0137
	DO 317 I=1,NDAT	SCF 0138
	KX=KMAX(I)	SCF 0139
	IF(LCORE(I).EQ.0) GO TO 319	SCF 0140
	DO 318 K=1,KX	SCF 0141
318	RHOTOT(K,NS)=ROCORE(K,NSC)	SCF 0142
	NSC=NSC+1	SCF 0143
	GO TO 317	SCF 0144

319	DO 323 K=1,KX	SCF 0145
323	RHOTOT(K,NS)=0	SCF 0146
317	NS=NS+1	SCF 0147
324	CONTINUE	SCF 0148
	NMX=1	SCF 0149
	DC 314 N=1,NSTS	SCF 0150
	CALL TIMING(ICPU,IEXCP)	SCF 0151
	WRITE(6,1001) ICPU,N	SCF 0152
1001	FORMAT(1H0,I8,' STATE',I3)	SCF 0153
	NNS=NSPIN(N)	SCF 0154
	VCON=VCONS(NNS)	SCF 0155
	IFX=NSFIX(NSYM(N))	SCF 0156
	IFL=NSPL(NSYM(N))	SCF 0157
	NDIM=ISTR(IFX)	SCF 0158
	IFX=IFX+1	SCF 0159
	NDG=ISTR(IFX)	SCF 0160
	IFX=IFX+1	SCF 0161
	NUATOM=ISTR(IFX)	SCF 0162
	IFX=IFX+1	SCF 0163
	DO 3 NN=1,NDIM	SCF 0164
	LN(NN)=ISTR(IFX)	SCF 0165
	IFX=IFX+1	SCF 0166
	NM=ISTR(IFX)	SCF 0167
	IFX=IFX+1	SCF 0168
	NMS(NN)=NM	SCF 0169
	DC 3 I=1,NM	SCF 0170
	MN(I,NN)=ISTR(IFX)	SCF 0171
	IFX=IFX+1	SCF 0172
	IN(I,NN)=ISTR(IFX)	SCF 0173
	IFX=IFX+1	SCF 0174
	NATOM(I,NN)=ISTR(IFX)	SCF 0175
	IFX=IFX+1	SCF 0176
	CN(I,NN)=STR(IFL)	SCF 0177
3	IFL=IFL+1	SCF 0178
	DC 4 I=1,NAT	SCF 0179
	NLEQ(I)=ISTR(IFX)	SCF 0180

IFX=IFX+1	SCF 0181
NLS(I)=ISTR(IFX)	SCF 0182
IFX=IFX+1	SCF 0183
NOL(I)=ISTR(IFX)	SCF 0184
IFX=IFX+1	SCF 0185
NO(I)=ISTR(IFX)	SCF 0186
IFX=IFX+1	SCF 0187
NTERMS(I)=ISTR(IFX)	SCF 0188
IFX=IFX+1	SCF 0189
LMAXN(I)=ISTR(IFX)	SCF 0190
IFX=IFX+1	SCF 0191
DO 4 NN=1,NDIM	SCF 0192
IMIN(NN,I)=ISTR(IFX)	SCF 0193
IFX=IFX+1	SCF 0194
IMAX(NN,I)=ISTR(IFX)	SCF 0195
4 IFX=IFX+1	SCF 0196
EMIN=ESTATE(N)	SCF 0197
EMAX=0.0	SCF 0198
ICORE=ISACOR(N)	SCF 0199
CALL EIGEN(0,6,DEST(N),EMAX,EMIN,THRESH,P,XA,PS,DPS,ESTATE(N),RAM	SCF 0200
1 F)	SCF 0201
GC TO 132	SCF 0202
131 CALL EIGEN(0,7,DEST(N),EMAX,EMIN,THRESH,P,XA,PS,DPS,ESTATE(N),RAM	SCF 0203
1 F)	SCF 0204
132 IF(EMAX.EQ.0.0.AND.EMIN.EQ.0.0) GO TO 6	SCF 0205
IF(N.EQ.1) GO TO 134	SCF 0206
N1=N-1	SCF 0207
DO 130 NP=1,N1	SCF 0208
IF(NSYM(NP).NE.NSYM(N).OR.NSPIN(NP).NE.NSPIN(N)) GO TO 130	SCF 0209
IF(ESTATE(N).GT.EMIN) GC TO 133	SCF 0210
IF(ESTATE(N).LE.ESTATE(NP).AND.ESTATE(NP).LE.ESTATE(N)+DEST(N)) GO	SCF 0211
1 TO 131	SCF 0212
GC TO 130	SCF 0213
133 IF(ESTATE(N).GE.ESTATE(NP).AND.ESTATE(NP).GE.ESTATE(N)-DEST(N)) GO	SCF 0214
1 TO 131	SCF 0215
130 CONTINUE	SCF 0216



134	CALL EIGEN (15,8,DEST(N),EMAX,EMIN,THRESH,P,XA,PS,DPS,ESTATE(N),RAM	SCF 0217
1	F)	SCF 0218
	IF (ESTATE(N).GE.ESTATE(NMX)) NMX=N	SCF 0219
	IF (IOUT.GE.0) WRITE (6,101) N,ITER,OCUP(N),ESTATE(N)	SCF 0220
101	FORMAT (/23X,I2,7H ITER=,I2,8H OCCUP=,F6.2,9H ENERGY=,1PE16.7/)	SCF 0221
	XC(1)=XA(1)/RAMF(1)	SCF 0222
	XCMA X=XC(1)	SCF 0223
	DO 4013 I=2,NDIM	SCF 0224
	XC(I)=XA(I)/RAMF(I)	SCF 0225
	IF (ABS(XC(I)).LE.ABS(XCMA X)) GO TO 4013	SCF 0226
	XCMA X=XC(I)	SCF 0227
4013	CONTINUE	SCF 0228
	DO 4014 I=1,NDIM	SCF 0229
	XA(I)=XA(I)/XCMA X	SCF 0230
4014	XC(I)=XC(I)/XCMA X	SCF 0231
	CALL NRMLIZ(P,XC,XA,Q,QINT,PS,DPS,RAMF)	SCF 0232
	NXGO=N XGE(N)	SCF 0233
	IF (NXGO.EQ.0) GO TO 700	SCF 0234
	NRIT=NWRIT(N)	SCF 0235
	XSYMF=1.0	SCF 0236
	IF (NXGO.EQ.2) XSYMF=SYMCR(N)	SCF 0237
	IF (NXGO.EQ.1) NSPINA=NSPIN(N)	SCF 0238
	IF (NXGO.EQ.2) NSPINB=NSPIN(N)	SCF 0239
	CALL OPTIK(XC,ESTATE(N),NXGO,NRIT,XOSC,XPROB,1,XSYMF)	SCF 0240
	IF (NXGO.EQ.2) MLOC=N	SCF 0241
700	WRITE(8) ((RHO(K,I),K=1,200),I=1,NDAT),(Q(I),I=1,NAT),QINT	SCF 0242
	IF (IOUT.GE.0) WRITE (6,106) (I,Q(I),I=1,NAT)	SCF 0243
106	FORMAT(6(' Q(' ,I2,' )=' ,1PE14.7))	SCF 0244
	IF (IOUT.GE.0) WRITE (6,107) QINT	SCF 0245
107	FORMAT(' INTERSPHERE CHARGE=' ,1P2E14.7)	SCF 0246
314	CONTINUE	SCF 0247
	IF (NTYP.EQ.2) GO TO 27	SCF 0248
	STATES=0.	SCF 0249
	OCUP(NMX)=0.	SCF 0250
	DO 25 N=1,NSTS	SCF 0251
	IFX=NSFIX(NSYM(N))	SCF 0252

IFX=IFX+1	SCF 0253
NDG=ISTR (IFX)	SCF 0254
NCCP=OCUP (N)	SCF 0255
IF (NOCP.NE.NDG.AND.N.NE.NMX) OCUP (N) =NDG	SCF 0256
STATES=STATES+OCUP (N)	SCF 0257
25 CONTINUE	SCF 0258
OCUP (NMX) =OCEL-STATES	SCF 0259
27 REWIND 8	SCF 0260
ETOT=ECSUM	SCF 0261
IF (NAV.EQ.0.OR.ITER.EQ.1) GO TO 18	SCF 0262
READ (8) ((RHO (K,I) ,K=1,200) ,I=1,NSAT)	SCF 0263
18 DC 315 N=1,NSTS	SCF 0264
ETOT=ETOT+OCUP (N)*ESTATE (N)	SCF 0265
IF (IOUT.EQ.-2) WRITE (6,101) N,ITER,OCUP (N) ,ESTATE (N)	SCF 0266
READ (8) ((RHO (K,I) ,K=1,200) ,I=1,NDAT) , (Q (I) ,I=1,NAT) , QINT	SCF 0267
NNS=NSPIN (N)	SCF 0268
QITOT (NNS) =QITOT (NNS) +QINT*OCUP (N)	SCF 0269
DC 315 I=1,NDAT	SCF 0270
KX=KMAX (I)	SCF 0271
IF (IOUT.EQ.-2) WRITE (6,116) (K1, (R (K1+ (K2-1) ,I) ,RHO (K1+ (K2-1)	SCF 0272
1 ,I) ,K2=1,4) ,K1=1,KX,4)	SCF 0273
116 FORMAT (1X,I3,8E15.7)	SCF 0274
NS=I+NDAT*(NNS-1)	SCF 0275
DO 316 K=1,KX	SCF 0276
316 RHOTOT (K,NS) =RHOTOT (K,NS) +RHO (K,I) *OCUP (N)	SCF 0277
315 CONTINUE	SCF 0278
IF (IOUT.NE.-2) GO TO 119	SCF 0279
DO 118 NNS=1,NSPINS	SCF 0280
WRITE (6,117)	SCF 0281
117 FCRMAT (1H1)	SCF 0282
DO 118 I=1,NDAT	SCF 0283
KX=KMAX (I)	SCF 0284
NS=I+NDAT*(NNS-1)	SCF 0285
118 WRITE (6,116) (K1, (R (K1+ (K2-1) ,I) ,RHOTOT (K1+ (K2-1) ,NS) ,K2=1,4) ,	SCF 0286
1 K1=1,KX,4)	SCF 0287
119 REWIND 8	SCF 0288

IF (NAV.EQ.0.OR.ITER.EQ.1) GO TO 220	SCF 0289
READ (8) ((RHO(K,I),K=1,200),I=1,NSAT)	SCF 0290
I=0	SCF 0291
DO 222 ISPIN=1,NSPINS	SCF 0292
DO 221 IAT=1,NDAT	SCF 0293
KX=KMAX(IAT)	SCF 0294
I=I+1	SCF 0295
DO 223 K=1,KX	SCF 0296
223 RHOTOT(K,I)=ALPH1*RHOTOT(K,I)+ALPH2*RHO(K,I)	SCF 0297
221 CCNTINUE	SCF 0298
222 QITOT(ISPIN)=ALPH1*QITOT(ISPIN)+ALPH2*QIOLD(ISPIN)	SCF 0299
220 CALL VGEN(Q,QITOT,RHOTOT,VN,VCN,VT,ETOT)	SCF 0300
I=0	SCF 0301
EPS=0.	SCF 0302
DO 321 ISEIN=1,NSPINS	SCF 0303
EPS=AMAX1(EPS,ABS((VCN(ISPIN)-VCONS(ISPIN))/VCONS(ISPIN)))	SCF 0304
IF (NAV.EQ.0.OR.ITER.EQ.1) GO TO 225	SCF 0305
GO TO 224	SCF 0306
225 VCN(ISPIN)=ALPH1*VCN(ISPIN)+ALPH2*VCONS(ISPIN)	SCF 0307
224 DO 321 IAT=1,NDAT	SCF 0308
I=I+1	SCF 0309
KX=KMAX(IAT)	SCF 0310
KPL=KPLACE(IAT)	SCF 0311
DO 320 K=1,KX	SCF 0312
IF (IAT.EQ.1.AND.NOUT.NE.0.AND.K.GT.KPL) GO TO 229	SCF 0313
CNUC=0.	SCF 0314
GO TO 230	SCF 0315
229 CNUC=QNUC	SCF 0316
230 EPS=AMAX1(EPS,ABS((VN(K,I)-V(K,I))/(VN(K,I)+CNUC/R(K,IAT))))	SCF 0317
IF (NAV.EQ.0.OR.ITER.EQ.1) GO TO 322	SCF 0318
GO TO 320	SCF 0319
322 VN(K,I)=ALPH1*VN(K,I)+ALPH2*V(K,I)	SCF 0320
320 CONTINUE	SCF 0321
321 CONTINUE	SCF 0322
WRITE(6,103) ITER, EPS	SCF 0323
103 FORMAT(///30X,'ITERATION ',I2,' EPS=',1PE16.7)	SCF 0324

17	WRITE (6,107) (QITOT(I SPIN),ISPIN=1,NSPINS)	SCF 0325
	WRITE (6,106) (I,Q(I),I=1,NAT)	SCF 0326
C	USE 1ST ORDER PERTURBATION THEORY TO FIND TRIAL ENERGY FOR NEXT	SCF 0327
C	ITERATION.	SCF 0328
	DO 120 N=1,NSTS	SCF 0329
	READ (8) ((RHO(K,I),K=1,200),I=1,NDAT), (Q(I),I=1,NAT), QINT	SCF 0330
	NNS=NSPIN(N)	SCF 0331
	DE=0	SCF 0332
	NID=2	SCF 0333
	IF(NOUT.EQ.0) NID=1	SCF 0334
	NS= NDAT*(NNS-1)	SCF 0335
	DO 125 I=1,NDAT	SCF 0336
	NS=NS+1	SCF 0337
	KX=KMAX(I)	SCF 0338
	DC 121 K=1,KX	SCF 0339
121	RHO(K,I)=RHO(K,I)*(VN(K,NS)-V(K,NS))	SCF 0340
	CALL INTEGR(RHO(1,I),R(1,I),KX,ICHG(1,I),EINTEG,NID)	SCF 0341
	NID=1	SCF 0342
	CALL INTERP(R(KPLACE(I)-3,I),EINTEG(KPLACE(I)-3),7,RS(I),QE(I),	SCF 0343
	1 ZILCH,.FALSE.)	SCF 0344
125	DE=DE+QE(I)	SCF 0345
	NDAT1=NDAT+1	SCF 0346
	IF(NDAT1.GT.NAT) GO TO 123	SCF 0347
	DO 122 I=NDAT1,NAT	SCF 0348
122	DE=DE+QE(NEQ(I))	SCF 0349
123	DE=DE+QINT*(VCN(NNS)-VCCNS(NNS))	SCF 0350
	EP=ESTATE(N)+DE	SCF 0351
	WRITE (6,105) N,OCUP(N),ESTATE(N),EP,NNS,NSYM(N)	SCF 0352
	ESTATE(N)=EP	SCF 0353
105	FORMAT(/6X,'STATE',I3,' OCCUP=',F6.2,' E=',1PE15.7,' NEXT E=',1	SCF 0354
	1 PE15.7,' SPIN=',I2,' SYMMETRY',I3)	SCF 0355
	IF (MLOC.EQ.N) WRITE(6,701) XPROB,XOSC	SCF 0356
701	FORMAT(1X,32HABSOLUTE TRANSITION PROBABILITY=,F12.6,20HOSCILLATOR	SCF 0357
	1STRENGTH=,F12.6)	SCF 0358
	WRITE (6,106) (I,Q(I),I=1,NAT)	SCF 0359
120	WRITE (6,107) QINT	SCF 0360

	WRITE (6,109) ETOT,VT	SCF 0361
109	FORMAT (/6X,'XALPHA STATISTICAL TOTAL ENERGY=',1PE15.7,' TOTAL K	SCF 0362
	KINETIC ENERGY=',1PE15.7)	SCF 0363
	IF (EPS.IT.TOL) GO TO 5	SCF 0364
	REWIND 8	SCF 0365
	IF (NAV.EQ.0) GO TO 514	SCF 0366
	WRITE (8) ((PHOTOT(K,I),K=1,200),I=1,NSAT)	SCF 0367
514	I=0	SCF 0368
	DO 124 ISPIN=1,NSPINS	SCF 0369
	QIOLD (ISPIN)=QITOT (ISPIN)	SCF 0370
	VCONS (ISPIN)=VCN (ISPIN)	SCF 0371
	DO 124 IAT=1,NDAT	SCF 0372
	I=I+1	SCF 0373
	KX=KMAX (IAT)	SCF 0374
	DO 124 K=1,KX	SCF 0375
124	V (K,I)=VN (K,I)	SCF 0376
	IF (ITER.EQ.NITER) GO TO 5	SCF 0377
	CALL OUTPUT (XC,IPR,IPU1,PS,DPS,P,E,EV,0.0)	SCF 0378
312	CONTINUE	SCF 0379
	6 WRITE (6,900) N	SCF 0380
900	FORMAT (' ERROR,ENERGY LEVEL',I4,' NOT FOUND')	SCF 0381
	5 CALL OUTPUT (XC,3 ,IPU2,PS,DPS,P,E,EV,0.0 )	SCF 0382
	DO 298 N=1,NSTS	SCF 0383
298	WRITE (7,299) OCUP (N) ,ESTATE (N) ,DEST (N) ,NSYM (N) ,NSPIN (N) ,	SCF 0384
	1 ISACOR (N)	SCF 0385
299	FORMAT (3F10.3,3I5)	SCF 0386
	STOP	SCF 0387
	END	SCF 0388

```

OPTICAL PROPERTIES SUBROUTINE (FOR USE IN SCF PROGRAM)
SUBROUTINE OPTIK (XC,E,NXGO,NRIT,XOSC,PABS ,JCONTR,XSYMF)
C OPTIK ROUTINE WRITTEN BY LOUIS NOODLEMAN
COMMON/STATE/CN (24,28) , MN (24,28) , IN (24,28) , NATCM (24,28) , LN (28) ,
1 NMS (28) , IMIN (28,18) , IMAX (28,18) , NLEQ (18) , KTAU (18) , NNS , ICORE ,
2 NUAT , NDG , NLS (18) , NOL (18) , NO (18) , NTERMS (18) , LMAXA (18) , NDIM
COMMON/PARAM/VCON,XE,EV,IOUA,KONSH,MOU,NAT,NDAT, NSPINS,
1 NACORE,RADION,QION,FAC1,EXFAC0,RS (18) ,XV (18) ,YV (18) ,ZV (18) ,ZP (18)
2 ,EXFACT (18) ,LMAXX (18) ,NZ (18) ,NSYMBL (18) ,NEQ (18) ,LCORE (18) ,KION
COMMON/FCNR/H (10) ,VCONS (2) ,R (200,10) ,V (200,20) ,ICHG (10,10) ,
1 KPLACE (18) ,KMAX (18)
COMMON/BESSEL/SBFC (9) ,DSBFC (9) ,SNFC (9) ,DSNFC (9)
COMMON/OP/NSPINA,NSPINB
REAL CI (6,9,5,10) ,CF (6,9,5,10) ,RI (200,5,5) ,RF (200,5,5) ,SUMAF (9) ,
1SUMBF (9) ,ZUM (5,5,10,3) ,ZUMP (3) ,RV (200,10) ,RSVP (200) ,BVP (200,10) ,
2Y (200) ,S (5,5,10) ,SUR (5,5,10) ,ST (5,5,10) ,A (200) ,VP (200,10) ,
3VS (200,10) ,I1P,Q (10) ,QAM (10,5) ,XC (28)
INTEGER LMAXN (18) ,KB (10) ,MVN (24,28) ,KI (18) ,NU (18) ,JAKE (5) ,
1 LMAXN1 (18)
DO 609 JKR=1,9
SBFC (JKR) =1.0
DSBFC (JKR) =1.0
SNFC (JKR) =1.0
609 DSNFC (JKR) =1.0
IF (NRIT.EQ.0) NRIT=1
IF (NXGO.EQ.1) EI=E
IF (NXGO.EQ.2) EF=E
NUATOM=NDAT
IF (NXGO.EQ.2) VC=VCONS (NSPINB)
DC 2 NN=1,NAT
IF (NXGO.EQ.1) LMAXN1 (NN) =LMAXA (NN)
2 IF (NXGO.EQ.2) LMAXN (NN) =MAX0 (LMAXN1 (NN) ,LMAXA (NN) )
DO 4 K=1,10
DC 4 KL=1,5
DO 4 M=1,9
DO 4 ML=1,6
OPT10001
OPT10002
OPT10003
OPT10004
OPT10005
OPT10006
OPT10007
OPT10008
OPT10009
OPT10010
OPT10011
OPT10012
OPT10013
OPT10014
OPT10015
OPT10016
OPT10017
OPT10018
OPT10019
OPT10020
OPT10021
OPT10022
OPT10023
OPT10024
OPT10025
OPT10026
OPT10027
OPT10028
OPT10029
OPT10030
OPT10031
OPT10032
OPT10033
OPT10034
OPT10035
OPT10036

```

IF (NXGO.EQ.1) CI (ML,M,KL,K)=0.0	OPT10037
4 IF (NXGO.EQ.2) CF (ML,M,KL,K)=0.0	OPT10038
IF (NXGO.EQ.1) GO TO 603	OPT10039
DO 504 NN=1,NUATOM	OPT10040
DO 504 JK=1,2	OPT10041
IF (JK.EQ.1) NS=NN+(NSPINA-1)*NUATCM	OPT10042
IF (JK.EQ.2) NS=NN+(NSPINB-1)*NUATCM	OPT10043
ICUT=1	OPT10044
IF (NN.EQ.1) IOUT=2	OPT10045
KX=KMAX (NN)	OPT10046
NLMAP=IMAXN (NN)+1	OPT10047
DO 503 LVAL=1,NLMAP	OPT10048
L=LVAL-1	OPT10049
Z=FLOAT (NZ (NN))	OPT10050
IF (JK.EQ.1) CALL TMAT (L,EI,RS (NN),KMAX (NN),Z,H (NN),R (1,NN),	OPT10051
1V (1,NS),ICHG (1,NN),IOUT,KPLACE (NN),RI (1,LVAL,NN),STMAT,PS,DPS,	OPT10052
2RAMF)	OPT10053
IF (JK.EQ.2) CALL TMAT (L,EF,RS (NN),KMAX (NN),Z,H (NN),R (1,NN),	OPT10054
1V (1,NS),ICHG (1,NN),IOUT,KPLACE (NN),RF (1,LVAL,NN),STMAT,PS,DPS,	OPT10055
2RAMF)	OPT10056
503 CONTINUE	OPT10057
IF (NRIT.EQ.1) GO TO 504	OPT10058
WRITE (6,506) NN,JK	OPT10059
506 FORMAT (1X,7HCENTER=,I4,6HSTATE=,I4)	OPT10060
DO 510 IS=1,KX	OPT10061
IF (JK.EQ.1) WRITE (6,505) LS,R (LS,NN), (RI (LS,LVAL,NN)	OPT10062
1 ,LVAL=1,NLMAP)	OPT10063
IF (JK.EQ.2) WRITE (6,505) LS,R (LS,NN), (RF (LS,LVAL,NN)	OPT10064
1 ,LVAL=1,NLMAP)	OPT10065
505 FORMAT (1X,I4,6 (4X,E14.7))	OPT10066
510 CONTINUE	OPT10067
504 CONTINUE	OPT10068
DC 13 I=2,NUATOM	OPT10069
NS=I+(NSPINB-1)*NUATCM	OPT10070
LMAF=LMAXN (I)+1	OPT10071
LY=KMAX (I)	OPT10072

```

      LP=KMAX(I)-1
      LD=KPLACE(I)
      DC 8 KM=1,LY
8     RV(KM,I) = R(KM,I)*V(KM,NS)
      DO 9 L=1,LP
      IF(L.LE.2) CALL INTERP(R(L,I),RV(L,I),4,R(L,I),DUMMY,RVP(L,I),
1     .TRUE.)
      IF(L.GT.2)
1    CALL INTERP(R(L-2,I),RV(L-2,I),4,R(L,I),DUMMY,RVP(L,I),.TRUE.)
      RSVP(L)=R(L,I)*RVP(L,I)-RV(L,I)
      IF(NRIT.EQ.1) GO TO 9
      WRITE(6,500) I,L,R(L,I),RV(L,I),RVP(L,I),V(L,NS),RSVP(L)
500  FORMAT(1X,7HNUATOM=,I5,2HL=,I5,2HR=,F10.5,3HRV=,F10.5,4HRVP=,
1     F10.5,3H V=,E14.7,6H RSVP=,E14.7)
      9 CONTINUE
      DO 13 J=1,LMAF
      DC 13 K=1,LMAF
      IF(IABS(J-K).GT.1) GO TO 12
      IF((K+J+1)/2 .LT. FLOAI(K+J+1)/2.0) GO TO 12
      DO 5 L=1,LP
      5 Y(L)=RI(L,K,I)*RF(L,J,I)*RSVP(L)
      CALL INTEGR(Y,R(1,I),KMAX(I)-1,ICHG(1,I),A,1)
      CALL INTERP(R(LD-3,I),A(LD-3),6,RS(I),ASA,DUMMY,.FALSE.)
      S(K,J,I)=ASA
      SUR(K,J,I)=RI(LD,K,I)*RF(LD,J,I)*(RS(I)**2)*(VC-V(LD,NS))
      ST(K,J,I)=S(K,J,I)+SUR(K,J,I)
      GO TO 13
12   ST(K,J,I)=0.0
13   CONTINUE
      LMAF=LMAXN(1)+1
      LP=KMAX(1)-1
      LD=KPLACE(1)
      NS=1+(NSEINB-1)*NUATOM
      DO 28 I=1,LP
      IF(L.LE.2) CALL INTERP(R(L,1),V(L,NS),4,R(L,1),VS(L,1),VP(L,1),
1     .TRUE.)

```

```

OPT10073
OPT10074
OPT10075
OPT10076
OPT10077
OPT10078
OPT10079
OPT10080
OPT10081
OPT10082
OPT10083
OPT10084
OPT10085
OPT10086
OPT10087
OPT10088
OPT10089
OPT10090
OPT10091
OPT10092
OPT10093
OPT10094
OPT10095
OPT10096
OPT10097
OPT10098
OPT10099
OPT10100
OPT10101
OPT10102
OPT10103
OPT10104
OPT10105
OPT10106
OPT10107
OPT10108

```



```

IF (L.GT.2) CALL INTERP(R(L-2,1),V(L-2,NS),4,R(L,1),VS(L,1),VP(L,1)
1 ,.TRUE.)
IF (NRIT.EQ.1) GO TO 28
WRITE(6,501) L,R(L,1),V(L,NS),VP(L,1)
501 FORMAT(1X,8HNUATOM=1,3H L=,I5,3H R=,F10.5,3H V=,E14.7,3HV=,F10.5)
28 RSVP(L) = (R(L,1)**2.0)*VP(L,1)
DO 30 J=1,LMAF
DC 30 K=1,LMAF
IF (IABS(J-K).GT.1) GO TO 36
IF ((K+J+1)/2 .LT. (FLOAT(K+J+1)/2.0)) GO TO 36
DO 29 L=1,LP
29 Y(L)=RI(L,K,1)*RF(L,J,1)*RSVP(L)
CALL INTEGR(Y,R(1,1),KMAX(1)-1,ICHG(1,1),A,3)
CALL INTERP(R(1,1),A,7,BS(1),AS,DUMMY,.FALSE.)
AINT=A(KMAX(1)-1)-AS
S(K,J,1)=AINT
SUR(K,J,1)=RI(LD,K,1)*RF(LD,J,1)*(RS(1)**2.)*(V(LD,NS)-VC)
ST(K,J,1)=S(K,J,1)+SUR(K,J,1)
GC TO 30
36 ST(K,J,1)=0.0
30 CCNTINUE
IF (NXGO.EQ.2) GO TO 93
603 DO 90 N=1,NAT
NU(N)=NEQ(N)
90 IF (NEQ(N).EQ.0) NU(N)=N
DC 91 N=1,NAT
IF (NU(N).EQ.N) KI(N)=1
IF (NU(N).EQ.N) KB(N)=1
IF (N.LE.NUATCM) GO TO 91
DO 92 I=1,NUATOM
IF (NU(N).EQ.I) KB(I)=KB(I)+1
92 IF (NU(N).EQ.I) KI(N)=KB(I)
91 CONTINUE
WRITE(6,602)
602 FORMAT(1X,5HNUATOM,3X,2HNU,2X,3HNEQ,3X,2HKB)
WRITE(6,601) (J,NU(J),NEQ(J),KI(J),J=1,NAT)

```

```

OPT10109
OPT10110
OPT10111
OPT10112
OPT10113
OPT10114
OPT10115
OPT10116
OPT10117
OPT10118
OPT10119
OPT10120
OPT10121
OPT10122
OPT10123
OPT10124
OPT10125
OPT10126
OPT10127
OPT10128
OPT10129
OPT10130
OPT10131
OPT10132
OPT10133
OPT10134
OPT10135
OPT10136
OPT10137
OPT10138
OPT10139
OPT10140
OPT10141
OPT10142
OPT10143
OPT10144

```

601	FCRMT (1X,4I5)	OPT10145
93	KK=NXGO	OPT10146
	IF (NRIT.EQ.1) GO TO 607	OPT10147
	WRITE(6,53) NDIM,NDG	OPT10148
53	FORMAT (1X,5HNDIM=,I5,5H NDG=,I5)	OPT10149
	WRITE(6,54) (XC(N),N=1,NDIM)	OPT10150
54	FORMAT (1X,10HSYMM COEF=,10F10.5)	OPT10151
607	DC 600 N=1,NDIM	OPT10152
	IF (NRIT.EQ.1) GO TO 608	OPT10153
	WRITE(6,52) LN(N),NMS(N)	OPT10154
52	FORMAT (1X,3H LN=,I5,5H NMS=,I5)	OPT10155
608	NMQ=NMS(N)	OPT10156
	DO 600 I=1,NMQ	OPT10157
	IF (NRIT.EQ.1) GO TO 605	OPT10158
	WRITE(6,55) MN(I,N),IN(I,N),NATCM(I,N),CN(I,N)	OPT10159
55	FORMAT (1X,3H MN=,I5,4H IN=,I5,7H NATCM=,I5,4H CN=,F10.5)	OPT10160
605	IF (MN(I,N).EQ.0 .AND. IN(I,N).EQ.1) MVN(I,N)=1	OPT10161
	IF (MN(I,N).NE.0 .AND. IN(I,N).EQ.-1) MVN(I,N)=2*MN(I,N)	OPT10162
	IF (MN(I,N).NE.0 .AND. IN(I,N).EQ.1) MVN(I,N)=2*MN(I,N)+1	OPT10163
600	CONTINUE	OPT10164
	DC 606 N=1,NDIM	OPT10165
	NMQ=NMS(N)	OPT10166
	LNT=LN(N)+1	OPT10167
	DO 606 K=1,NMQ	OPT10168
	KTA=NATCM(K,N)	OPT10169
	KIT=KI(KTA)	OPT10170
	MVNT=MVN(K,N)	OPT10171
	NUE=NU(KTA)	OPT10172
	IF (KK.EQ.1) CI(KIT,MVNT,LNT,NUE)=CI(KIT,MVNT,LNT,NUE)+CN(K,N)	OPT10173
	1 *XC(N)	OPT10174
	IF (KK.EQ.2) CF(KIT,MVNT,LNT,NUE)=CF(KIT,MVNT,LNT,NUE)+CN(K,N)	OPT10175
	1 *XC(N)	OPT10176
606	CONTINUE	OPT10177
	IF (NXGO.EQ.2) GO TO 94	OPT10178
	RETURN	OPT10179
C	X,Y,Z POLARIZATION OF E FIELD	OPT10180

94 DC 20 IX=1,3	OPT10181
DO 20 I=1,NUATOM	OPT10182
LMAF=LMAXN(I)+1	OPT10183
DO 20 J=1,LMAF	OPT10184
DO 20 JP=1,LMAF	OPT10185
IF (IABS(J-JP).GT.1) GO TO 19	OPT10186
IF ((J+JP+1)/2 .LT.FLOAT(J+JP+1)/2.0) GO TO 19	OPT10187
SUMC=0.0	OPT10188
MF=(2*J)-1	OPT10189
DO 17 M=1,MF	OPT10190
SUMB=0.0	OPT10191
MPP=(2*JP)-1	OPT10192
DO 16 MP=1,MPP	OPT10193
SUMA=0.0	OPT10194
KBF=KB(I)	OPT10195
DO 15 KJ=1,KBF	OPT10196
15 SUMA=SUMA+CF(KJ,MP,JP,I)*CI(KJ,M,J,I)	OPT10197
SUMAF(MP)=SUMA*I1P(MP,M,JP-1,J-1,IX)	OPT10198
XIPT=I1P(MP,M,JP-1,J-1,IX)	OPT10199
16 SUMB=SUMB+SUMAF(MP)	OPT10200
SUMBF(M)=SUMB	OPT10201
17 SUMC=SUMC+SUMBF(M)	OPT10202
18 ZUM(JP,J,I,IX)=SUMC	OPT10203
GO TO 20	OPT10204
19 ZUM(JP,J,I,IX)=0.0	OPT10205
20 CCNTINUE	OPT10206
DO 23 IX=1,3	OPT10207
ZUM1=0.0	OPT10208
DO 22 I=1,NUATOM	OPT10209
LMAF=LMAXN(I)+1	OPT10210
DO 22 J=1,LMAF	OPT10211
DO 22 JP=1,LMAF	OPT10212
WRITE(6,50) JP,J,I,IX,ZUM(JP,J,I,IX),JP,J,I,ST(J,JP,I)	OPT10213
50 FORMAT(1X,4HZUM,4I3,2H =,F10.5,3HST,3I3,2H =,F10.5)	OPT10214
22 ZUM1=ZUM1+ZUM(JP,J,I,IX)*ST(J,JP,I)	OPT10215
23 ZUMP(IX)=ZUM1	OPT10216

```

      ZUMPS=0.0
      DO 40 IM=1,3
40    ZUMPS=ZUMPS+ZUMP(IM)**2
      WRITE(6,528) XSYMF
528  FORMAT(1X,'XSYMF ',F8.4)
      PREL=ZUMPS/(EI-EF)**4
      PABS=(4.0/3.0)*PREL*XSYMF
      XCSC=PABS*(EF-EI)
      DO 822 KC=1,2
      DC 815 I=1,NUATOM
      LMAF=LMAXN(I)+1
      LY=KMAX(I)
      LP=KMAX(I)-1
      LD=KPLACE(I)
      Q(I)=0.0
      DO 815 J=1,LMAF
      DC 810 KM=1,LY
      IF (KC.EQ.1) Y(KM)=(RI(KM,J,I)*R(KM,I))**2
      IF (KC.EQ.2) Y(KM)=(RF(KM,J,I)*R(KM,I))**2
810  CONTINUE
      IF (I.GT.1) GO TO 813
      CALL INTEGR(Y,R(1,1),KMAX(1)-1,ICHG(1,1),A,3)
      CALL INTERP(R(1,1),A,7,RS(1),AS,DUMMY,.FALSE.)
      RADFS=A(KMAX(1)-1)-AS
      GO TO 814
813  CALL INTEGR(Y,R(1,I),LP,ICHG(1,I),A,1)
      CALL INTERP(R(LD-3,I),A(LD-3),6,RS(I),RADFS,DUMMY,.FALSE.)
814  MF=2*J-1
      CRT=0.0
      DC 811 M=1,MF
      IF (KC.EQ.1) CRT=CRT+CI(1,M,J,I)**2
      IF (KC.EQ.2) CRT=CRT+CF(1,M,J,I)**2
811  CONTINUE
      QAM(I,J)=CRT*RADFS
815  Q(I)=Q(I)+CRT*RADFS
808  WRITE(6,820) KC, (I,Q(I),I=1,NUATOM)

```

```

OPT10217
OPT10218
OPT10219
OPT10220
OPT10221
OPT10222
OPT10223
OPT10224
OPT10225
OPT10226
OPT10227
OPT10228
OPT10229
OPT10230
OPT10231
OPT10232
OPT10233
OPT10234
OPT10235
OPT10236
OPT10237
OPT10238
OPT10239
OPT10240
OPT10241
OPT10242
OPT10243
OPT10244
OPT10245
OPT10246
OPT10247
OPT10248
OPT10249
OPT10250
OPT10251
OPT10252

```

820	FORMAT(1X,6HSTATE=,I4,4(1HQ,I2,1H=,F8.4))	OPT10253
	DO 822 I=1,NUATOM	OPT10254
	LMAF=LMAXN(I)+1	OPT10255
	DO 823 J=1,LMAF	OPT10256
823	JAKE(J)=J-1	OPT10257
822	WRITE(6,821) KC,I,(JAKE(J),QAM(I,J),J=1,LMAF)	OPT10258
821	FCRMT(1X,6HSTATE=,I4,5HATOM=,I4,5(2HQL,I2,1H=,F8.4))	OPT10259
	WRITE(6,41) EL,EF	OPT10260
41	FORMAT(1X,15HTRANSITION FROM,F10.5,11HRYDBERGS TO,F10.5,	OPT10261
	1 8HPYDBEFGS)	OPT10262
	DO 45 IX=1,3	OPT10263
	IF (IX.EQ.1) WRITE(6,42)	OPT10264
	IF (IX.EQ.2) WRITE(6,43)	OPT10265
	IF (IX.EQ.3) WRITE(6,44)	OPT10266
42	FORMAT(1X,32HTRANSITION AMPLITUDE X COMPONENT)	OPT10267
43	FORMAT(1X,32HTRANSITION AMPLITUDE Y COMPONENT)	OPT10268
44	FORMAT(1X,32HTRANSITION AMPLITUDE Z COMPONENT)	OPT10269
	WRITE(6,46) ZUMP(IX)	OPT10270
46	FORMAT(4X,E14.6)	OPT10271
45	CONTINUE	OPT10272
	WRITE(6,47) PREL	OPT10273
47	FORMAT(1X,32HRELATIVE TRANSITION PROBABILITY=,E14.6)	OPT10274
	WRITE(6,48) PABS	OPT10275
48	FORMAT(1X,33HABSOLUTE TRANSITION PROBABILITY=,F12.6)	OPT10276
	WRITE(6,49) XOSC	OPT10277
49	FORMAT(1X,20HOSCILLATOR STRENGTH=,F12.6)	OPT10278
527	CONTINUE	OPT10279
	RETURN	OPT10280
	END	OPT10281

	I1P SUBPROGRAM FOR GAUNT INTEGRALS	I1P 0001
	REAL FUNCTION I1P(M3V,M1V,J3,J1,IX)	I1P 0002
C I1P	ROUTINE WRITTEN BY LOUIS NOODLEMAN	I1P 0003
	DATA PI/3.1415927/,PI4/12.566371/	I1P 0004
	CCOMPLEX XSIN,XSINC,CMLPX,CONJG,TINT1,TINT3,A1(3)	I1P 0005
	XSIN=(0.,1.)	I1P 0006
	XSINC=CONJG(XSIN)	I1P 0007
	DO 7 K=1,2	I1P 0008
	IF(K.EQ.1) MV=M1V	I1P 0009
	IF(K.EQ.2) MV=M3V	I1P 0010
	IF((MV-(MV/2)*2).EQ.1) GO TO 2	I1P 0011
	MN=MV/2	I1P 0012
	IN=-1	I1P 0013
	GO TO 6	I1P 0014
2	IN=1	I1P 0015
	MN=(MV-1)/2	I1P 0016
6	IF(K.EQ.1) MN1=MN	I1P 0017
	IF(K.EQ.1) IN1=IN	I1P 0018
	IF(K.EQ.2) MN3=MN	I1P 0019
	IF(K.EQ.2) IN3=IN	I1P 0020
7	CCONTINUE	I1P 0021
	DO 15 KX=1,3	I1P 0022
	MX=KX-2	I1P 0023
	A1(KX)=(0.0,0.0)	I1P 0024
	DC 14 J=1,2	I1P 0025
	DC 14 JJ=1,2	I1P 0026
	IF(J.EQ.1) GO TO 10	I1P 0027
	MNT1=-MN1	I1P 0028
	IF(IN1.EQ.1) TINT1=CMLPX((-1.0)**MN1,0.0)	I1P 0029
	IF(IN1.EQ.-1) TINT1=(-1)**MN1*XSIN	I1P 0030
	IF(MN1.EQ.0) TINT1=(0.0,0.0)	I1P 0031
	GO TO 11	I1P 0032
10	MNT1=MN1	I1P 0033
	IF(IN1.EQ.-1) TINT1=XSINC	I1P 0034
	IF(IN1.EQ.1) TINT1=(1.0,0.0)	I1P 0035
	IF(MN1.EQ.0) TINT1=(2.**0.5)*(1.0,0.0)	I1P 0036

11	IF (JJ.EQ.1) GO TO 12	I1P 0037
	MNT3=-MN3	I1P 0038
	IF (IN3.EQ.1) TINT3=CMPLX((-1.0)**MN3,0.0)	I1P 0039
	IF (IN3.EQ.-1) TINT3=(-1)**MN3*XSINC	I1P 0040
	IF (MN3.EQ.0) TINT3=(0.0,0.0)	I1P 0041
	GO TO 13	I1P 0042
12	MNT3=MN3	I1P 0043
	IF (IN3.EQ.1) TINT3=(1.0,0.0)	I1P 0044
	IF (IN3.EQ.-1) TINT3=XSIN	I1P 0045
	IF (MN3.EQ.0) TINT3=(2.**0.5)*(1.0,0.0)	I1P 0046
13	CONTINUE	I1P 0047
	LK=MNT1+MX	I1P 0048
	IF (MNT3.NE.LK) GO TO 14	I1P 0049
	A1(KX)=A1(KX)+((PI/3.）**0.50)*TINT1*TINT3*CGC(J1,1,J3,MNT1,MX)	I1P 0050
	1 *CGC(J1,1,J3,0,0) *SQRT((2.*J1+1)*3./(PI4*(2.*J3+1)))	I1P 0051
14	CONTINUE	I1P 0052
15	CCONTINUE	I1P 0053
	IF (IX.EQ.1) I1P=(2.**0.5)*REAL(A1(3))*(-1.)	I1P 0054
	IF (IX.EQ.2) I1P=(2.**0.5)*ATMAG(A1(3))*(-1.)	I1P 0055
	IF (IX.EQ.3) I1P= REAL(A1(2))	I1P 0056
	RETURN	I1P 0057
	END	I1P 0058

SCATTERED WAVE NON-SELF CONSISTENT FIELD PROGRAM

C SCATTERED-WAVE MODEL FOR POLYATOMIC MOLECULES AND CLUSTERS  
 C PROGRAM WRITTEN BY F. C. SMITH, JR. AND K. H. JOHNSON, M.I.T.  
 C NON-SELF-CONSISTENT SPIN-UNRESTRICTED MAIN PROGRAM  
 C CALCULATES ONE-ELECTRON ENERGIES FOR GIVEN NUMERICAL POTENTIAL  
 C USED TO START SCF CALCULATION  
 C ALL ELECTRONS OR FROZEN CORES  
 C THIS VERSION DIMENSIONED FOR 18 CENTERS (INCLUDING ATOMS, OUTER OR  
 C WATSON SPHERE, AND INTERATOMIC SPHERES), PARTIAL-WAVE LMAX=6 PER  
 C PAIR OF ATOMS, 10 DIFFERENT ATOMS (WITH A TOTAL OF 26 DIFFERENT L  
 C VALUES), 2 DIFFERENT INTERATOMIC POTENTIALS, A 28X28 SECULAR  
 C MATRIX, AND A MAXIMUM OF 24 COMPONENTS PER BASIS FUNCTION.  
 COMMON/STATE/CN(24,28),MN(24,28),IN(24,28),NATOM(24,28),LN(28),  
 1 NMS(28),IMIN(28,18),IMAX(28,18),NLEQ(18),KTAU(18),NNS,ICORE,  
 2 NUATOM,NDG,NLS(18),NOL(18),NO(18),NTERMS(18),LMAXN(18),NDIM  
 COMMON/PARAM/VCON,XE,EV,IOUT,KONSW,NOUT,NAT,NDAT, NSPINS,  
 1 NACORE,RADICN,QION,FAC1,EXFACO,RS(18),XV(18),YV(18),ZV(18),Z(18)  
 2 ,EXFACT(18),LMAXX(18),NZ(18),NSYMBL(18),NEQ(18),LCORE(18),KION  
 COMMON/FCNR/H(10),VCONS(2),R(200,10),V(200,20),ICHG(10,10),  
 1 KPLACE(18),KMAX(18)  
 COMMON/OP/NSPINA,NSPINB,NLP1,NLP2,NREP1,NREP2,NIRREP  
 DIMENSION P(200,26),PS(26),DPS(26),XC(28),XA(28),RAME(28),Q(18)  
 DIMENSION XCI(28),XCF(28)  
 IPR=1  
 IPU=0  
 NEMAX=12  
 THRESH=1.E-5  
 IOUT0=0  
 KONSW=1  
 140 CALL INPUT  
 IF(IOUT.EQ.0) GO TO 302  
 IPR1=3  
 IPU1=0  
 IF(IOUT.EQ.2) IPU1=3  
 CALL OUTPUT(XC,IPR1,IPU1,PS,DPS,P,E,RAME)

NSCF0001  
 NSCF0002  
 NSCF0003  
 NSCF0004  
 NSCF0005  
 NSCF0006  
 NSCF0007  
 NSCF0008  
 NSCF0009  
 NSCF0010  
 NSCF0011  
 NSCF0012  
 NSCF0013  
 NSCF0014  
 NSCF0015  
 NSCF0016  
 NSCF0017  
 NSCF0018  
 NSCF0019  
 NSCF0020  
 NSCF0021  
 NSCF0022  
 NSCF0023  
 NSCF0024  
 NSCF0025  
 NSCF0026  
 NSCF0027  
 NSCF0028  
 NSCF0029  
 NSCF0030  
 NSCF0031  
 NSCF0032  
 NSCF0033  
 NSCF0034  
 NSCF0035  
 NSCF0036



IOUT=IOUT0	NSCF0037
NIP1=0	NSCF0038
NIP2=0	NSCF0039
302 CALL SETUP	NSCF0040
100 PCRMAT(16I5)	NSCF0041
127 READ(5,103) ID,NNS,DE,EMAX,EMIN,ICORE,NXGO,NRIT,XYMP,NIRREP	NSCF0042
103 PCRMAT(2I5,3F10.2,3I5,F10.5,I5)	NSCF0043
IF(ID.GT.0) GO TO 5	NSCF0044
IF(NNS.EQ.0) GO TO 4	NSCF0045
IF(NNS.EQ.1) GO TO 302	NSCF0046
IF(NNS.EQ.2) GO TO 140	NSCF0047
READ(5,100) IOUT,IPB,IPU,NEMAX,NTHR	NSCF0048
IOUT0=IOUT	NSCF0049
THRESH=10.**(-NTHR)	NSCF0050
IF(NTHR.EQ.0) THRESH=1.F-5	NSCF0051
IF(NEMAX.EQ.0) NEMAX=12	NSCF0052
GO TO 127	NSCF0053
5 IF(NXGO.EQ.1) NSPINA=NNS	NSCF0054
IF(NXGO.EQ.2) NSPINB=NNS	NSCF0055
IF(NXGO.EQ.0) GO TO 128	NSCF0056
IF(NIRREP.EQ.0) GO TO 128	NSCF0057
IF(NXGO.EQ.2) GO TO 8	NSCF0058
NREP1=NIRREP	NSCF0059
DO 6 M=1,NIRREP	NSCF0060
WRITE(9) NDIM,NDG	NSCF0061
WRITE(9) (LN(N),NMS(N),N=1,NDIM)	NSCF0062
DC 7 N=1,NDIM	NSCF0063
NMN=NMS(N)	NSCF0064
7 WRITE(9) (CN(I,N),MN(I,N),IN(I,N),NATCH(I,N),I=1,NMN)	NSCF0065
IF(M.EQ.NIRREP) GO TO 128	NSCF0066
6 CALL SETUP	NSCF0067
GO TO 128	NSCF0068
8 NREP2=NIRREP	NSCF0069
DC 9 M=1,NIRREP	NSCF0070
WRITE(10) NDIM,NDG	NSCF0071
WRITE(10) (LN(N),NMS(N),N=1,NDIM)	NSCF0072

DO 10 N=1,NDIM	NSCF0073
MHN=MNS(N)	NSCF0074
10 WRITE(10) (CN(I,N),MN(I,N),IN(I,N),NATOM(I,N),I=1,MHN)	NSCF0075
IF(M.EQ.NIRREP) GO TO 128	NSCF0076
9 CALL SETUP	NSCF0077
128 IF(NNS.EQ.0) NNS=1	NSCF0078
VCON=VCCNS(NNS)	NSCF0079
CALL TIMING(ICPU,IEXCP)	NSCF0080
WRITE(6,100) ICPU,IEXCP	NSCF0081
CALL EIGEN(NEMAX,ID,DE,EMAX,EMIN,THRESH,P,XA,PS,DPS,E,RAMF)	NSCF0082
IF(EMAX.EQ.0.0.AND.EMIN.EQ.0.0) GO TO 304	NSCF0083
WRITE(6,101) E	NSCF0084
101 FCRMAT(/30X,'FINAL ENERGY=',1PE16.7)	NSCF0085
IF(IPR.EQ.0.AND.IPU.EQ.0) GO TO 304	NSCF0086
XC(1)=XA(1)/RAMF(1)	NSCF0087
XC MAX=XC(1)	NSCF0088
DO 4013 N=2,NDIM	NSCF0089
XC(N)=XA(N)/RAMF(N)	NSCF0090
IF(ABS(XC(N)).LE.ABS(XC MAX)) GO TO 4013	NSCF0091
XC MAX=XC(N)	NSCF0092
4013 CONTINUE	NSCF0093
IF(XC MAX.EQ.0.0) GO TO 4015	NSCF0094
DO 4014 N=1,NDIM	NSCF0095
XA(N)=XA(N)/XC MAX	NSCF0096
4014 XC(N)=XC(N)/XC MAX	NSCF0097
EV=E-VCCN	NSCF0098
CALL NRMLIZ(P,XC,XA,Q,OINT,PS,DPS,RAMF)	NSCF0099
CALL OUTPUT(XC,1,0,PS,DPS,P,E,XA,0.0)	NSCF0100
CALL TIMING(ICPU,IEXCP)	NSCF0101
WRITE(6,100) ICPU,IEXCP	NSCF0102
4015 CALL OUTPUT(XC,IPR,IPU,PS,DPS,P,E,XA,0.0)	NSCF0103
IF(NXGO.EQ.0) GO TO 304	NSCF0104
DC 14 N=1,NDIM	NSCF0105
IF(NXGO.EQ.1) XCI(N)=XC(N)	NSCF0106
14 IF(NXGO.EQ.2) XCF(N)=XC(N)	NSCF0107
IF(NXGO.EQ.2) REWIND 10	NSCF0108

IF (NXGO.EQ.2) GO TO 17	NSCF0109
IF (NIRREP.EQ.0) GO TO 12	NSCF0110
REWIND 9	NSCF0111
18 NLP2=0	NSCF0112
NLP1=NLP1+1	NSCF0113
NXGO=1	NSCF0114
READ (9) NDIM,NDG	NSCF0115
READ (9) (LN (N) , NMS (N) , N=1, NDIM)	NSCF0116
DC 13 N=1,NDIM	NSCF0117
NMN=NMS (N)	NSCF0118
13 READ (9) (CN (I, N) , MN (I, N) , IN (I, N) , NATOM (I, N) , I=1, NMN)	NSCF0119
DO 15 N=1,NDIM	NSCF0120
15 XC (N) =XCI (N)	NSCF0121
GO TO 12	NSCF0122
17 NXGO=2	NSCF0123
NLP2=NLP2+1	NSCF0124
READ (10) NDIM,NDG	NSCF0125
READ (10) (LN (N) , NMS (N) , N=1, NDIM)	NSCF0126
DC 16 N=1,NDIM	NSCF0127
NMN=NMS (N)	NSCF0128
16 READ (10) (CN (I, N) , MN (I, N) , IN (I, N) , NATOM (I, N) , I=1, NMN)	NSCF0129
DC 19 N=1,NDIM	NSCF0130
19 XC (N) =XCF (N)	NSCF0131
12 CALL OPTIK (XC, E, NXGO, NRIT, XOSC, XPROB, 2, XSYMF)	NSCF0132
IF (NIRREP.EQ.0) GO TO 304	NSCF0133
IF (NLP2.EQ.0.AND. NLP1.EQ.1) GO TO 304	NSCF0134
IF (NLP2.LT.NREP2) GO TO 17	NSCF0135
IF (NLP1.EQ.NREP1) GO TO 304	NSCF0136
IF (NLP2.EQ.NREP2) REWIND 10	NSCF0137
IF (NLP2.EQ.NREP2) GO TO 18	NSCF0138
304 GC TO 127	NSCF0139
4 STOP	NSCF0140
END	NSCF0141

OPTICAL PROPERTIES SUBROUTINE (FOR USE IN NSCF PROGRAM)	OPT20001
SUBROUTINE OPTIK (XC, E, NXGO, NRIT, XOSC, PABS, JCONTR, XSYMF)	OPT20002
C OPTIK ROUTINE WRITTEN BY LOUIS NOODLEMAN	OPT20003
COMMON/STATE/CN(24,28), MN(24,28), IN(24,28), NATOM(24,28), LN(28),	OPT20004
1 NMS(28), IMIN(28,18), IMAX(28,18), NLEQ(18), KTAU(18), NNS, ICORE,	OPT20005
2 NUAT, NDG, NLS(18), NOL(18), NO(18), NTERMS(18), LMAXA(18), NDIM	OPT20006
COMMON/PARAM/VCON, XE, EV, IOUA, KONSW, NOUT, NAT, NDAT, NSPINS,	OPT20007
1 NACORE, RADION, QION, FAC1, EXFAC0, RS(18), XV(18), YV(18), ZV(18), ZP(18)	OPT20008
2, EXFACT(18), LMAXX(18), NZ(18), NSYMBL(18), NEQ(18), LCORE(18), KION	OPT20009
COMMON/FCNR/H(10), VCONS(2), R(200,10), V(200,20), ICHG(10,10),	OPT20010
1 KPLACE(18), KMAX(18)	OPT20011
COMMON/BESSEL/SBFC(7), DSBFC(7), SNFC(7), DSNFC(7)	OPT20012
COMMON/OP/NSPINA, NSPINB, NLP1, NLP2, NREP1, NREP2, NIRREP	OPT20013
REAL CI(6,9,5,10), CF(6,9,5,10), RI(200,5,5), RF(200,5,5), SUMAF(9),	OPT20014
1 SUMBF(9), ZUM(5,5,10,3), ZUMP(3), RV(200,10), RSVP(200), RVP(200,10),	OPT20015
2 Y(200), S(5,5,10), SUR(5,5,10), ST(5,5,10), A(200), VP(200,10),	OPT20016
3 VS(200,10), I1P, Q(10), QAM(10,5), XC(28)	OPT20017
INTEGER LMAXN(18), KB(10), MVN(24,28), KI(18), NU(18), JAKE(5),	OPT20018
1 LMAXN1(18)	OPT20019
DO 4 K=1,10	OPT20020
DO 4 KL=1,5	OPT20021
DO 4 M=1,9	OPT20022
DO 4 ML=1,6	OPT20023
IF (NXGO.EQ.1) CI(ML,M,KL,K)=0.0	OPT20024
4 IF (NXGO.EQ.2) CF(ML,M,KL,K)=0.0	OPT20025
IF (NLP1.GT.1 .OR. NLP2.GT.1) GO TO 93	OPT20026
OSSUM=0.0	OPT20027
DC 609 JKR=1,7	OPT20028
SBFC(JKR)=1.0	OPT20029
DSBFC(JKR)=1.0	OPT20030
SNFC(JKR)=1.0	OPT20031
609 DSNFC(JKR)=1.0	OPT20032
IF (NRIT.EQ.0) NRIT=1	OPT20033
IF (NXGO.EQ.1) EI=E	OPT20034
IF (NXGO.EQ.2) EF=E	OPT20035
NUATOM=NDAT	OPT20036

IF (NXGO.EQ.2) VC=VCONS(NSPINB)	OPT20037
DO 2 NN=1,NAT	OPT20038
IF (NXGO.EQ.1) LMAXN1 (NN)=LMAXA (NN)	OPT20039
2 IF (NXGO.EQ.2) LMAXN (NN)=MAX0 (LMAXN1 (NN) , LMAXA (NN) )	OPT20040
IF (NXGO.EQ.1) GO TO 603	OPT20041
DC 504 NN=1,NUATOM	OPT20042
DO 504 JK=1,2	OPT20043
IF (JK.EQ.1) NS=NN+(NSPINA-1)*NUATOM	OPT20044
IF (JK.EQ.2) NS=NN+(NSPINE-1)*NUATCM	OPT20045
IOUT=1	OPT20046
IF (NN.EQ.1) IOUT=2	OPT20047
KX=KMAX (NN)	OPT20048
NLMAP=LMAXN (NN) +1	OPT20049
DO 503 LVAL=1,NLMAP	OPT20050
L=LVAL-1	OPT20051
Z=FLOAT (NZ (NN) )	OPT20052
IF (JK.EQ.1) CALL TMAT (L, EI, RS (NN) , KMAX (NN) , Z, H (NN) , R (1, NN) ,	OPT20053
1V (1, NS) , ICHG (1, NN) , IOUT, KPLACE (NN) , RI (1, LVAL, NN) , STMAT, PS, DPS,	OPT20054
2RAMF)	OPT20055
IF (JK.EQ.2) CALL TMAT (L, EF, RS (NN) , KMAX (NN) , Z, H (NN) , R (1, NN) ,	OPT20056
1V (1, NS) , ICHG (1, NN) , ICUT, KPLACE (NN) , RF (1, LVAL, NN) , STMAT, PS, DPS,	OPT20057
2RAMF)	OPT20058
503 CONTINUE	OPT20059
IF (NRIT.EQ.1) GO TO 504	OPT20060
WRITE (6,506) NN,JK	OPT20061
506 FORMAT (1X,7HCENTER=,I4,6HSTATE=,I4)	OPT20062
DO 510 LS=1,KX	OPT20063
IF (JK.EQ.1) WRITE (6,505) LS,R (LS,NN) , (RI (LS, LVAL, NN)	OPT20064
1 ,LVAL=1,NLMAP)	OPT20065
IF (JK.EQ.2) WRITE (6,505) LS,R (LS,NN) , (RF (LS, LVAL, NN)	OPT20066
1 ,LVAL=1,NLMAP)	OPT20067
505 FORMAT (1X,I4,6 (4X,E14.7) )	OPT20068
510 CCNTINUE	OPT20069
504 CONTINUE	OPT20070
DC 13 I=2,NUATOM	OPT20071
NS=I+(NSPINB-1)*NUATCM	OPT20072

LMAF=LMAXN(I)+1	OPT20073
LY=KMAX(I)	OPT20074
LP=KMAX(I)-1	OPT20075
ID=KPLACE(I)	OPT20076
DO 8 KM=1,LY	OPT20077
8 RV(KM,I) = R(KM,I)*V(KM,NS)	OPT20078
DO 9 L=1,LP	OPT20079
IF(L.LE.2) CALL INTERP(R(L,I),RV(L,I),4,R(L,I),DUMMY,RVP(L,I),	OPT20080
1 .TRUE.)	OPT20081
IF(L.GT.2)	OPT20082
1CALL INTERP(R(L-2,I),RV(L-2,I),4,R(L,I),DUMMY,RVP(L,I),.TRUE.)	OPT20083
RSVP(L)=R(L,I)*RVP(L,I)-RV(L,I)	OPT20084
IF(NRIT.EQ.1) GO TO 9	OPT20085
WRITE(6,500) I,L,R(L,I),RV(L,I),RVP(L,I),V(L,NS),RSVP(L)	OPT20086
500 FOFMAT(1X,7HNUATOM=,I5,2HL=,I5,2HR=,F10.5,3HRV=,F10.5,4HRVP=,	OPT20087
1 F10.5,3H V=,E14.7,6H RSVP=,E14.7)	OPT20088
9 CCNTINUE	OPT20089
DO 13 J=1,LMAF	OPT20090
DO 13 K=1,LMAF	OPT20091
IF(IABS(J-K).GT.1) GO TO 12	OPT20092
IF((K+J+1)/2 .LT. FICAT(K+J+1)/2.0) GO TO 12	OPT20093
DO 5 L=1,LP	OPT20094
5 Y(L)=RI(L,K,I)*RF(L,J,I)*RSVP(L)	OPT20095
CALL INTEGR(Y,R(1,I),KMAX(I)-1,ICHG(1,I),A,1)	OPT20096
CALL INTERP(R(LD-3,I),A(LD-3),6,RS(I),ASA,DUMMY,.FALSE.)	OPT20097
S(K,J,I)=ASA	OPT20098
SUR(K,J,I)=RI(LD,K,I)*RF(LD,J,I)*(RS(I)**2)*(VC-V(LD,NS))	OPT20099
ST(K,J,I)=S(K,J,I)+SUR(K,J,I)	OPT20100
GO TO 13	OPT20101
12 ST(K,J,I)=0.0	OPT20102
13 CONTINUE	OPT20103
LMAF=LMAXN(1)+1	OPT20104
LP=KMAX(1)-1	OPT20105
ID=KPLACE(1)	OPT20106
NS=1+(NSEINB-1)*NUATOM	OPT20107
DO 28 L=1,LP	OPT20108

IF (L.LE.2) CALL INTERP (R (L,1) , V (L,NS) , 4, R (L,1) , VS (L,1) , VP (L,1) ,	OPT20109
1 .TRUE.)	OPT20110
IF (L.GT.2) CALL INTERP (R (L-2,1) , V (L-2,NS) , 4, R (L,1) , VS (L,1) , VP (L,1)	OPT20111
1 ,.TRUE.)	OPT20112
IF (NRIT.EQ.1) GO TO 28	OPT20113
WRITE (6,501) L, R (L,1) , V (L,NS) , VP (L,1)	OPT20114
501 FORMAT (1X,8HNUATOM=1,3H L=,I5,3H R=,F10.5,3H V=,E14.7,3HVP=,F10.5)	OPT20115
28 RSVP(L) = (R (L,1) **2.0) * VP (L,1)	OPT20116
DO 30 J=1,LMAF	OPT20117
DC 30 K=1,LMAF	OPT20118
IF (IABS (J-K) .GT. 1) GO TO 36	OPT20119
IF ((K+J+1) /2 .LT. (FLOAT (K+J+1) /2.0)) GO TO 36	OPT20120
DO 29 L=1,LP	OPT20121
29 Y(L)=RI (L,K,1) *RF (L,J,1) *RSVP(L)	OPT20122
CALL INTEGR (Y, R (1,1) , KMAX (1) -1, ICHG (1,1) , A,3)	OPT20123
CALL INTERP (R (1,1) , A,7, RS (1) , AS,DUMMY, .FALSE.)	OPT20124
AINT=A (KMAX (1) -1) -AS	OPT20125
S (K,J,1) =AINT	OPT20126
SUR (K,J,1) =RI (LD,K,1) *RF (LD,J,1) * (RS (1) **2.) * (V (LD,NS) -VC)	OPT20127
ST (K,J,1) =S (K,J,1) +SUR (K,J,1)	OPT20128
GO TO 30	OPT20129
36 ST (K,J,1) =0.0	OPT20130
30 CONTINUE	OPT20131
IF (NXGO.EQ.2) GO TO 93	OPT20132
603 DC 90 N=1,NAT	OPT20133
NU(N) =NEQ(N)	OPT20134
90 IF (NEQ (N) .EQ.0) NU (N) =N	OPT20135
DO 91 N=1,NAT	OPT20136
IF (NU (N) .EQ.N) KI (N) =1	OPT20137
IF (NU (N) .EQ.N) KB (N) =1	OPT20138
IF (N.LE.NUATOM) GO TO 91	OPT20139
DO 92 I=1,NUATOM	OPT20140
IF (NU (N) .EQ.I) KB (I) =KB (I) +1	OPT20141
92 IF (NU (N) .EQ.I) KI (N) =KB (I)	OPT20142
91 CCNTINUE	OPT20143
WRITE (6,602)	OPT20144

602	FORMAT (1X,5HNATOM,3X,2HNU,2X,3HNEQ,3X,2HKI)	OPT20145
	WRITE (6,601) (J,NU(J),NFQ(J),KI(J),J=1,NAT)	OPT20146
601	FORMAT (1X,4I5)	OPT20147
93	KK=NXGO	OPT20148
	IF (NRIT.EQ.1) GO TO 607	OPT20149
	WRITE (6,53) NDIM,NDG	OPT20150
53	FORMAT (1X,5HNDIM=,I5,5H NDG=,I5)	OPT20151
	WRITE (6,54) (XC(N),N=1,NDIM)	OPT20152
54	FORMAT (1X,10HSYMM COEF=,10F10.5)	OPT20153
607	DC 600 N=1,NDIM	OPT20154
	IF (NRIT.EQ.1) GO TO 608	OPT20155
	WRITE (6,52) LN(N),NMS(N)	OPT20156
52	FORMAT (1X,3HLN=,I5,5H NMS=,I5)	OPT20157
608	NMQ=NMS(N)	OPT20158
	DO 600 I=1,NMQ	OPT20159
	IF (NRIT.EQ.1) GO TO 605	OPT20160
	WRITE (6,55) MN(I,N),IN(I,N),NATCM(I,N),CN(I,N)	OPT20161
55	FORMAT (1X,3HMN=,I5,4H IN=,I5,7H NATCM=,I5,4H CN=,F10.5)	OPT20162
605	IF (MN(I,N).EQ.0 .AND. IN(I,N).EQ.1) MVN(I,N)=1	OPT20163
	IF (MN(I,N).NE.0 .AND. IN(I,N).EQ.-1) MVN(I,N)=2*MN(I,N)	OPT20164
	IF (MN(I,N).NE.0 .AND. IN(I,N).EQ.1) MVN(I,N)=2*MN(I,N)+1	OPT20165
600	CONTINUE	OPT20166
	DC 606 N=1,NDIM	OPT20167
	NMQ=NMS(N)	OPT20168
	LNT=LN(N)+1	OPT20169
	DO 606 K=1,NMQ	OPT20170
	KTA=NATCM(K,N)	OPT20171
	KIT=KI(KTA)	OPT20172
	MVNT=MVN(K,N)	OPT20173
	NUE=NU(KTA)	OPT20174
	IF (KK.EQ.1) CI (KIT,MVNT,LNT,NUE) =CI (KIT,MVNT,LNT,NUE) +CN (K,N)	OPT20175
	1 *XC (N)	OPT20176
	IF (KK.EQ.2) CF (KIT,MVNT,LNT,NUE) =CF (KIT,MVNT,LNT,NUE) +CN (K,N)	OPT20177
	1 *XC (N)	OPT20178
606	CONTINUE	OPT20179
	IF (NXGO.EQ.2) GO TO 94	OPT20180



	RETURN	OPT20181
C	X, Y, Z POLARIZATION OF E FIELD	OPT20182
94	DO 20 IX=1,3	OPT20183
	DC 20 I=1,NUATOM	OPT20184
	LMAF=LMAXN(I)+1	OPT20185
	DO 20 J=1,LMAF	OPT20186
	DO 20 JP=1,LMAF	OPT20187
	IF (IABS(J-JP) .GT.1) GO TO 19	OPT20188
	IF ((J+JP+1)/2 .LT.FLOAT(J+JP+1)/2.0) GO TO 19	OPT20189
	SUMC=0.0	OPT20190
	MF= (2*J) - 1	OPT20191
	DO 17 M=1,MF	OPT20192
	SUMB=0.0	OPT20193
	MPF= (2*JP) - 1	OPT20194
	DC 16 MP=1,MPF	OPT20195
	SUMA=0.0	OPT20196
	KBF=KB(I)	OPT20197
	DO 15 KJ=1,KBF	OPT20198
15	SUMA=SUMA+CF(KJ,MP,JP,I)*CI(KJ,M,J,I)	OPT20199
	SUMAF(MP)=SUMA*I1P(MP,M,JP-1,J-1,IX)	OPT20200
	XIPT=I1P(MP,M,JP-1,J-1,IX)	OPT20201
16	SUMB=SUMB+SUMAF(MP)	OPT20202
	SUMBF(M)=SUMB	OPT20203
17	SUMC=SUMC+SUMBF(M)	OPT20204
18	ZUM(JP,J,I,IX)=SUMC	OPT20205
	GC TO 20	OPT20206
19	ZUM(JP,J,I,IX)=0.0	OPT20207
20	CCONTINUE	OPT20208
	DO 23 IX=1,3	OPT20209
	ZUM1=0.0	OPT20210
	DO 22 I=1,NUATOM	OPT20211
	LMAF=LMAXN(I)+1	OPT20212
	DO 22 J=1,LMAF	OPT20213
	DO 22 JP=1,LMAF	OPT20214
	IF(NRIT.EC.1) GO TO 22	OPT20215
	WRITE(6,50) JP,J,I,IX,ZUM(JP,J,I,IX),JP,J,I,ST(J,JP,I)	OPT20216

50	FORMAT (1X,4HZUM ,4I3,2H =,F10.5,3HST ,3I3,2H =,F10.5)	OPT20217
22	ZUM1=ZUM1+ZUM (JP ,J ,I ,IX) *ST (J ,JP ,I)	OPT20218
23	ZUMP (IX) =ZUM1	OPT20219
	ZUMPS=0.0	OPT20220
	DO 40 IM=1,3	OPT20221
40	ZUMPS=ZUMPS+ZUMP (IM) **2	OPT20222
	WRITE (6,528) XSYMF	OPT20223
528	FORMAT (1X, 'XSYMF ',F8.4)	OPT20224
	PREL=ZUMPS/ (EI-EF) **4	OPT20225
	PABS=(4.0/3.0) *PREL *XSYMF	OPT20226
	XOSC=PABS* (EF-EI)	OPT20227
	IF (JCONTR.EQ.1) GO TO 527	OPT20228
	IF (NIRREP.EQ.0) GO TO 522	OPT20229
	IF (NLP1.NE.NREP1 .OR. NLP2.NE.NREP2) GO TO 51	OPT20230
522	DO 822 KC=1,2	OPT20231
	DO 815 I=1,NUATOM	OPT20232
	LMAF=LMAXN (I) +1	OPT20233
	LY=KMAX (I)	OPT20234
	LF=KMAX (J) -1	OPT20235
	LD=KPLACE (I)	OPT20236
	Q (I) =0.0	OPT20237
	DO 815 J=1,LMAF	OPT20238
	DC 810 KM=1,LY	OPT20239
	IF (KC.EQ.1) Y (KM) = (RI (KM,J,I) *R (KM,I) ) **2	OPT20240
	IF (KC.EQ.2) Y (KM) = (RF (KM,J,I) *R (KM,I) ) **2	OPT20241
810	CONTINUE	OPT20242
	IF (I.GT.1) GO TO 813	OPT20243
	CALL INTEGR (Y, R (1,1) ,KMAX (1) -1, ICHG (1,1) ,A,3)	OPT20244
	CALL INTERP (R (1,1) ,A,7,BS (1) ,AS,DUMMY, .FALSE.)	OPT20245
	PADFS=A (KMAX (1) -1) -AS	OPT20246
	GO TO 814	OPT20247
813	CALL INTEGR (Y, R (1,I) ,LP, ICHG (1,I) ,A,1)	OPT20248
	CALL INTERP (R (LD-3,I) ,A (LD-3) ,6,RS (I) ,RADFS,DUMMY, .FALSE.)	OPT20249
814	MF=2 *J-1	OPT20250
	CRT=0.0	OPT20251
	DC 811 M=1,MF	OPT20252

```

      IF (KC.EQ.1) CRT=CRT+CI(1,M,J,I)**2
      IF (KC.EQ.2) CRT=CRT+CF(1,M,J,I)**2
811  CCNTINUE
      QAM(I,J)=CRT*RADFS
815  Q(I)=Q(I)+CRT*RADFS
808  WRITE(6,820) KC, (I,Q(I),I=1,NUATOM)
820  FORMAT(1X,6HSTATE=,I4,4(1HQ,I2,1H=,F8.4))
      DO 822 I=1,NUATOM
      LMAF=LMAXN(I)+1
      DC 823 J=1,LMAF
823  JAKE(J)=J-1
822  WRITE(6,821) KC,I,(JAKE(J),QAM(I,J),J=1,LMAF)
821  FORMAT(1X,6HSTATE=,I4,5HATOM=,I4,5(2HQL,I2,1H=,F8.4))
      51 WRITE(6,700) NLP1,NLP2
700  FORMAT(1X,'INITIAL STATE PARTNER=',I5,'FINAL STATE PARTNER=',I5)
      WRITE(6,41) EI,EF
      41 FORMAT(1X,15HTRANSITION FROM,F10.5,11HRYDBERGS TO,F10.5,
      1 8HRYDBERGS)
      DO 45 IX=1,3
      IF (IX.EQ.1) WRITE(6,42)
      IF (IX.EQ.2) WRITE(6,43)
      IF (IX.EQ.3) WRITE(6,44)
      42 FCRMAT(1X,32HTRANSITION AMPLITUDE X COMPONENT)
      43 FCRMAT(1X,32HTRANSITION AMPLITUDE Y COMPONENT)
      44 FCRMAT(1X,32HTRANSITION AMPLITUDE Z COMPONENT)
      WRITE(6,46) ZUMP(IX)
      46 FCRMAT(4X,E14.6)
      45 CONTINUE
      WRITE(6,47) PREL
      47 FORMAT(1X,32HRELATIVE TRANSITION PROBABILITY=,E14.6)
      WRITE(6,48) PABS
      48 FCRMAT(1X,33HABSOLUTE TRANSITION PROBABILITY=,F12.6)
      WRITE(6,49) XOSC
      49 FCRMAT(1X,20HOSCILLATOR STRENGTH=,F12.6)
      IF (NIRREP.EQ.0) GO TO 527
      IF (NLP1.EQ.1 .AND. NLP2.EQ.1) OSTEM=XOSC

```

```

OPT20253
OPT20254
OPT20255
OPT20256
OPT20257
OPT20258
OPT20259
OPT20260
OPT20261
OPT20262
OPT20263
OPT20264
OPT20265
OPT20266
OPT20267
OPT20268
OPT20269
OPT20270
OPT20271
OPT20272
OPT20273
OPT20274
OPT20275
OPT20276
OPT20277
OPT20278
OPT20279
OPT20280
OPT20281
OPT20282
OPT20283
OPT20284
OPT20285
OPT20286
OPT20287
OPT20288

```

```
OSSUM=OSSUM+XOSC
IF(NLP1.NE.NREP1 .OR. NLP2.NE.NREP2) GO TO 527
WRITE(6,520) OSSUM
520 FORMAT(1X,'SUM OF OSCILLATOR STRENGTHS =',F12.6)
IF(OSTEM.LT.0.0001) GO TO 527
FACTOR=OSSUM/OSTEM
WRITE(6,521) FACTOR
521 FORMAT(1X,'TOTAL OSCILLATOR STRENGTH/FIRST OSCILLATOR STRENGTH =',
1,F12.6)
527 CONTINUE
RETURN
END
```

```
OPT20289
OPT20290
OPT20291
OPT20292
OPT20293
OPT20294
OPT20295
OPT20296
OPT20297
OPT20298
OPT20299
OPT20300
```

```

          TMAT SUBROUTINE WITH PHOTO-EMISSION OPTION
          SUBROUTINE TMAT(L,E,RS,KMAX,Z,DELH,R,V,ICHG,IOUT,KPLACE,P,STMAT,
          1 PS,DPS,RAMP)
C PHOTO-EMISSION OPTION ADDED BY LOUIS NOODLEMAN
          REAL*8 PKM,PK1,PK,DKM,DK1,DK,GK,GK1,GKM
          COMMON/PARAM/VCON,XE,EV,NOUT
          REAL          NEUO(7),DNEUO(7),BESO(7),DBESO(7),NER(7),BER(7),
          1 DNER(7),DBER(7),NEMO,NERR
C          T-MATRIX CALCULATION FOR MULTIPLE-SCATTERING MODEL FOR POLYATOMIC
C          MOLECULES. INTEGRATES RADIAL SCHRODINGER EQUATION USING NUMEROV
C          DOES OUTWARD INTEGRATION FOR ATOMIC SPHERES, INWARD FOR OUTER
C          SPHERES. GIVES INVERSE OF T-MATRIX AND LOG DERIVATIVE AT SPHERE
C          SURFACE.
          DIMENSION V(KMAX),P(KMAX),P(KMAX),ICHG(10)
          COMMON/BESSEL/SBFC(9),DSBFC(9),SNFC(9),DSNFC(9)
          LOGICAL IGCTP,ALLOW
          ALLOW=.FALSE.
          KSTOP=1
          A=L*(L+1)
          IGCTP=IOUT.NE.3.AND.NOUT.EQ.0
          IF(IOUT.EQ.2) GO TO 60
C          OUTWARD INTEGRATION FOR ATOMIC SPHERES
          CALL PSTART(DELH,Z,L,E,V,P(1),P(2))
          HSQ=DELH**2
          PKM=P(1)
          PK1=P(2)
          DKM=- (E-V(1)-A/R(1)**2)*HSQ*PKM/12.
          DK1=- (E-V(2)-A/R(2)**2)*HSQ*P(2)/12.
          N=1
          DO 34 K=3,KMAX
          GK= (E-V(K)-A/R(K)**2)*HSQ/12.
          PK = (2.*(PK1 +5.*DK1)- (PKM-DKM))/(1.+GK)
          P(K)=PK
          IF(IGCTP) GO TO 50
          IF(ALLOW) GO TO 51
          IF(GK.LT.0) GO TO 53

```

```

TMAT0001
TMAT0002
TMAT0003
TMAT0004
TMAT0005
TMAT0006
TMAT0007
TMAT0008
TMAT0009
TMAT0010
TMAT0011
TMAT0012
TMAT0013
TMAT0014
TMAT0015
TMAT0016
TMAT0017
TMAT0018
TMAT0019
TMAT0020
TMAT0021
TMAT0022
TMAT0023
TMAT0024
TMAT0025
TMAT0026
TMAT0027
TMAT0028
TMAT0029
TMAT0030
TMAT0031
TMAT0032
TMAT0033
TMAT0034
TMAT0035
TMAT0036

```

```

ALLOW=.TRUE.
GC TO 53
51 IF (GK.GE.0) GO TO 53
   IGCTP=.TRUE.
   IF (IOUT.EQ.3) GO TO 54
   GO TO 53
54 KSTOP=K+3
   IF (KSTOP.EQ. ICHG (N)-1) KSTOP=ICHG (N)
   GC TO 53
50 IF (K.EQ.KSTOP) GO TO 52
53 IF (K.LT. ICHG (N)) GO TO 30
   N=N+1
   HSQ=4.*HSQ
   DKM=4.*DKM
   DK1=-4.*GK*PK
   PK1=PK
   GO TO 34
30 PKM=PK1
   DKM=DK1
   DK1=-GK*PK
   PK1=PK
34 CONTINUE
   IF (IOUT.NE.3) GO TO 78
   WRITE (6,104) E
104 FORMAT (' ERROR - LEVEL E=',E14.7,' SHOULD NOT BE A CORE LEVEL' /)
   STOP
52 DC 40 K=1,KSTOP
40 P (K)=P (K)/R (K)
   KSTOP=KSTOP-6
   CALL INTERP (P (KSTOP), P (KSTOP), 7, R (KSTOP+3), PS, DPS, .TRUE.)
   PS=P (KSTOP+3)
C   INWARD INTEGRATION FOR OUTER SPHERE
C   ADDITIONAL SEQUENCE FOR PHOTOEMISSION OPTION
60 N=11
   IF (E.GT.0.0) GO TO 181
61 N=N-1

```

```

TMAT0037
TMAT0038
TMAT0039
TMAT0040
TMAT0041
TMAT0042
TMAT0043
TMAT0044
TMAT0045
TMAT0046
TMAT0047
TMAT0048
TMAT0049
TMAT0050
TMAT0051
TMAT0052
TMAT0053
TMAT0054
TMAT0055
TMAT0056
TMAT0057
TMAT0058
TMAT0059
TMAT0060
TMAT0061
TMAT0062
TMAT0063
TMAT0064
TMAT0065
TMAT0066
TMAT0067
TMAT0068
TMAT0069
TMAT0070
TMAT0071
TMAT0072

```

```

KN=ICHG (N)
IF (KN.GE.KMAX) GO TO 61
IF (KN.LE.0) GO TO 61
IF (N.EQ.0) GO TO 66
KN=KMAX
GO TO 62
64 KN=ICHG (N)
N=N-1
IF (N.EQ.0) GO TO 66
62 IF ((V (KN)-E) *R (KN) **2+A-2400.) 63,63,64
66 IF (KN.GT.3) GO TO 63
N=1
KN=ICHG (2)
63 HSQ=DELH**2*4**N
PKM= EXP (- SQRT ((V (KN)-E) *R (KN) **2+A) )
DKM=- (E-V (KN)-A/R (KN) **2 ) *PKM*HSQ/12.
P (KN) =PKM
PK1= EXP (- SQRT ((V (KN-1)-E) *R (KN-1) **2+A) )
P (KN-1) =PK1
DK1=- (E-V (KN-1)-A/R (KN-1) **2) *HSQ*PK1/12.
K=KN+1
IF (K.GT.KMAX) GO TO 79
DO 76 I=K,KMAX
76 P (I) =0.
79 K=KN-1
73 K=K-1
74 GK= (E-V (K)-A/R (K) **2) *HSQ/12.
PK = (2.* (PK1 +5.*DK1) - PKM+DKM) / (1.+GK)
P (K) =PK
IF (IGCTP) GO TO 71
IF (ALLOW) GO TO 56
IF (GK.LT.0) GO TO 71
IF (L.EQ.0) GO TO 59
ALLOW=.TRUE.
GC TO 71
56 IF (GK.GE.0) GO TO 71

```

```

TMAT0073
TMAT0074
TMAT0075
TMAT0076
TMAT0077
TMAT0078
TMAT0079
TMAT0080
TMAT0081
TMAT0082
TMAT0083
TMAT0084
TMAT0085
TMAT0086
TMAT0087
TMAT0088
TMAT0089
TMAT0090
TMAT0091
TMAT0092
TMAT0093
TMAT0094
TMAT0095
TMAT0096
TMAT0097
TMAT0098
TMAT0099
TMAT0100
TMAT0101
TMAT0102
TMAT0103
TMAT0104
TMAT0105
TMAT0106
TMAT0107
TMAT0108

```

59	IGCTP=.TRUE.	TMAT0109
	IF(E.GT.0.0) GO TO 71	TMAT0110
	GO TO 71	TMAT0111
71	IF(K.EQ.KSTOP) GO TO 78	TMAT0112
	IF(N.EQ.0) GO TO 65	TMAT0113
	IF(K.GT.ICHG(N)) GO TO 65	TMAT0114
	IF(K.LE.2) GO TO 75	TMAT0115
	N=N-1	TMAT0116
	DK=-PK *GK	TMAT0117
	GK1=(E-V(K-2)-A/R(K-2)**2)*HSQ/12.	TMAT0118
	PK1=(2.*(PK +5.*DK) - PK1 +DK1)/(1.+GK1)	TMAT0119
	DK1=-PK1*GK1/4.	TMAT0120
	HSQ=HSQ/4.	TMAT0121
	GKM=(E-V(K-1)-A/R(K-1)**2)*HSQ/12.	TMAT0122
	DK=DK/4.	TMAT0123
	PKM =0.5*((PK -DK)+(PK1-DK1))/(1.-5.*GKM)	TMAT0124
	DKM=-PKM*GKM	TMAT0125
	K=K-3	TMAT0126
	P(K+2)=PKM	TMAT0127
	IF(K+1.LT.KSTOP) GO TO 78	TMAT0128
	P(K+1)=PK1	TMAT0129
	IF(K+1.EQ.KSTOP) GO TO 78	TMAT0130
	GO TO 74	TMAT0131
65	PKM=PK1	TMAT0132
	DKM=DK1	TMAT0133
	DK1=-PK *GK	TMAT0134
	PK1=PK	TMAT0135
	GO TO 73	TMAT0136
75	WRITE(6,103)	TMAT0137
	STOP	TMAT0138
103	FCRMAT(18H ERROR STOP - TMAT)	TMAT0139
181	N=N-1	TMAT0140
	MMAX=50	TMAT0141
180	KN=ICHG(N)	TMAT0142
	IF(KN.LT.MMAX) GO TO 105	TMAT0143
	N=N-1	TMAT0144



```

GO TO 180
105 XEP=SQRT (E-V (MMAX))
ARG1=XEP*R (MMAX)
LP=L+1
LV=MAX0 (LP, 3)
CALL OSNF (ARG1,XEP, LV, NEUC,DNEUC)
CALL OSBF (ARG1,XEP, LV, BESO, DBESO)
NEMO=NEUC (LP)
BEMO=BESO (LP)
MDMAX=MMAX-2
DC 106 I=MDMAX,KMAX
IF (I.GE.MMAX) P (I)=0.0
IF (I.GE.MMAX) GO TO 106
ARG2=XEP*R (I)
CALL OSNF (ARG2,XEP, LV, NER,DNER)
CALL OSBF (ARG2,XEP, LV, BER,DBER)
NERR=NER (LP)
BERR=BER (LP)
P (I) =R (I) * (NEMO*BERR-BEMO*NERR)
106 CONTINUE
HSQ=DELH**2*4**N
PKM=P (MMAX-1)
PK1=P (MMAX-2)
KN=MMAX-1
DKM=- (E-V (KN)-A/R (KN)**2 ) *PKM*HSQ/12.
DK1=- (E-V (KN-1)-A/R (KN-1)**2) *HSQ*PK1/12.
GO TO 79
78 IF (IOUT.EQ.3) GO TO 57
DC 77 K=1,KMAX
77 P (K)=P (K)/R (K)
107 CALL INTERP (R (KPLACE-3),P (KPLACE-3),7,RS,PS,DPS,.TRUE.)
X=DPS/PS
21 STMAT=(DSNFC (L+1)-X*SNFC (L+1))/(DSBFC (L+1)-X*SBFC (L+1))
IF (IOUT.EQ.2) STMAT=1./STMAT
STMAT=STMAT*XE
IF (IOUT.EQ.2) RAMF=X*SNFC (L+1)-DSNFC (L+1)

```

```

TMAT0145
TMAT0146
TMAT0147
TMAT0148
TMAT0149
TMAT0150
TMAT0151
TMAT0152
TMAT0153
TMAT0154
TMAT0155
TMAT0156
TMAT0157
TMAT0158
TMAT0159
TMAT0160
TMAT0161
TMAT0162
TMAT0163
TMAT0164
TMAT0165
TMAT0166
TMAT0167
TMAT0168
TMAT0169
TMAT0170
TMAT0171
TMAT0172
TMAT0173
TMAT0174
TMAT0175
TMAT0176
TMAT0177
TMAT0178
TMAT0179
TMAT0180

```

```

IF (IOUT.NE.2) RAMF=DSBFC (L+1) -X*SBFC (L+1)
RAMF=-RAMF*PS*RS**2*XF
IF (MOD (L,2) .NE.0 .OR.EV.GT.0.00) RETURN
STMAT=-STMAT
RETURN
57 RATIO=PS* R(KSTCP+3) /P (KSTOP+3)
DO 58 K=KSTOP,KMAX
58 P (K) =P (K) *RATIO/R (K)
CALL INTERP (R (KSTOP) ,P (KSTOP) ,7,R (KSTOP+3) ,PS,DPS1,.TRUE.)
RAMF=1.
STMAT=DPS1-DPS
RETURN
END

```

```

TMAT0181
TMAT0182
TMAT0183
TMAT0184
TMAT0185
TMAT0186
TMAT0187
TMAT0188
TMAT0189
TMAT0190
TMAT0191
TMAT0192
TMAT0193

```

APPENDIX B  
 DETAILED DERIVATION OF MATRIX ELEMENT  
 FORMULA IN THE  $\vec{\nabla}V$  FORMALISM

By definition

$$x = r \sin \theta \cos \phi, \quad y = r \sin \theta \sin \phi, \quad z = r \cos \theta$$

$\hat{i}, \hat{j}, \hat{k}$  are unit vectors in the  $x, y, z$  directions

$\vec{u}_r, \vec{u}_\theta, \vec{u}_\phi$  are unit vectors in the  $r, \theta, \phi$  directions

$Y_L(\hat{r}_B)$  = normalized spherical harmonic about origin at

$$\vec{r}_B = 0$$

$L = (\ell, m)$  = angular momentum indices

$d\Omega_B$  = angular integration =  $\sin \theta \, d\theta \, d\phi$  referred to  
 origin at center  $B$  (of atom  $B$ )

$$\tilde{Y}_{11}(\hat{r}) = \sin \theta \cos \phi, \quad \tilde{Y}_{1-1}(\hat{r}) = \sin \theta \sin \phi, \quad \tilde{Y}_{10}(\hat{r}) = \cos \theta$$

$$V_C = \bar{V}_{II} = \text{constant potential}$$

Matrix Elements

$$\begin{aligned} (\psi_m, \vec{\nabla}_x V \psi_n) &= \sum_B \sum_L \sum_{L'} C_L^B C_{L'}^{B'} \int_0^{4\pi} \int_0^{b_B} R_\ell^B(E_m, r_B) R_{\ell'}^{B'}(E_n, r_B) \\ &\quad \cdot \frac{\partial V}{\partial r_B} \cdot \tilde{Y}_{11}(\hat{r}_B) Y_L(\hat{r}_B) d\Omega_B r_B^2 dr_B + (\psi_m, \vec{\nabla}_x V \psi_n)_{\text{surface}} \end{aligned}$$

$$\begin{aligned} \text{where } (\psi_m, \vec{\nabla}_x V \psi_n)_{\text{surface}} &= \sum_B \sum_L \sum_{L'} C_L^B C_{L'}^{B'} \left[ \int \tilde{Y}_{11}(\hat{r}_B) Y_L(\hat{r}_B) Y_{L'}(\hat{r}_B) d\Omega_B \right] \\ &\quad \cdot R_\ell^B(E_m, b_B) R_{\ell'}^{B'}(E_n, b_B) b_B^2 (\bar{V}_{II} - V_{\text{inside on}})_{\text{surface}} \end{aligned}$$

(For the outer sphere,  $B = 0$ , we have  $(V(\text{outside on surface}) - \bar{V}_{II}) = \Delta V$  in the surface term. Also, we have  $\int_{b_0}^{\infty}$  for the limits of integration. See the text for the final answer. The matrix elements  $(\Psi_m, \vec{\nabla}_y V \Psi_n)$  and  $(\Psi_m, \vec{\nabla}_z V \Psi_n)$  are derived analogously.

#### Derivation of Surface Terms

$$\begin{aligned}
 (\Psi_m, \nabla_x V \Psi_n)_{\text{surface}} &= \sum_B \int_{b_B - \delta}^{b_B + \delta} \int_0^{4\pi} \Psi_m(\vec{r}_B) \frac{\partial V}{\partial r_B} \Psi_n(\vec{r}_B) \tilde{Y}_{11}(\hat{r}_B) d\Omega_B r_B^2 dr_B \\
 &\quad \lim_{\delta \rightarrow 0} \\
 &= \sum_B \sum_L \sum_{L'} C_L^B C_{L'}^B \left[ \int_{b_B - \delta}^{b_B + \delta} R_L^B(E_m, r_B) R_{L'}^B(E_n, r_B) \frac{\partial V}{\partial r_B} r_B^2 dr_B \right] \\
 &\quad \lim_{\delta \rightarrow 0} \left[ \int_0^{4\pi} \tilde{Y}_{11}(\hat{r}_B) Y_L(\hat{r}_B) Y_{L'}(\hat{r}_B) d\Omega_B \right]
 \end{aligned}$$

The important surface integral is

$$\int_{b_B - \delta}^{b_B + \delta} R_L^B(E_m, r_B) R_{L'}^B(E_n, r_B) \frac{\partial V}{\partial r_B} r_B^2 dr_B$$

$\lim_{\delta \rightarrow 0}$

Integrate by parts  $\int_a^b u dv = uv \Big|_a^b - \int_a^b v du$

$$\text{Let } u = R_\ell^B R_{\ell'}^B r_B^2$$

$$dv = \frac{\partial V}{\partial r_B} dr_B$$

$$V = \begin{cases} V_{\text{inside}} & r_B < b_B \\ V_c = \bar{V}_{II} & r_B > b_B \end{cases}$$

The preceding expression becomes

$$\left[ R_\ell^B R_{\ell'}^B r_B^2 V \right]_{b_B - \delta}^{b_B + \delta} - \int_{b_B - \delta}^{b_B + \delta} V \frac{\partial}{\partial r_B} [R_\ell^B R_{\ell'}^B r_B^2] dr_B$$

$\lim_{\delta \rightarrow 0}$

Since  $R_\ell^B$  and  $R_{\ell'}^B$  are continuous across the boundary

they go to a single limit as  $\delta \rightarrow 0$

$$R_\ell^B \rightarrow R_\ell^B(E_m, b_B) \text{ as } \delta \rightarrow 0$$

$$R_{\ell'}^B \rightarrow R_{\ell'}^B(E_m, b_B) \text{ as } \delta \rightarrow 0$$

The first derivatives are also continuous at the boundary

and  $V$  is always finite so the second term is 0.

$$\lim_{\delta \rightarrow 0} \int_{b_B - \delta}^{b_B + \delta} V \frac{\partial}{\partial r_B} [R_\ell^B R_{\ell'}^B r_B^2] dr_B = 0$$

Therefore the surface integral is

$$\lim_{\delta \rightarrow 0} \left[ R_{\ell}^B R_{\ell'}^B r_B^2 V \right]_{b_B - \delta}^{b_B + \delta} = R_{\ell}^B(E_m, b_B) R_{\ell'}^B(E_n, b_B) b_B^2 (V_c - V_{\text{inside on surface}})$$

A similar derivation gives the outer sphere surface term. Let

$$I_{11}(L; L') = \int \tilde{Y}_{11}(\hat{r}) Y_L(\hat{r}) Y_{L'}(\hat{r}) d\Omega$$

$$I_{1-1}(L; L') = \int \tilde{Y}_{1-1}(\hat{r}) Y_L(\hat{r}) Y_{L'}(\hat{r}) d\Omega$$

$$I_{10}(L; L') = \int \tilde{Y}_{10}(\hat{r}) Y_L(\hat{r}) Y_{L'}(\hat{r}) d\Omega$$

Then we obtain directly the result given in the text of the thesis.

### Gaunt Integrals

From Rose (page 62, equation 4.34) we obtain<sup>104</sup>

$$\int d\Omega Y_{\ell_3 m_3}^* Y_{\ell_2 m_2} Y_{\ell_1 m_1} = \left[ \frac{(2\ell_1 + 1)(2\ell_2 + 1)}{4\pi(2\ell_3 + 1)} \right] \cdot C(\ell_1, \ell_2, \ell_3; m_1, m_2, m_3) \cdot C(\ell_1, \ell_2, \ell_3; 000)$$

The spherical harmonics are complex, the C's are Clebsch Gordon coefficients calculated via equation 3.18 of Rose in the CGC routine of the scattered wave program. Relation of complex to real spherical harmonics: for  $m \neq 0$ , both real and complex harmonics are normalized

$$Y_{lm}^{\cos} = \frac{1}{\sqrt{2}} (Y_{lm} + Y_{lm}^*) = \frac{1}{\sqrt{2}} (Y_{lm} + (-1)^m Y_{l-m})$$

$$Y_{lm}^{\sin} = \frac{1}{\sqrt{2}i} (Y_{lm} - Y_{lm}^*) = \frac{-i}{\sqrt{2}} (Y_{lm} - (-1)^m Y_{l-m})$$

for  $m=0$

$$Y_{l0}^{\cos} = 1 Y_{l0} + 0 Y_{l-0}$$

This is the method of formulation used in subprogram IIP to obtain real Gaunt integrals from the complex Gaunt integrals.

Also:

$$\operatorname{Re} Y_{lm} = \frac{Y_{lm} + Y_{lm}^*}{2}$$

$$\operatorname{Im} Y_{lm} = \frac{1}{2i} (Y_{lm} - Y_{lm}^*)$$

for  $m \neq 0$

$$Y_{lm}^{\cos}(\hat{r}) = \sqrt{2} \operatorname{Re} Y_{lm}(\hat{r})$$

$$Y_{lm}^{\sin}(\hat{r}) = \sqrt{2} \operatorname{Im} Y_{lm}(\hat{r})$$

for  $m = 0$

$$Y_{l_0}^{\cos(\hat{r})} = Y_{l_0}$$

Products of 3 real spherical harmonics:

$$I_{\substack{l_3 \cos \\ m=0 \\ \sin}}(L_3; L_1) = \int Y_{L_3}^{\text{Real}} \cdot \left(\frac{4\pi}{3}\right)^{\frac{1}{2}} \cdot \begin{pmatrix} Y_{l_1 \cos} \\ Y_{l_1 0} \\ Y_{l_1 \sin} \end{pmatrix} \cdot Y_{L_1}^{\text{Real}} d\Omega$$

For real harmonics, each  $L$  means  $(l, |m|, \cos \phi \text{ or } \sin \phi)$  or for  $m = 0$ ,  $L = (l, 0, \text{no } \phi \text{ dependence})$ . Therefore, in the preceding equation, there are many possible matrix elements. The terms in brackets will correspond to the  $\begin{pmatrix} \cos \phi \\ m=0 \\ \sin \phi \end{pmatrix}$  terms respectively.

$$I_{\substack{l_3 \cos \phi \\ m=0 \\ \sin \phi}}(L_3; L_1) = \left(\frac{4\pi}{3}\right)^{\frac{1}{2}} \left(\frac{1}{\sqrt{2}}\right)^2 \int d\Omega \left( \begin{pmatrix} 1 \\ \sqrt{2} \\ i \end{pmatrix} Y_{l_3 m_3}^* + \begin{pmatrix} 1 \\ 0 \\ -i \end{pmatrix} (-1)^{m_3} Y_{l_3 - m_3}^* \right) \cdot \begin{pmatrix} Y_{l_1 \cos} \\ Y_{l_1 0} \\ Y_{l_1 \sin} \end{pmatrix} \cdot \left( \begin{pmatrix} 1 \\ \sqrt{2} \\ -i \end{pmatrix} Y_{l_1 m_1} + \begin{pmatrix} 1 \\ 0 \\ +i \end{pmatrix} (-1)^{m_1} Y_{l_1 - m_1} \right)$$

$$I_{l_0}(L_3; L_1) = \left(\frac{4\pi}{3}\right)^{\frac{1}{2}} \frac{1}{2} \int d\Omega \left( \begin{pmatrix} 1 \\ \sqrt{2} \\ i \end{pmatrix} Y_{l_3 m_3}^* + \begin{pmatrix} 1 \\ 0 \\ -i \end{pmatrix} (-1)^{m_3} Y_{l_3 - m_3}^* \right) \cdot Y_{l_0} \cdot \left( \begin{pmatrix} 1 \\ \sqrt{2} \\ -i \end{pmatrix} Y_{l_1 m_1} + \begin{pmatrix} 1 \\ 0 \\ +i \end{pmatrix} (-1)^{m_1} Y_{l_1 - m_1} \right)$$



$$I_{\frac{\cos}{\sin}}(L_3; L_1) = -\left(\frac{4\pi}{3}\right)^{\frac{1}{2}} \frac{\sqrt{2}}{2} \int d\Omega \left( \begin{pmatrix} 1 \\ \sqrt{2} \\ i \end{pmatrix} Y_{\ell_3 m_3}^* + \begin{pmatrix} 1 \\ 0 \\ -i \end{pmatrix} (-1)^{m_3} Y_{\ell_3 -m_3}^* \right) \\ \cdot \begin{pmatrix} \text{Re} \\ \text{Im} \\ Y_{\ell_1+1} \end{pmatrix} \cdot \left( \begin{pmatrix} 1 \\ \sqrt{2} \\ -i \end{pmatrix} Y_{\ell_1 m_1} + \begin{pmatrix} 1 \\ 0 \\ +i \end{pmatrix} (-1)^{m_1} Y_{\ell_1 -m_1} \right)$$

The integrals over complex spherical harmonics are evaluated via Rose, equation 4.34.

In the integrals  $I_{\frac{\cos}{\sin}}$  the Re and Im parts of the

entire integral yield the same answer as taking  $\begin{pmatrix} \text{Re} \\ \text{Im} \\ Y_{\ell_1} \end{pmatrix}$  before integrating. This is the way we evaluate the terms of  $I_{\frac{\cos}{\sin}}(L_3; L_1)$  in the function subprogram IIP.

#### Function Subroutine IIP

In IIP, (MNI, IN1) = initial state (MN, IN); (MN3, IN3) = final state (MN, IN) where MN = |m|, IN = +1 for cos, -1 for sin, and for MN = 0, IN = +1. TINT1 and TINT3 are coefficients preceding  $Y_{\ell_1 m_1}$  and  $Y_{\ell_1 -m_1}$  for TINT1, and preceding  $Y_{\ell_3 m_3}$  and  $Y_{\ell_3 -m_3}$  for TINT3. IX is again the x, y, z electric field polarization direction. The algorithm follows from the preceding description.

## APPENDIX C

RELATION OF THE MOLAR EXTINCTION COEFFICIENT  
 $\epsilon_m$  AND THE OSCILLATOR STRENGTH  $f$  TO THE AB-  
 SORPTION COEFFICIENT  $\eta$ .

In the preceding discussion,  $\eta$  was defined in terms of theoretically obtained quantities. In an absorption experiment, the intensity  $I$  (which is the same as the Poynting's vector previously defined) is attenuated according to the equation.

$$C1) \quad I(\nu) = I_0(\nu)e^{-\eta \ell}$$

$I(\nu)$  = intensity per unit frequency range at  
 frequency  $\nu$

$I_0(\nu)$  = intensity per unit frequency at zero penetration into the material. This is the incident intensity minus the reflected intensity at the material surface, since it is this energy flux which penetrates the material and is attenuated by absorption,

$\ell$  = Penetration distance into the material at which  $I(\nu)$  is measured.

Equation C1 (identical to equation 6.19 in the text) arises from a differential absorption law

$$C2) -dI = I\eta dl \text{ or } \frac{1}{I}(-\frac{dI}{dl}) = \eta$$

Since  $-\frac{dI}{dl}$  is the rate of energy absorption per unit volume we can see that the phenomenological definition of equation C2 coincides with the previous definition of equation 6.18

$$C3) \eta = \frac{\frac{1}{2} \operatorname{Re}(\vec{J}_0 \cdot \vec{E}_0^*)}{\frac{c}{8\pi} \operatorname{Re}(\vec{E}_0 \times \vec{B}_0^*)} = \frac{4\pi}{c} \frac{\operatorname{Re}(\sum_j \sigma_{jj}) |E_{0x}|^2}{3 |E_{0x}|^2}$$

By definition,

$$C4) \epsilon_m = \frac{\eta}{\bar{c} l \eta_{10}}$$

Where  $\bar{c}$  is the molecular density, in moles/liter.  $f$  is then defined in terms of  $\epsilon_m$ .<sup>23</sup> This relation is given by equation 6.22 (The molecular density  $\bar{N}$  is in molecules/cm<sup>3</sup>).

## APPENDIX D

PHOTOEMISSION USING THE  $\vec{V}$  FORMALISM

As part of the present work, we have attempted to calculate photoemission intensities from  $\text{CH}_4$  using the  $\vec{V}$  method. The positive energy eigenstates were confined to a large spherical box (radius of about  $15a_0$ ). This produced a discrete set of final states. The density of final states was sufficiently low so that the intensity for each transition may be evaluated, and a profile of photoemission intensity versus the kinetic energy of the final state electron may be constructed. The radial functions for the final state are required to go to 0 at the box radius. The inward integration to obtain the positive energy radial functions for the outer sphere region is begun by assuming the radial functions take the form

$$D1) \quad R_\ell(r_0) = A j_\ell(Kr_0) + B n_\ell(Kr_0)$$

$$\text{where } \frac{A}{B} = \frac{-n_\ell(Kb_x)}{j_\ell(Kb_x)}$$

$$D2) \quad R_\ell(b_x) = 0 \text{ with } b_x = \text{box radius}$$

Equation D1 is only used for the first few points inside  $b_x$ . Then the inward integration is performed in the standard manner using the outer sphere potential from the scattered wave program.

The additional photoemission sequence may be found in the TMAP routine of Appendix A from statement 181 to 106.

(It is also necessary to override the statement in EIGEN which prohibits searching for positive energy eigenstates.)

The photoemission program should be run using the new NSCF MAIN program. A set of transitions from a single initial state may be calculated at one time by letting  $NXGP(N) = 1$  for the initial state and  $NXGP(N) = 2$  for each final state.

The photoemission intensities for  $CH_4$  calculated by the author were completely unreliable. However, only  $\ell = 0$  and  $\ell = 1$  partial waves were used in the calculation, and it is now clear that  $\ell = 2$  must be included as well to obtain accurate intensities. Once this defect is corrected, we will be better able to evaluate the accuracy of this approach for determining photoemission intensities.

1. J.H. Van Vleck, *Phys. Rev.* 24, 330 (1924).
2. E. V. Condon and G.H. Shortley, The Theory of Atomic Spectra (Cambridge University Press, 1959).
3. H.F. Schaefer, The Electronic Structure of Atoms and Molecules (Addison-Wesley Publishing Company, Reading, Mass., 1972).
4. B.D. Bird and P. Day, *J. Chem. Phys.* 49, 392 (1968).
5. J.G. Slater, in Advances in Quantum Chemistry, Vol. 6, edited by P.O. Lowdin (Academic Press, New York, 1972), p.1.
6. K.H. Johnson, in Advances in Quantum Chemistry, Vol. 7, edited by P.O. Lowdin (Academic Press, New York, 1973), p. 143.
7. R. S. Mulliken and C.A. Rieke, *Repts. Progr. Phys.* 8, 231 (1941).
8. K.H. Johnson, J.G. Norman, Jr., and J.W.D. Connolly in Computational Methods for Large Molecules and Localized States in Solids, edited by F. Herman, A.D. MacLean and R.K. Nesbet (Plenum Press, New York, 1973), p. 161; and references therein.
9. K.H. Johnson and F.C. Smith, Jr., *Phys. Rev.* B5, 831 (1972).
10. H. Fraunfelder, M.I.T. Physics Colloquium, 1974.
11. C.J. Ballhausen and H.B. Gray in Coordination Chemistry 1, edited by A.E. Martell (Van Nostrand Reinhold Company, New York, 1971), pp. 3-37.
12. R.F. Fenske and C.A. Sweeney, *Inorg. Chem.* 3, 1113 (1964).
13. A. van der Avoird and P. Ros, *Theoret. Chim. Acta* 4, 13 (1966).
14. P. Ros and G.C.A. Shuit, *Theoret. Chim. Acta* 4, 1 (1966).
15. G. Herzberg, Spectra of Diatomic Molecules (Van Nostrand Reinhold Company, New York, 1950).
16. A. Einstein, *Physik. Z.* 18, 121 (1917).
17. R.M. Eisberg, Fundamentals of Modern Physics (John Wiley and Sons, Inc., New York, 1961), pp. 453-468.

18. B. Schiff and C.L. Perk anis, Phys, Rev. A 134, 638 (1964).
19. J.N. Murrell, S.F.A.Kettle and J.M. Tedder, Valence Theory (John Wiley and Sons, Inc., London, 1970) pp. 82-86.
20. W. Kauzmann, Quantum Chemistry (Academic Press, New York, 1957).
21. K. Nakamoto in Coordination Chemistry Vol. 1, edited by A.E. Martell (Van Nostrand Reinhold Company, New York, 1971), p. 134.
22. H.E. Popkie and W.H. Henneker, J. Chem. Phys. 55, 617 (1971); and references therein.
23. H. Suzuki, Electronic Absorption Spectra and Geometry of Organic Molecules (Academic Press, New York, 1967).
24. S. Bashkin in Beam-Foil Spectroscopy (Gordon and Breach, New York, 1968).
25. O. Sinanoglu, Comments on At. and Mol. Physics II, No. 2, 73 (1970).
26. G.M. Lawrence and B.D. Savage, Phys. Rev. 141, 67 (1966).
27. L. Heroux, Phys. Rev. 153, 156 (1967).
28. E. Hinnov, J. Opt. Soc. Am. 56, 1179 (1966).
29. G.M. Lawrence and J. Hesser, unpublished work quoted in: P. Westhaus and O. Sinanoglu, Astrophys. J. 157, 997 (1969).
30. P.G. Ellis and O. Goscinski, Physica Scripta 9, 104 (1974); and references therein.
31. T. Andersen, K.A. Jessen, and G. Sorensen, Phys. Letts. A29, 384 (1969).
32. J.K. Link, J. Opt. Soc. Am. 56, 1195 (1966).
33. S. Ehrenson and P.E. Phillipson, J. Chem. Phys. 34, 1224 (1961).
34. K.L. Wolf and K.F. Herzfeld, Handbuch der Physik 20, 492 (1928).
35. J.R. Peterson and J.T. Mosely, J. Chem. Phys. 58, 172 (1973); and references therein.
36. D.C. Cartwright, J. Chem. Phys. 58, 178 (1973).
37. S.E. Johnson, G. Capelle, and H.P. Broida, J. Chem. Phys. 56, 663 (1972).

38. R.C.L. Mooney, Phys. Rev. 37, 1306 (1931).
39. W.C.McCrone, Anal. Chem. 22, 1459 (1950).
40. G.J. Palenik, Inorg. Chem. 6, 503 (1967).
41. S.L. Holt and C.J. Ballhausen, Theoret. Chim Acta 7, 313 (1967).
42. J. Teltow, Z. Phys. Chem. B40, 397 (1938); B42, 198 (1939).
43. G. den Boef, H.J. van der Beek, and T. Braef, Rec. Trav. Chem. Pay-Bas 77, 1064 (1958).
44. L.W. Johnson and S.P. McGlynn, Chem. Phys. Lett. 7, 618 (1970).
45. R.R. Richards and N.W. Gregory, J. Phys. Chem. 69, 239 (1965).
46. A.B. Lever, Inorganic Electronic Spectroscopy (Elsevier Publishing Company, Amsterdam, the Netherlands, 1968).
47. P. Day and C.K. Jorgensen, J. Chem. Soc. 6226 (1964).
48. F.A. Cotton, D.M.L. Goodgame, and M. Goodgame, J. Am. Chem. Soc. 83, 4690 (1961).
49. J. Ferguson, J. Chem. Phys. 39, 116 (1963).
50. M.B. Quinn and D.W. Smith, J. Chem. Soc. A., 2496 (1971).
51. N.A. Beach and H.B. Gray, J. Am. Chem. Soc. 90, 5713 (1968).
52. M. Wrighton and M.A. Schroeder, J. Am. Chem. Soc. 95, 5764 (1973).
53. K.H. Johnson, personal communication.
54. D.R. Bates, K. Ledsham, and A.L. Stewart, Proc. Phys. Soc. (London) A66, 1124 (1954).
55. D.R. Bates, K. Ledsham, and A.L. Stewart, Phil. Trans. Roy. Soc. (London) Ser. A246, 215 (1953).
56. W. Lamb, R. Young, and S.R. La Paglia, J. Chem. Phys. 49, 2868 (1968).
57. W. Kolos and L. Wolniewicz, J. Chem. Phys. 41, 3663 (1964); 43, 2409 (1965); 45, 509 (1966); L. Wolniewicz, J. Chem. Phys. 51, 5002 (1969).



58. P.E. Cade, K.D. Sales, and A.C. Wahl, *J. Chem. Phys.* 44, 1973 (1966).
59. R.P. Messmer and D.R. Salahub, unpublished results.
60. H.H. Michels, *J. Chem. Phys.* 56, 665 (1972).
61. M. Yoshimine, A.D. McLean, and B. Liu, *J. Chem. Phys.* 58, 4412 (1973).
62. P. Jorgensen and J. Oddershude, *J. Chem. Phys.* 57, 277 (1972).
63. M. Wolfsberg and L. Helmholz, *J. Chem. Phys.* 20, 837 (1952).
64. C.J. Ballhausen and A.D. Liehr, *J. Mol. Spectry.* 2, 342 (1958); 4, 190 (1960).
65. A. Viste and H.B. Gray, *Inorg. Chem.* 3, 1113 (1964).
66. A.P. Mortola, H. Basch, and J. W. Moskowitz, *Intern. J. Quantum Chem.* 3, 725 (1973).
67. C. Carrington, D.J.E. Ingram, K.A.K. Lott, D.S. Schonland, and M.C.R. Symons, *Proc. Roy. Soc.* A254, 101 (1960).
68. D.S. Schonland, *Proc. Roy. Soc.* A254, 101 (1960).
69. D.E. Ellis and F.W. Averill, *J. Chem. Phys.* 60, 2856 (1974).
70. Z. Jaeger and R. Englman, *Chem. Phys. Lett.* 19, 242 (1973).
71. J. C. Slater, Quantum Theory of Atomic Structure, Vol. II (McGraw Hill Book Company, New York, 1960), pp. 1-30.
72. C.C.J. Roothaan, *Rev. Mod. Phys.* 23, 69 (1951).
73. D.E. Ellis, A.J. Freeman, and P. Ros, *Phys. Rev.* 176, 688 (1968).
74. J. C. Slater, The Self-Consistent Field for Molecules and Solids (McGraw Hill Book Company, New York, 1974), pp. 1-11.
75. E. Merzbacher, Quantum Mechanics (John Wiley and Sons, Inc., New York, 1970).
76. N.Q. Chako, *J. Chem. Phys.* 2, 644 (1934).
77. L. Onsager, *J. Am. Chem. Soc.* 58, 1486 (1936).
78. W.B. Person, *J. Chem. Phys.* 28, 319 (1958).
79. J. Schuyler, *Rec. Trav. Chim.* 72, 933 (1953).

80. J. B. Marion, Classical Electromagnetic Radiation (Academic Press, New York, 1965), pp. 130-148.
81. M. Born and E. Wolf, Principles of Optics (Pergamon Press, London, 1959), pp. 83-107.
82. P. Nozieres and D. Pines, Il Nuovo Cimento, X 9, 470 (1958).
83. J.B. Ziman, Principles of the Theory of Solids (Cambridge University Press, 1969), p. 221.
84. J. C. Slater, Phys Rev. 81, 385 (1951); 82, 538 (1951).
85. P. Hohenberg and W. Kohn, Phys.Rev. B136, 864 (1964).
86. W. Kohn and L.J. Sham, Phys. Rev. A140, 1133 (1965).
87. J.P. Dahl, Concepts in the X<sub>α</sub> Method (Notes from Scandinavian Summer School in Quantum Chemistry, University of Copenhagen, 1972).
88. F. Herman and S. Skillman, Atomic Structure Calculations (Prentice Hall, Inc., Englewood, Cliffs, New Jersey, 1963).
89. K. Schwarz, Phys. Rev. B5, 2466 (1972).
90. F. Herman, A.R. Williams, and K.H. Johnson, IBM Research Report, June 1974, to be published.
91. J. Korrynga, Physica 13, 392 (1947).
92. W. Kohn and N. Rostoker, Phys. Rev. 94, 111 (1954).
93. A.R. Williams and J. van W. Morgan, J. Phys. C5, 1293 (1972); J. Phys. C7, 36 (1974).
94. J. C. Slater, Intern. J. of Quantum Chem. S. No. 8, 81 (1974).
95. K.H. Johnson, unpublished results.
96. D.R. Salahub, R.P. Messmer, and K.H. Johnson, to be published.
97. W. Klemperer, K.H. Johnson, and L. Noodleman, to be published.
98. H. Ehrenreich and M.H. Cohen, Phys. Rev. 115, 786 (1959).
99. W.A. Harrison, Solid State Theory (McGraw Hill Book Company, New York, 1970), pp. 290-295, 317-321.
100. O. Sinanoglu and K. A. Brueckner, Three Approaches to Electron Correlation in Atoms (Yale University Press,

New Haven, Conn., 1970).

101. J.I. Steinfeld, Molecules and Radiation (Harper and Row, New York, 1974), pp. 22-29.
102. G.F. Koster, J.O. Dimmock, R.G. Wheeler, and H. Statz, Properties of the 32 Crystallographic Point Groups (M.I.T. Press, Cambridge, Mass., 1963), pp. 13-14, 88-89.
103. The preliminary form of this result, without the surface terms, is due to R.P. Messmer and K.H. Johnson, personal communication. The existence of surface terms was first noted by G.A. Coulson.
104. M.E. Rose, Elementary Theory of Angular Momentum (John Wiley and Sons, Inc., New York, 1957), pp. 61-63.
105. P.S. Bagus and B.I. Bennett, IBM Research Paper (1974), to be published.
106. J.A. Tossell, D.J. Vaughan, and K.H. Johnson, *Nature (Phys. Sci.)* 244, 42 (1973).
107. J.A. Tossell, D.J. Vaughan, and K.H. Johnson, *Amer. Minerol.* 59, 319 (1974).
108. L. Noodleman, Masters Thesis, Department of Materials Science and Engineering, M.I.T. (1971).
109. J.C. Slater and K.H. Johnson, *Physics Today*, p. 34 (October, 1974).
110. J. Aleksandrowicz, Sc.D. Thesis, M.I.T., Department of Chemical Engineering, Cambridge, Massachusetts (1970).
111. K.H. Johnson, to be published in *Ann.Rev.Phys.Chem.* 26 (1975).
112. J.G. Norman, personal communication.
113. B. Ritchie, *J.Chem.Phys.* 61, 3279 (1974); 61, 3291 (1974).
114. A. Schweig and W. Theil, *J.Chem.Phys.* 60, 951 (1974).
115. D. Dill and J.L. Dehmer, *J.Chem.Phys.* 61, 692 (1974).
116. J.L. Dehmer and D. Dill, to be published.
117. K.H. Johnson and R.P. Messmer, personal communication.

## Biographical Note

The author was born in Dayton, Ohio on January 3, 1950. After living for 14 years in Dayton and Cincinnati, he moved with his family to Blacksburg, Virginia, his present home. The author attended Blacksburg High School and subsequently Virginia Polytechnic Institute. In 1968, he transferred to M.I.T., and graduated in June, 1971 with an S.B. in physics. In September, 1972 he received his S.M. without specification of field from the Department of Metallurgy and Materials Science. His work has centered on the fields of solid state physics and chemistry. The author also has a deep interest in the history and philosophy of science. In his spare time, the author plays tennis and communes with nature.